COFIRING OF COAL AND DAIRY BIOMASS IN A 100,000 BTU/HR FURNACE

A Thesis

by

BENJAMIN DANIEL LAWRENCE

Submitted to the Office of Graduate Studies of
Texas A&M University
in partial fulfillment of the requirements for the degree of

MASTER OF SCIENCE

December 2007

Major Subject: Mechanical Engineering

COFIRNG OF COAL AND DAIRY BIOMASS IN A 100,000 BTU/HR FURNACE

A Thesis

by

BENJAMIN DANIEL LAWRENCE

Submitted to the Office of Graduate Studies of
Texas A&M University
in partial fulfillment of the requirements for the degree of

MASTER OF SCIENCE

Approved by:

Chair of Committee,	Kalyan Annamalai
Committee Members,	Jerald Caton
	John Sweeten
Head of Department,	Dennis O'Neal

December 2007

Major Subject: Mechanical Engineering

ABSTRACT

Cofiring Of Coal and Dairy Biomass in a 100,000 BTU/hr Furnace.

December 2007

Benjamin Daniel Lawrence, B.S. Kansas State University;

Chair of Advisory Committee: Dr. Kalyan Annamalai

Dairy biomass (DB) is evaluated as a possible co-firing fuel with coal. Cofiring of DB offers a technique of utilizing dairy manure for power/steam generation, reducing greenhouse gas concerns, and increasing financial returns to dairy operators. The effects of cofiring coal and DB have been studied in a 30 kW (100,000 BTU/hr) burner boiler facility. Experiments were performed with Texas Lignite coal (TXL) as a base line fuel. The combustion efficiency from co-firing is also addressed in the present work.

Two forms of partially composted DB fuels were investigated: low ash separated solids and high ash soil surface. Two types of coal were investigated: TXL and Wyoming Powder River Basin coal (WYO).

Proximate and ultimate analyses were performed on coal and DB. DB fuels have much higher nitrogen (kg/GJ) and ash content (kg/GJ) than coal. The HHV of TXL and WYO coal as received were 14,000 and 18,000 kJ/kg, while the HHV of the LA-PC-DB-SepS and the HA-PC-DB-SoilS were 13,000 and 4,000 kJ/kg. The HHV based on stoichiometric air were 3,000 kJ/kg for both coals and LA-PC-DB-SepS and 2,900 kJ/kg

for HA-PC-DB-SoilS. The nitrogen and sulfur loading for TXL and WYO ranged from 0.15 to 0.48 kg/GJ and from 0.33 to 2.67 for the DB fuels.

TXL began pyrolysis at 640 K and the WYO at 660 K. The HA-PC-DB-SoilSs began pyrolysis at 530 K and the LA-PC-DB-SepS at 510 K. The maximum rate of volatile release occurred at 700 K for both coals and HA-PC-DB-SoilS and 750K for LA-PC-DB-SepS.

The NO_x emissions for equivalence ratio (ϕ) varying from 0.9 to 1.2 ranged from 0.34 to 0.90 kg/GJ (0.79 to 0.16 lb/mmBTU) for pure TXL. They ranged from 0.35 to 0.7 kg/GJ (0.82 to 0.16 lb/mmBTU) for a 90:10 TXL:LA-PC-DB-SepS blend and from 0.32 to 0.5 kg/GJ (0.74 to 0.12 lb/mmBTU) for a 80:20 TXL:LA-PC-DB-SepS blend over the same range of ϕ. In a rich environment, DB:coal cofiring produced less NO_x and CO than pure coal. This result is probably due to the fuel bound nitrogen in DB is mostly in the form of urea which reduces NO_x to non-polluting gases such as nitrogen (N_2).

DEDICATION

This thesis is dedicated to my parents, Rod and Hatsie Lawrence for their patience, support, and loving guidance through all of my journeys. Thank you Mom and Dad for providing me with the opportunity, means, and desire to pursue all of my dreams.

ACKNOWLEDGEMENTS

One of my favorite quotes regarding education and learning in general comes from Abigail Adams. Mrs. Adams once said "Learning is not attained by chance; it must be sought for with ardor and attended to with diligence." I would like to take a moment to recognize all of those individuals who have diligently assisted me along this arduous adventure; beginning with my colleagues at Texas A&M University.

I want to thank all of the graduate students, past and present, who have worked in the Coal and Biomass Lab. In particular: Nathan Coon, Paul Goughnor, Brandon Martin, Giacomo Colegma, Madhu Babu, Uday Sarathy, Hyukjin Oh, Gerardo Gordillo, Nicholas Carlin, and Pat Gomez. Although research has not always been the most pleasant experience, working with you all has been.

I want to thank all the professors at Texas A&M University that have helped me with my studies: S.C. Lau, J.C. Han, Warren Heffington, Gerald Morrison, Mariah Hahn, and Timothy Jacobs. Your patience, guidance, and insight has been invaluable.

I want to thank all of my committee members for taking the time to serve on my committee: Jerald Caton, John Sweeten, and Kalyan Annamalai. Special recognition goes to Kalyan Annamalai for serving as my committee chair. I appreciate all the energy you have invested in furthering me.

Special recognition goes to Kevin Heflin at the Agricultural Research and Extension Center. Mr. Heflin received, composted, dried, ground, and shipped all of the fuel samples. Without his hard work, none of this could have been accomplished.

I want to thank all the secretaries and business coordinators and administrative aides and receptionists at all the institutions I have attended. You do not receive a quarter of the credit you deserve. Without your hard work, all other work would grind to a halt very quickly. Although the students and faculty often get all the glory, you provide the effort that propels us forward.

I want to thank all of my friends in the Bryan/College Station area. Any list of the people that belong in this group would take longer than the 4 pages I am allotted for my acknowledgements. Know that your absence on paper does not constitute absence in my heart.

I want to thank the professors at Kansas State University who have helped me with my studies: David Pacey, Bill Dunn, Bruce Babin, Charlie Zheng, Jack Xin, Dale Schinstock, Prakash Krishnaswami, Warren White, Steve Eckles, Don Fenton, Kevin Lease, Byron Jones, Mohamed Hosni, John Schlupe, and Bob Peterman.

I want to thank all of my friends from the Manhattan area. My time at Kansas State University was wonderful. I carry nothing but the fondest of memories from that time. You all have left a permanent mark on my heart.

I want to thank the professors at Johnson County Community College: Ron Palcic, Chris Imm, Carl Anderson, Mike Martin, Barry Herron, Kevin Canless, Bill Karnaze, Susan Johnson, Cindy Koons, and Bob Hunt. I am as proud of my degree from Johnson County Community College as I am of any other degree that I currently hold or will hold. Being a Cavalier moved me from being a teenager into a young man. I grew so much as a person in my time there.

I want to thank all my friends from the Kansas City area. Although my childhood was not perfect, (no one's is) I have several fond memories of growing up in one of the best cities in the world.

I want to thank all of my family. I don't think you are aware of how much inspiration and motivation you have given me along the way. Most of the time you were doing it unconsciously. Just by being such excellent role models for me as to how to live my life and conduct my affairs. Getting to where I am now has not been an easy trek, but I have always known that I could depend upon you to support me.

I want to thank all the funding agencies for giving me the opportunity and financial means to do this work.

Lastly, I want to thank my beautiful fiancée Jenna Escue. This is a major step in preparing for our life together. You have been wonderfully patient and understanding. Thank you for allowing me the time to continue to work on this project; I know it has been a sacrifice for you. I cherish all the past memories I have with you, and I eagerly look forward to all the memories we are going to make in the future. Thanks Babe.

NOMENCLATURE

AB	Agricultural Biomass
b	Pre-exponential Constant Used in Size Distribution Analysis
BF	Burnt Fraction
BTU	British Thermal Units
CAFO	Confined Animal Feeding Operation
CB	Cattle Biomass
CMF	Cumulative Mass Fraction
CO	Carbon Monoxide In Exhaust Gas Stream
CO_2	Carbon Dioxide In Exhaust Gas Stream
DAF	Dry Ash Free
DB	Dairy Biomass
DOE	Department Of Energy
DTA	Differential Thermal Analysis
FB	Feedlot Biomass
FC	Fixed Carbon
FS	Full Scale
ft^2/hd	Foot Squared per Head
GJ	Gigajoule
HA-PC-DB-SoilS	High Ash Partially Composted Dairy Biomass Soil Surfaced Pens
HHV	Higher Heating Value

kJ	Kilojoule
kW	Kilowatt
LA-PC-DB-SepS	Low Ash Partially Composted Dairy Biomass Separated Solids
lb	Pound
LB	Litter Biomass
m^2/hd	Meter Squared per Head
m^3	Meter Cubed
mmBTU	Million British Thermal Units
n	Exponential Constant Used in Size Distribution Analysis
NO_x	Nitrous Oxides In Exhaust Gas Stream
O_2	Oxygen In Exhaust Gas Stream
$O_{2,A}$	Oxygen In Ambient Air
PC	Partially Composted
PM	Particulate Matter
PPM	Parts Per Million
SCFH	Standard Cubic Feet Per Hour
Sep	Separated
SLPM	Standard Liters Per Minute
SMD	Sauter Mean Diameter
SO_2	Sulfur Dioxide
TCEQ	Texas Commission on Environmental Quality
TGA	Thermo-gravimetric Analysis

TSP	Total Suspended Particles
TXL	Texas Lignite Coal
VM	Volatile Matter
WYO	Wyoming Powder River Basin Coal (a subbituminous coal)
X_i	Measured Value from Instrument I (Used in Uncertainty Analysis)
Y_i	Mass Fraction of Compound i
ϕ	Equivalence Ratio
ϕ_{flow}	Equivalence Ratio based upon fuel and air flow rates
ϕ_{flue}	Equivalence Ratio based on exhaust gas analysis
μg	Microgram

TABLE OF CONTENTS

Page

LIST OF FIGURES

FIGURE Page

FIGURE Page

FIGURE Page

LIST OF TABLES

TABLE Page

1. INTRODUCTION: THE IMPORTANCE OF RESEARCH

The overall objective of the current research is to evaluate the combustion and emission behavior of coal:DB blends. The combustion behavior was evaluated by measuring product gas composition. The coal fuels included TXL and WYO. The DB fuels considered were LA-PC-DB-SepS and HA-PC-DB-SoilS. LA-PC-DB-SepS was collected from the flushed manure from the milking house of a dairy. The flushed manure was then passed through a mechanical separator to remove most fine solids including ash prior to air drying and grinding. This made LA-PC-DB-SepS low in ash. HA-PC-DB-SoilS was scraped from dairy farms that used soil as open pen surface and was high in entrained soil including ash. The DB was blended (on a mass basis) with the two types of coals and cofired in a 100,000 BTU/hr furnace. The gas compositions of products were used to characterize the combustion efficiency and emission behavior. TGA analysis was also performed on the pure fuels to determine pyrolysis behavior.

The HHV of TXL and WYO coal as received were 14,000 and 18,000 kJ/kg, while the HHV of the LA-PC-DB-SepS and the HA-PC-DB-SoilS were 13,000 and 4,000 kJ/kg. However, the HHV based on stoichiometric air were 3,000 kJ/kg for both coals and LA-PC-DB-SepS and 2,000 kJ/kg for HA-PC-DB-SoilS. All solid fuels should have approximately the same HHV based upon stoichiometric air. The Boie equation

---

This thesis follows the style of *Combustion Science and Technology*.

was used to approximate the HHV of the fuels based upon the ultimate analysis of each fuel. The Boie HHV was within 13% of the experimental HHV for the coals and LA-PC-DB-SepS. The nitrogen and sulfur loading from fuel input into the boiler for TXL and WYO ranged from 0.15 to 0.48 kg/GJ and from 0.33 to 2.67 for the DBs.

TXL began to pyrolize at 640K and the WYO began to pyrolize at 660K. The DBs began to pyrolize at lower temperatures, 530K for the HA-PC-DB-SoilS and 510K for the LA-PC-DB-SepS. This lower pyrolysis temperature delayed NO_x formation in rich combustion during cofiring experiments. The maximum rate of volatile release occurred at 700K for both coals and HA-PC-DB-SoilS and at 750K for LA-PC-DB-SepS.

The emissions of NO_x for ϕ varying from 0.9 to 1.2 ranged from 340 to 90 kg/GJ for pure TXL. They ranged from 350 to 70 kg/GJ for a 90:10 TXL:LA-PC-DB-SepS blend and from 320 to 50 kg/GJ for a 80:20 TXL:LA-PC-DB-SepS blend over the same range of ϕ.

2. LITERATURE REVIEW

Intensive animal feeding operations (dairy and cattle farms) create large amounts of animal waste that must be safely disposed of in order to avoid environmental degradation. CAFOs, which include cattle feedlot and dairy operations, are a cornerstone of the agricultural economy in Texas and neighboring states in the Southern Great Plains. In feedlots, cattle are confined to relatively small pens of 10 to 40 m^2/hd (100 to 430 ft^2/hd) and fed a high calorie grain diet in preparation for slaughter. Figure 2.1 shows a schematic of a 450 kg (1000 lb) cattle waste production process from excretion to collection (Tranchida, 2007).

Among dairy cattle, each animal, having a live weight between 1200 and 2000 lb, produces between 60 and 125 lb of wet manure per day per animal. This manure contains 85-90 % moisture and 10-15 % solids (including volatile matter, nutrients, ash and combustibles) (Carlin et al., 2007). Manure collected from a feedlot is called FB, while manure collected from a dairy is called DB. The sum of FB and DB together is commonly called CB. Potentially harvestable CB from all of the CAFOs in the U. S. easily exceeds 100 million tons per year on a dry basis and 6-12 million dry tons in the Texas Panhandle alone.

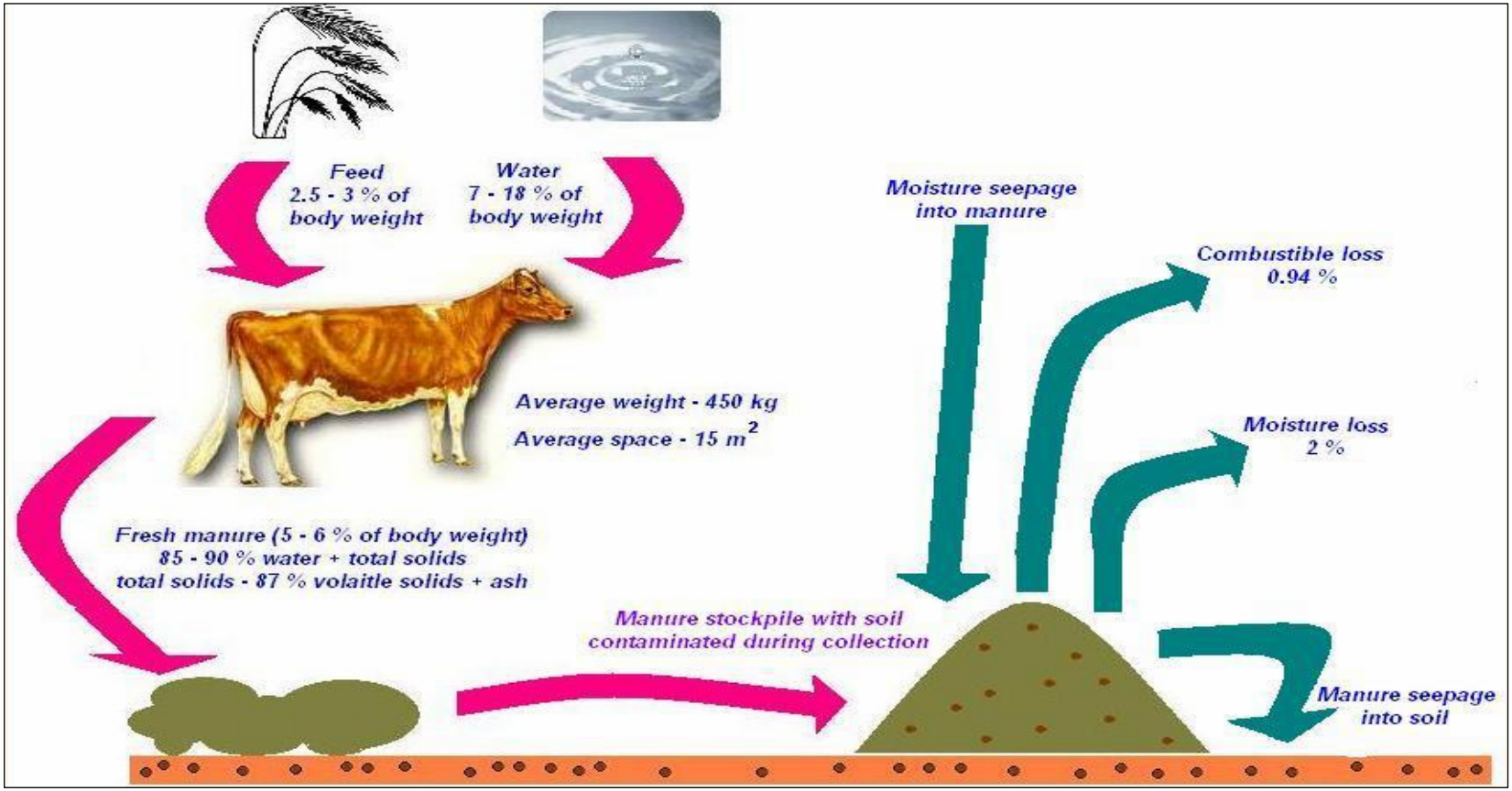

Figure 2.1: Schematic of a 450 kg (1000 lb) cattle waste production process from excretion to collection. Adapted from Tranchida (2007).

Another example of CAFOs is chicken houses. In chicken houses, thousands of chickens are kept in close proximity. Biomass derived from chicken litter will be called little biomass. If FB, DB and LB are not beneficially utilized as fertilizer or properly disposed of, these by-products may become sources of air, water, or soil pollution in some areas of the U.S., including the Southern Great Plains.

When the CB gets very dry, the cattle's feet grind the dry manure, creating a dust problem. PM or dust from feedlot ranges from 8.5 to 12 microns (Sweeten, 1979). TSP in feedlot dust can range from 150 $\mu g/m^3$ to 400 $\mu g/m^3$ (Sweeten, 1979). The PM 10 regulation requires the concentration of particles less than 10 μm should be less than 150 $\mu g/m^3$.

FB, DB and LB could be used as a fuel by mixing it with coal and firing it in an existing coal suspension fired combustion systems. This technique is known as co-firing. The high temperatures produced by the coal will allow the biomass to be completely combusted. These biomass fuels are higher in ash, lower in heat content, higher in moisture, and higher in nitrogen and sulfur (which can cause air pollution) compared to coal. Previous work (Frazzita et al., 1999), (Arumugam et al., 2005), (Annamalai et al., 2006), (Annamalai et al., 2003a), (Sweeten et al., 2003) (Annamalai et al., 2003b) was concerned with cofiring FB with coal

With support from DOE-Golden, Colorado and TCEQ to develop new technologies for use of FB and DB as an alternative renewable fuel, a comprehensive inter-disciplinary research initiative is currently being undertaken.

DB fuel properties (chiefly ash content) depend greatly on the collection technique used when the manure is gathered from the dairy; this is due in large part to the surface of the dairy. Most dairies have a soil base with an interfacial layer which consists of mixed soil and manure. If the manure is not harvested carefully some of the interfacial layer will be disturbed or collected with the manure. This leads to higher ash content in the manure. Collection techniques vary between dairies but usually one of the following methods is used: wheel loader alone, chisel-plow followed by wheel loader, and box scraper. (Sweeten, 1990) See Figure 2.2.

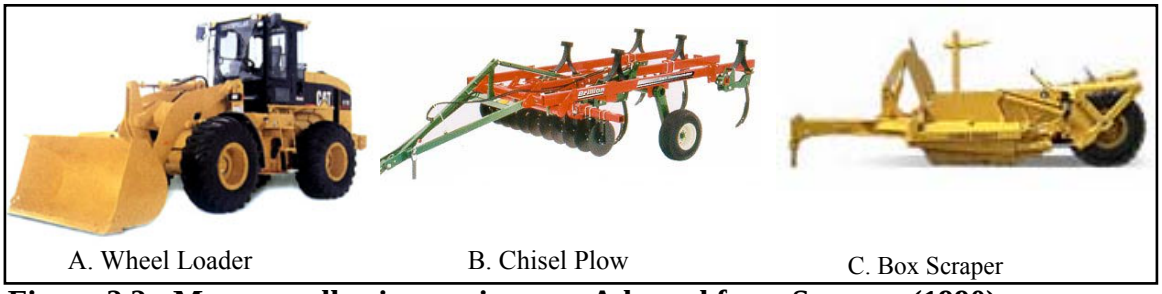

Figure 2.2: Manure collection equipment. Adapted from Sweeten (1990).

When the milking herd is moved inside the concrete floored milking house, fresh manure is collected by flushing the milking house floor with water or scraping the manure. This manure does not contain soil. The flushing water is then passed through a mechanical separator to remove the volatile solids from the flushing liquids. This liquid can then be used as lagoon water. The removed volatile solids can be combusted. This technique was used to collect the LA-PC-DB-SepS (Stokes and Gamroth, 1999).

The United States dairy industry is currently in the middle of a paradigm shift. In general, the total number of dairies is decreasing, but the size of each individual dairy is increasing and dairies are moving west. The rate of size increase of individual dairies is outpacing the rate of decrease of total number of dairies. Thus, the total dairy production rate is increasing. Figure 2.3 summarizes how the number of small dairies is deceasing, while the number of large dairies is increasing. These trends are predicted to continue.

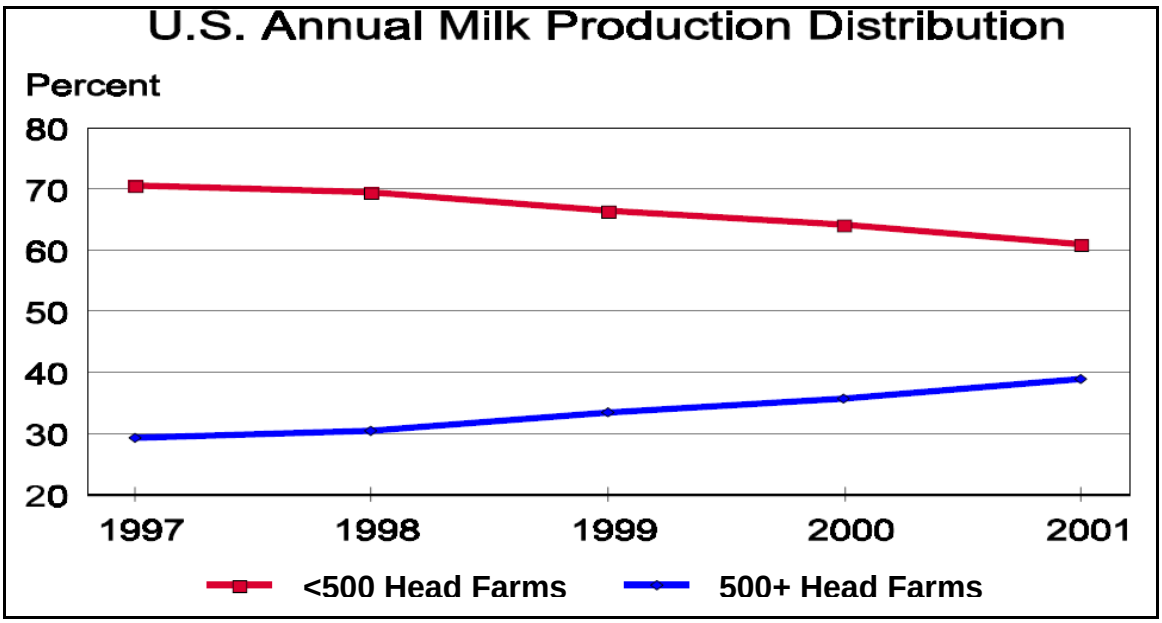

Figure 2.3: U.S. annual milk production distribution. Despite the decrease in the number of small dairies, total dairy production is increasing due to the number of large dairies increasing. Adapted from NASS (2002).

United States dairies are also becoming more efficient which means more milk is being produced per cow as demonstrated by Figure 2.4. The increased efficiency of dairy

operation is due to increased research in the areas of animal diets and improved milking systems.

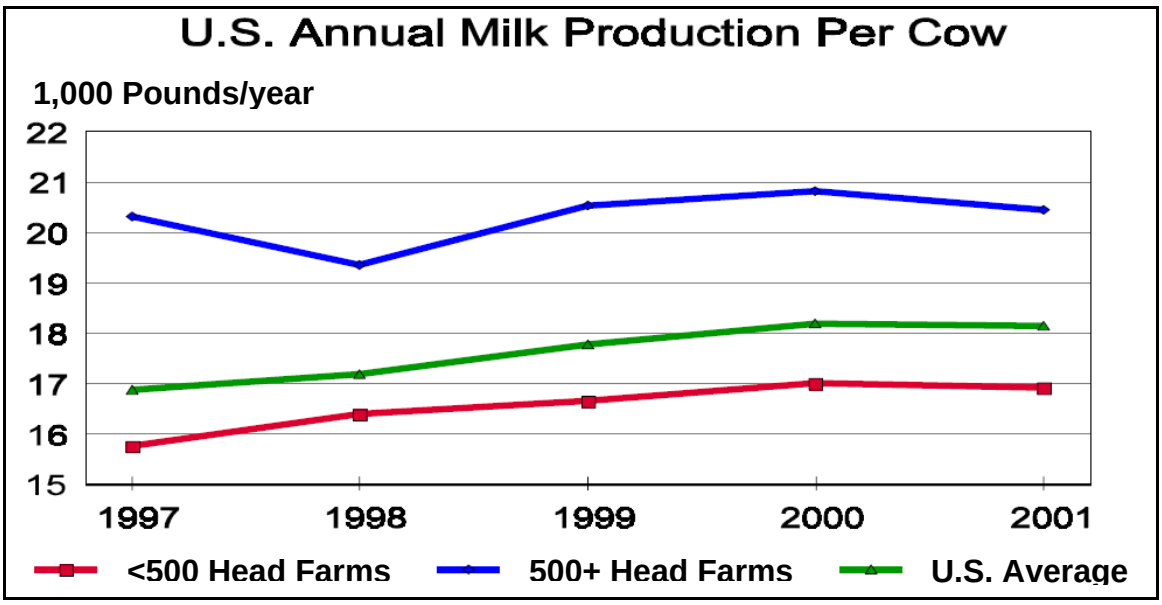

Figure 2.4: U.S. annual milk production per cow. Increased dairy efficiency leads to higher milk production per head of cow. Adapted from NASS (2002).

Figures 2.5, adapted from NASS (2002), illustrates the movement of dairies to the west. Note that the Midwest has seen a decline in the number of dairies, while the western states have seen a general increase in the number of dairies. Also note that the total milk production has increased in the western states. Note that the number of dairies in Iowa and the Dakotas has decreased, but the amount of milk produced in those states has either increased or stayed relatively unchanged. This further attests to how dairy production has become more efficient. Washington, Nevada, Oklahoma, and Montana also demonstrate this trend.

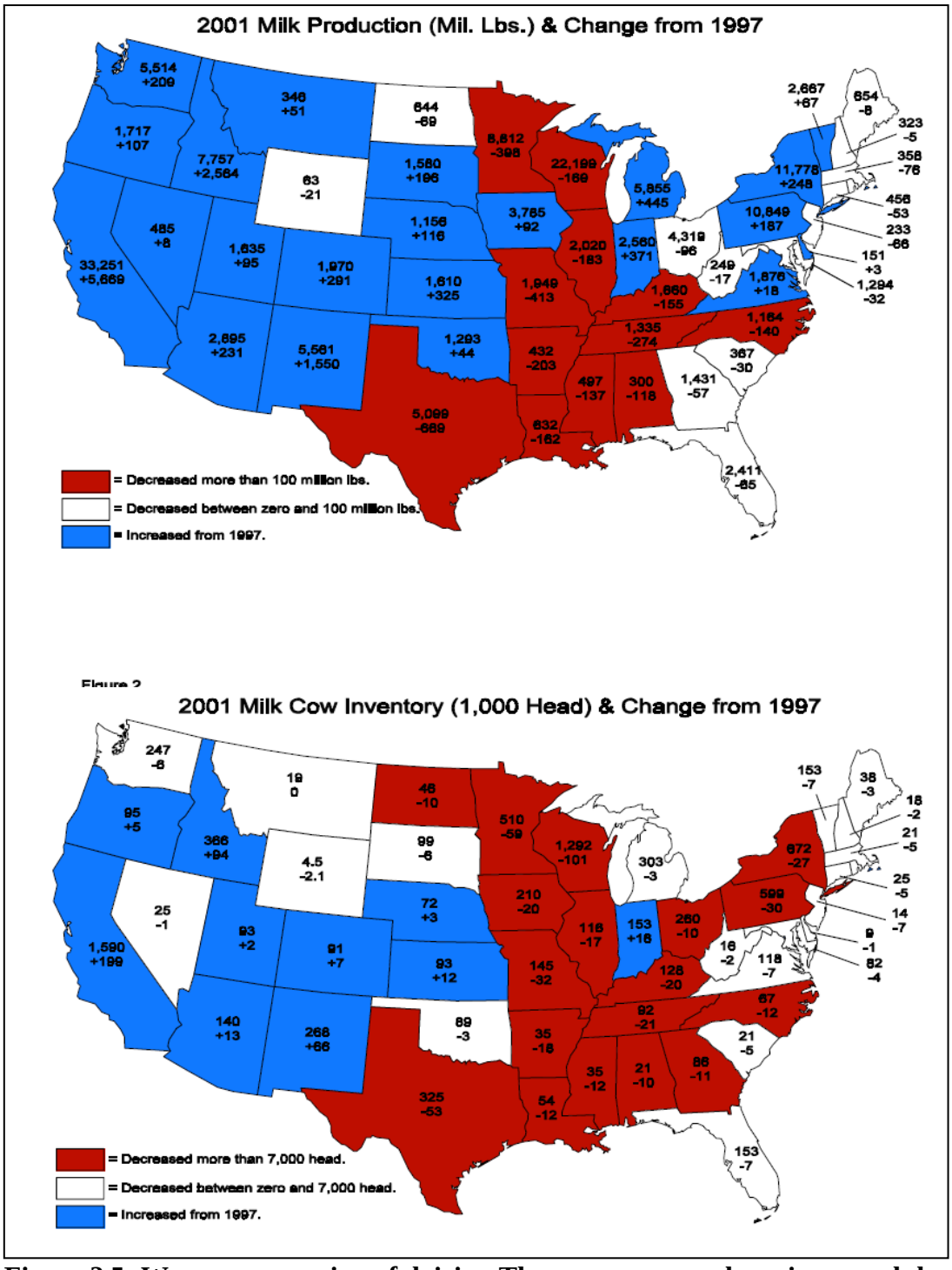

Figure 2.5: Western expansion of dairies. The western states have increased the number of dairies and the amount of dairy production. The Midwest states have decreased the number of dairies, but some have increased the total dairy production. This demonstrates how dairy efficiency has improved. Adapted from NASS (2002).

Although this work is primarily concerned with biomass derived from dairy manure, this is not the sole source for biomass (Volk, et al., 2002). Biomass can also come from agricultural crop residues, energy plantations, and municipal and industrial wastes. Biomass is considered to be both a renewable fuel and a carbon neutral fuel. Although combustion of biomass does release carbon into the atmosphere, this carbon is in turn used by vegetation to create more biomass. Thus, the net carbon balance remains approximately level.

NO_x causes lung deterioration and affects blood hemoglobin which deprives the body of oxygen. NO_x also plays a role in altering ozone levels. NO_x is absorbed in the atmosphere to create acid rain. (Annamalai and Puri, 2007) CO is a poisonous gas which can be fatal to humans.

Lundgren (2002) studied using horse manure from ranches for on site heat production. He found that the horse manure could be effectively disposed of by firing it in a small burner and the heat created could be used for on site purposes. The primary draw back to this technique was the elevated NO_x emissions. Lundgren reported 370 mg/m^3 of NO_x at 10% excess O_2. He did not discuss any rich combustion results.

Miller et al. (2002) has cofired LB with coal. The primary focus of his research was rendering chicken fat into a useable fuel. However, he has provided detailed ash analyses for several different cofired fuels. His work suggests that DB has a higher energy content than FB and both CB have higher energy content than LB.

Table 2.1 summarizes the feed rates of coal and various forms of biomass Miller used in cofiring experiments in his 200 million BTU/hr furnace.

Table 2.1: Firing rates of fuels investigated by Miller. (2002)

Feedstock	Maximum Firing Rate (kg/hr AR)	Maximum Thermal Input (kW)
Coal	36744	46389
Sewage Sludge	1720	139
Swine Manure	1576	34.2
Dairy Manure	8378	3107
Beef Manure	650	277
Sheep Manure	168	85.1
Covered Barn Manure	741	149
Reed Canary Grass	377	108
Plastics	1.32	3.37
Wood Chips/Shavings	12566	8323

The full fuel properties and ash analysis of fuels used by Miller are presented in Table 2.2. Of particular note is that all of the biomass fuels are higher in moisture than the coal. On a DAF basis, the manure biomass and AB fuels are higher in VM than coal. This is typical of most AB fuels. All of the biomass fuels are lower in FC than the coal. The AB fuels have less nitrogen than the coal. Hence, the AB fuels being higher in volatiles and lower in nitrogen help contribute to NO_x mitigation when the AB fuels are cofired with coal.

Table 2.2: Proximate, ultimate, and ash analyses of fuels investigated by Miller. (2002)

	Cofire Coal	Pine Shavings	Reed Canary Grass	Sheep Manure	Dairy Free-Stall	Dairy Tie-Stall Manure	Misc. Manure	Poultry Litter
Moisture	5.0	45.0	65.2	47.8	70.3	69.8	50.5	20.0
Proximate analysis (wt.%, db)								
Volatile matter	24.16	84.7	76.1	65.2	30.6	30.1	21.8	55.3
Ash	14.70	0.1	4.1	20.9	62.3	62.5	73.5	17.0
Fixed carbon	61.14	15.2	19.8	14.0	7.1	7.4	4.8	7.7
Ultimate analysis (wt. %, db)								
Carbon	72.75	49.1	45.8	40.6	22.1	22.6	19.6	38.1
Hydrogen	3.91	6.4	6.1	5.1	2.9	2.9	2.5	5.6
Nitrogen	1.50	0.2	1.0	2.1	1.1	1.1	1.0	3.5
Sulfur	2.27	0.2	0.1	0.6	0.1	0.1	0.1	0.6
Oxygen	4.87	44.0	42.9	30.7	11.5	10.8	3.3	30.9
HHV (Btu/lb, db)	13,118	8,373	7,239	6,895	3,799	8,203	3,114	6,399
Bulk density (lb/ft^3)	--	11.9	3.12	23.1	50.5	50.5	43.7	--
Ash Analysis (wt.%)								
Al_2O_3	25.34	13.4	1.66	3.08	0.96	2.26	1.34	9.14
BaO	--	0.15	0.05	0.05	0.02	0.02	0.01	0.05
CaO	2.28	8.75	9.57	12.8	6.38	23.3	3.44	12.7
Fe_2O_3	18.34	5.94	1.47	1.95	1.29	1.37	0.93	4.04
K_2O	2.22	4.94	18.1	23.4	6.75	10.7	1.77	9.94
MgO	0.82	3.35	5.29	5.74	2.65	8.91	1.06	4.01
MnO	--	0.49	0.11	0.17	0.17	0.14	0.03	0.36
Na_2O	0.25	1.38	2.34	4.64	1.32	7.04	0.88	3.60
P_2O_5	0.4	1.44	13.8	9.21	2.90	14.7	2.54	14.0
SiO_2	48.2	57.2	43.0	29.3	74.98	26.0	84.82	39.4
SO_3	0.67	0.05	0.02	5.52	0.04	0.14	0.01	2.58
SrO	--	0.80	0.11	0.03	0.10	0.11	0.14	0.03
TiO_2	--	1.16	4.99	0.20	2.06	5.08	1.20	0.51

Tillman (2000) has investigated cofiring coal with all forms of biomass for several years for the Foster Wheeler Corporation. One of the most important topics he has studied is emissions mitigation through use of biomass. The results from Tillman's experiments on cofiring coal and biomass are summarized as follows:

1. blends of wood waste and coal will flow through bunkers to pulverizers or cyclone feeders with minimum bridging;
2. blends of wood waste and coal can be stacked and stored outside through summer months and, if the piles are constructed correctly, spontaneous combustion will not occur;
3. blends of wood waste or switchgrass and coal can be burned with minimum impact on boiler operations; the blend may be largely transparent to the boiler operator if the percentage of biomass in the blend is low;
4. there are no technical show stoppers to cofiring biomass fuels with coal in existing boilers, although there are efficiency and emissions impacts and there can be capacity impacts.
5. The parametric test experience further documented the following impacts when cofiring biomass with coal:
    - reduced boiler efficiency, with the reduction being manageable;
    - reduced NO_x emissions, with reductions greater than originally expected;
    - reduced fossil CO_2 emissions, typically on the order of 3.15 ton fossil CO_2 avoided per ton of biomass burned;

- The NO_x emissions reductions, for all major tests, expressed on a percentage basis, were combined to yield the following approximation equation:

$RNO_x = 0{:}75B$; Eq. 2.2

where RNO_x is the percentage reduction in NO_x emissions, and B is the percentage of biomass in the blend. The R^2 for Eq. 2.2 is 0.78. Another form of this NO_x reduction equation is:

$RNO_x = 0{:}0008C^2 + 0{:}0006C + 0{:}075$; Eq. 2.3

where C is the percentage biomass cofiring on either a caloric or BTU basis. The R^2 for Eq. 2.3 is 0.72. The NO_x benefit is disproportional to the fuel input on a caloric basis, up to some maximum biomass input.

Figure 2.6 demonstrates the synergistic effects of cofiring coal with biomass on NO_x emissions.

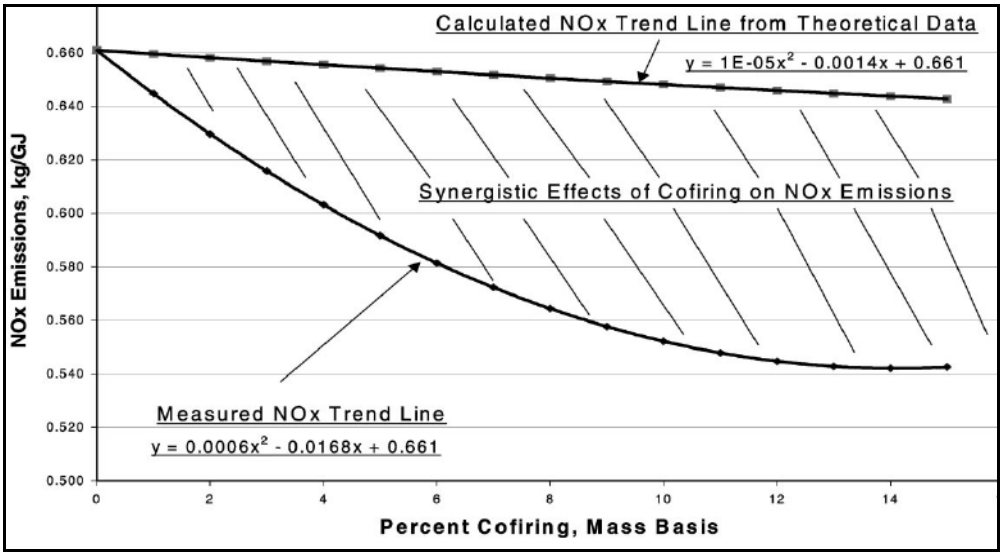

Figure 2.6: Tillman's (2000) NO_x reduction from cofiring coal with AB fuels. Note the measured NO_x trend line is lower than the predicted NO_x trend line.

Schmidt (2003) conducted an extensive study on biomass recovery opportunities for the utility industry. Table 2.3 helps identify promising biomass options by showing how much biomass is available. The first column gives the amount of manure produced. The second column gives the percentage of manure that can be collected. The third column gives the amount of manure that can be collected per animal per year. This table does not take into account the numbers of each animal. Note that of all forms of animal manure, dairy manure is the most plentiful on a per animal basis. This is due in large part to larger animal size, and high forage ratios that are lower in digestibility than a higher concentration ratio.

Di Nola (2007) used an FTIR instrument to measure the concentrations of HCN and NH_3 in the early flame stages of flames fired with coal and coal:LB blends. His work showed that coal alone can produce upwards of 700 ppm of HCN and approximately 80 ppm of NH_3. When 20% by mass LB was blended with the coal, HCN decreased to approximately 250 ppm and NH_3 increased to approximately 200 ppm. These experiments demonstrated that cofiring coal with LB has the potentially to reduce the formation of NO_x because it is known the high concentrations of HCN work to produce NO_x, whereas high concentrations of NH_3 work to reduce NO_x.

There is no previous research regarding cofiring DB with coal at the various equivalence ratios studied.

Table 2.3: Collectible quantities of dry manure available per animal. Adapted from Schmidt. (2003)

Collectible Tons of Dry Animal Manure			
Livestock	Tons Dry Manure Excreted/Animal/Year	Percent of Manure Collectible	Tons Dry Manure Collectible/Animal/Year
Cattle and Calves	0.73	100	0.73
Milk Cows and Dairy Cattle	2.13	80	1.704
Hogs and Pigs	0.27	100	0.27
Chickens	0.01644	100	0.01644
Sheep and Lambs	0.106	50	0.053

3. OBJECTIVE AND TASKS

The overall objective of the present research was to develop energy conversion technologies for utilization of CB. The specific objective of current work was to study combustion and emission behavior when DB is cofired with coal. In order to achieve the objective, the following tasks were preformed:

1. Obtain thermo-chemical characteristics of coals and DB fuels including ultimate and proximate analyses.
2. Conduct tests on pyrolysis characteristics of coals and DB fuels.
3. Grind coals and DB fuels and obtain particle size distributions.
4. Perform cofiring experiments under constant heat input
5. Obtain combustion and emissions characteristics.

4. EXPERIMENTAL SETUP AND PROCEDURE

4.1 Experimental Facility

All of the experiments were conducted using a 30 kW (100,000 BTU/hr) small scale furnace capable of firing most types of ground fuels. Solid fuel was fed at approximately 6.80 kg/hr (15 lb/hr). This furnace is part of the Coal and Biomass Laboratory of Mechanical Engineering at Texas A&M University. This facility operates with coal and coal:biomass blends and has been in operation for over 10 years. A schematic of the furnace is shown in Figure 4.1. Propane and natural gas (see Table 4.1 for composition) are used to heat the furnace to the operating temperature of 1100 C (2000 F). Type K (shielded, ungrounded) thermocouples are used to measure the temperature along the axial length of the furnace. These thermocouples provide a detailed temperature profile of the furnace throughout the combustion zone. A solid fuel hopper feeds coal and coal/biomass blends during experiments. Primary air is necessary to propel the solid fuel through the fuel line and to the furnace. Solid fuel comes out of the solid fuel line as a finely ground powder lightly dispersed in an air stream.

Table 4.1: Natural gas composition

Natural Gas Composition	
Component	Mole Fraction
Methane	94.45
Ethane	2.34
Propane	0.59
Isobutane	0.12
N-Butane	0.14
Isopentane	0.06
N-Pentane	0.04
Hexanes	0.12
Carbon Dioxide	1.69
Nitrogen	0.45
HHV (kJ/kg)	55304

At the base of the furnace, a probe is used to sample the flue gases. Prior to ventilation, all exhaust gases pass through a water-cooling spray to significantly lower the temperature of the gases. A sump pump pumps this water out of the furnace. More details are provided in Frazitta et al. (1999), Arumugam et al. (2006), and Annamalai et al. (2005).

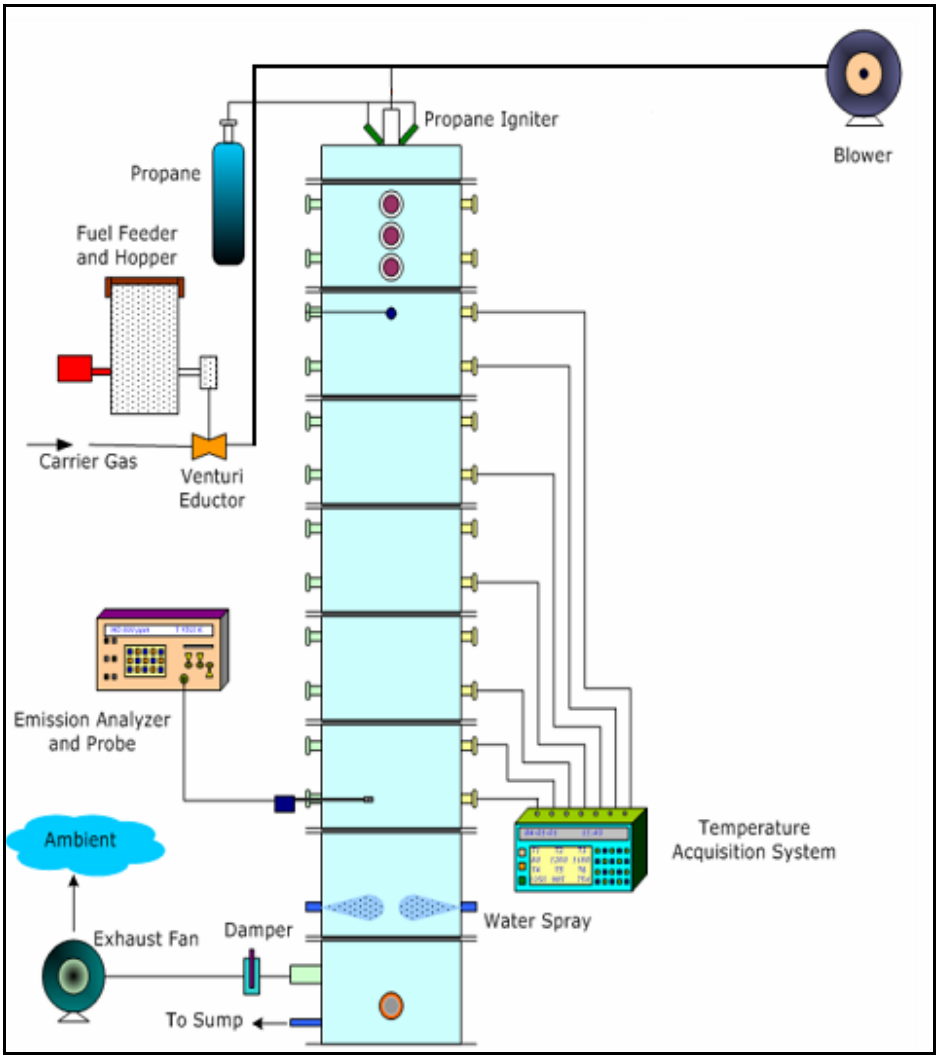

Figure 4.1: Schematic of boiler burner facility at Coal and Biomass Laboratory at Texas A&M University. (Annamalai et al., 2003a)

Thien (2002) built the current 100,000 BTU/hr furnace used. Figure 4.2 gives dimensions of the furnace.

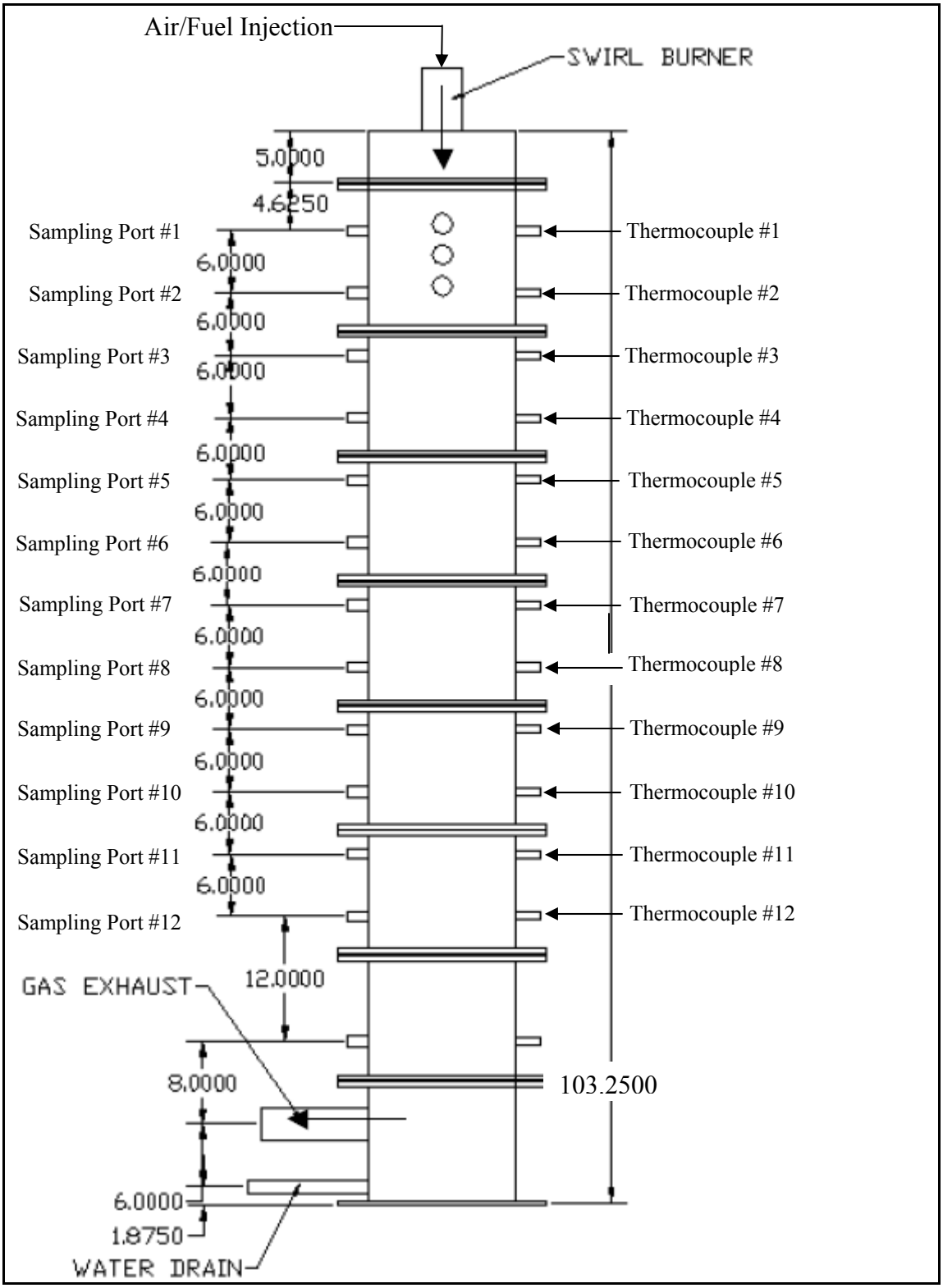

Figure 4.2: Dimensioned 100,000 BTU/hr furnace constructed by Thien (2002).

Figure 4.3 shows the cross section of one piece of the furnace. The refractory is made of greencast 94 ceramic. Table 4.2 following the figure gives the composition of greencast 94. The thermocouple ports are the same distance apart as the sampling ports: 6 inches. Also note that greencast 94 could react with SO_2 causing readings to be in error.

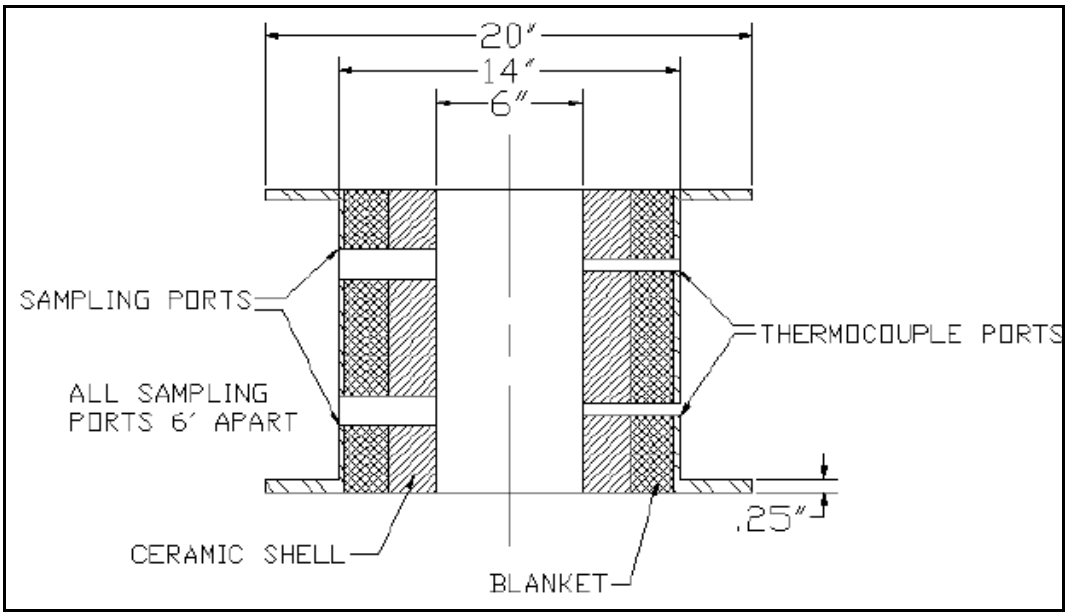

Figure 4.3: Dimensioned cross-section of greencast 94 refractory sections used in furnace. Adapted from Thien (2002).

Table 4.2: Composition of greencast 94. Adapted from Thien (2002).

Ingredient	Formula	Percent
Silica	SiO_2	0.2
Alumina	Al_2O_3	94.1
Titania	TiO_2	0.1
Iron Oxide	Fe_2O_3	0.2
Lime*	CaO	5.1
Magnesia*	MgO	0.1
Alkalies*	Na_2O+K_2O	0.2
* These alkaline oxides may react with SO_2		

The quarl at the top of the furnace is necessary to diffuse the coal and primary air into the secondary air stream and ensure sufficient mixing for thorough combustion. Figure 4.4 details the channels of the burner nozzle and swirlers which induce swirl to the secondary air. Table 4.3 details the parameters of the nozzle and gives the quarl angle of 24°.

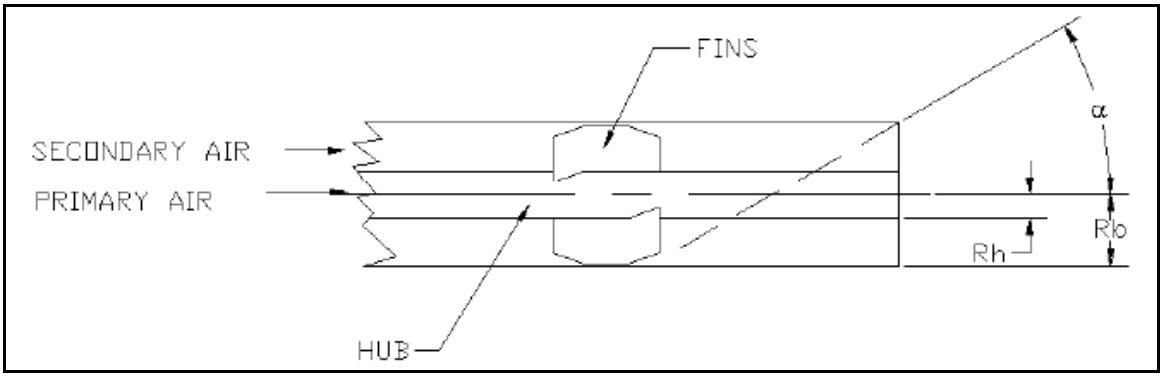

Figure 4.4: Detailed cross-section of fins used to mix primary and secondary air. Adapted from Thien (2002).

Table 4.3: Quarl and blade angle details. Adapted from Thien (2002).

Parameter	Value
Rh	0.0127m (.5in)
Rb	0.0206375m (.8125in)
Quarl Half Angle	24˚
Blade Angle	45˚
Swirl Number	0.7

4.2 Instrumentation

Flue gas concentrations were measured using an E-Instruments (2003) 8000 Portable Flue Gas Analyzer capable of detecting CO, CO_2, NO_x, SO_2, and O_2 in a flue gas stream. The analyzer uses electrochemical cells to detect flue gases in low range applications and NDIR in middle range applications.

Primary air flow measurements were made using Dwyer RMC Rate-Master Flow Meters. Two flow meters were used, one for motive air and one for eductor air. Each flow meter was calibrated to be accurate in the range of 20-200 SCFH of air with an accuracy of plus or minus 5 SCFH. Secondary air was measured using a Dwyer GFC Gas Mass Flow Controller. The flow meter was calibrated to be accurate in the range of 0-1000 SLPM of air with an accuracy of plus or minus 1.5% FS of the flow meter.

Appendix C gives an uncertainty analysis.

4.3 Experimental Procedure

The experimental procedure is as follows:

1. Secondary air flow is started.
2. A propane torch is used to fire natural gas into the furnace to heat the furnace to 650 C (1200 F) as indicated by thermocouple #1.

3. The air flow rate is gradually increased for about an hour until the flame is close to stoichiometric. This period is used to preheat the furnace.
4. At 650 C (as indicated by the first thermocouple), the propane line is shut off and the second half of the heating phase is done burning exclusively natural gas. Natural gas is used to heat the furnace to 1100 C. At this temperature, coal is able to self-ignite and maintain stable flame.
5. The natural gas line is closed and the solid fuel line and feeder air lines are opened. The solid feeder is turned on. The furnace is visually inspected to ensure that flame is still present. The thermocouple readings can also verify that a flame is present in the furnace.
6. From the known HHV of the fuel, the required fuel and air flow rates to obtain a 100,000 BTU/hr flame are calculated for all desired equivalence ratios.
7. The feeder and air lines are set to the proper flow rates for stoichiometric combustion.
8. The secondary air is adjusted to achieve the desired equivalence ratio. The primary air must stay at a constant value for all experiments. This is a requirement for the solid feeder to operate properly. The blower output can be increased to provide more secondary air.
9. After allowing 30 minutes for the furnace to stabilize, an initial analysis of the flue gases is taken to verify that the flame is at stoichiometric. The flue gas analyzer will require three minutes to self-calibrate and self-zero. After the initial start up, the analyzer is connected to the exhaust port.

10. This air flow rate is recorded as it will be used to calculate other air flow rates for all equivalence ratios.
11. After the reading at stoichiometric combustion has been recorded, the air flow rate can be adjusted to achieve any desired equivalence ratio. It is important to wait 10 minutes between readings to allow transients to dampen out.
12. Once all readings have been taken, the furnace is shut down by turning off the solid feeder and closing the feeder air lines. The secondary air line is cut to 100 L/min and the furnace to cools to ambient conditions.

5. RESULTS AND DISCUSSION

5.1 Introduction

This chapter presents the fuel properties for the four fuels considered. Fuel properties played a significant impact on the burnt fraction and the emissions created by combustion. In addition, this chapter presents the results from the cofiring experiments performed and discusses their role in evaluating the combustion performance of the fuels. The performance was evaluated by measuring combustion efficiency (burnt fraction) and the emissions levels of pollutants which include NO_x and CO. In addition, overall fuel nitrogen conversion efficiency to NO_x was also determined. The mercury emissions are presented elsewhere.

When BF is very high, near unity, it implies that all of the fuel was combusted. When fuel nitrogen conversion efficiency is very low, it means that most fuel bound nitrogen is converted to something other than NO_x. Unfortunately, optimizing one criterion is often at the expense of another criterion. To increase BF, typically fuel nitrogen conversion efficiency may be increased as well.

5.2 Fuel Properties

5.2.1 Proximate and Ultimate Analysis

All fuel samples were analyzed by Hazen Laboratories in Colorado for ultimate, proximate, and heat analyses. Table 5.1 presents the fuel properties. Note that the DB fuels are much higher in nitrogen than coal fuels. However, most AB fuels (e.g. saw dust, corn stalks, switch grass, nut shells, rice hulls, etc.) are lower in nitrogen than coal.

Manure based biomass is the exception to this generality. LA-PC-DB-SepS was almost 3 times richer in nitrogen than WYO. Both the DB fuels were higher in ash content than the coal fuels. The ash in HA-PC-DB-SoilS was more than 10 times more that of WYO. Although, LA-PC-DB-SepS was more than 4 times lower in ash than HA-PC-DB-SoilS, it was still higher in ash than either coal. The DB fuels contained less FC. The reduced FC for HA-PC-DB-SoilS caused the DB fuels to have a lower HHV. WYO had a 5.5 times larger HHV than HA-PC-DB-SoilS. The FC on a DAF basis was still low for HA-PC-DB-SoilS and lower even compared to LA-PC-DB-SepS.

TXL had the most sulfur, which is characteristic of a lignite coal. (Annamalai and Puri, 2007) WYO was lower in sulfur. It had less sulfur than LA-PC-DB-SepS, but more than HA-PC-DB-SoilS on a mass basis. On a heat basis, the biomass fuels had higher nitrogen and sulfur contents than coal.

Both of the biomass fuels had less moisture than either of the coals. This is due to the preparation of the biomass. Prior to grinding, the biomass fuels were composted for 90 days in a greenhouse. (Heflin and Sweeten, 2006) During the composting process, the biomasses were also air dried. Hence, specially prepared DB fuels contained less moisture. HA-PC-DB-SoilS had approximately the same amount of VM as the two coals. LA-PC-DB-SepS had almost twice the volatiles as HA-PC-DB-SoilS, TXL, or WYO.

The Boie HHV was the HHV predicted by the Boie equation (Annamalai and Puri, 2007):

$HHV(kJ * kg^{-1}) = 35160 * Y_C + 116225 * Y_H - 11090 * Y_O + 6280 * Y_N + 10465 * Y_S$. Eq. 5.2.1.

Table 5.1: Ultimate and proximate fuel properties.

	HA-PC-DB-SoilS	LA-PC-DB-SepS	TXL	WYO
Dry Loss (% Moisture)	12.21	25.26	38.34	32.88
Ash	59.89	14.86	11.46	5.64
FC	3.92	13.00	25.41	32.99
VM	23.99	46.88	24.79	28.49
Carbon, C	18.04	35.21	37.18	46.52
Hydrogen, H	1.45	3.71	2.12	2.73
Nitrogen, N	1.15	1.93	0.68	0.66
Oxygen, O (diff)	7.07	18.60	9.61	11.29
Sulfur, S	0.19	0.43	0.61	0.27
HHV (kJ/kg) As Received	4311.63	12844.17	14286.82	18193.02
HHV (kJ/kg) Dry	4911.11	17185.90	23169.07	27106.57
HHV (kJ/kg) DAF	15452.02	21449.85	28459.80	29593.38
HHV (kJ/kg of stoich Air) AR	1931.41	2886.07	3155.51	3191.89
Boie HHV (kJ/kg)	7340.86	14799.49	14582.32	18347.96
A:F AR	2.23	4.45	4.53	5.70
A:F DAF	8.00	7.44	8.77	9.22
FC DAF	14.04	21.72	50.62	53.66
VM DAF	85.96	78.28	49.38	46.34
Ash kg/GJ	138.90	11.57	8.02	3.10
Nitrogen kg/GJ	2.67	1.50	0.48	0.36
Sulfur kg/GJ	0.43	0.33	0.42	0.15

5.2.2 Fuel Particle Size Distribution

Table 5.2 gives the Rosin-Rammler parameters for the fuels considered. Appendix A explains how the fuels were analyzed for size distribution and defines the variables in Table 5.2. Note that the coals had a larger SMD than the DB fuels. The dirt that got collected with the DB fuels passed through all of the sieves and collected in the pan. This caused the DBs to have a smaller SMD. The larger SMD of the coals caused clogging difficulties.

Table 5.2: Size distribution parameters.

Size Distribution Parameters				
	TXL	WYO	LA-PC-DB-SepS	HA-PC-DB-SoilS
n	1.2991	1.4369	1.0934	1.2612
b	0.000934	0.00042	0.0024	0.0013
SMD (microns)	396	396	96.7	91.6

5.2.3 Thermogravimetric Analysis

Thermogravimetric analyses on the coal and DB fuels were performed using a TA SDT Q600 TGA-DSC instrument. A10 mg fuel sample was heated at 20 K/min from ambient to 1573 K in an inert (nitrogen environment). The mass of the sample as a function of temperature was recorded. All fuels were analyzed as received.

A reference pan was also heated in the same furnace at the same rate. The temperature of the reference pan was recorded with the temperature of the sample pan. The difference in the temperatures between the two pans can be used to create a DTA trace. Figures 5.1 through 5.4 give the TGA and DTA traces for the fuels considered. Point A marks the beginning of the traces. Point B marks the peak of the drying

(endothermic) process. Point C marks the beginning of the pyrolytic exotherm. Point D marks the peak of the pyrolytic exotherm. Point E marks the end of the pyrolytic exotherm. Following pyrolysis, the remaining fixed carbon and ash is heated. Point F marks the peak of this heating endotherm. Point G marks the end of the trace. A horizontal line has been added to the figures at 0.0 on the DTA scale. All portions of the trace above this line are exothermic and all portions below are endothermic.

Of particular interests are the temperatures at which pyrolysis began, ended, and the percentage of mass lost due to pyrolysis. The portion between points A and B on the TGA trace defines the amount of mass lost do to drying (moisture loss). The portion between points C and E on the TGA trace defines the amount of mass lost due to pyrolysis. The peak of the DTA trace has been marked. This is the point of maximum mass lost during pyrolysis. The temperature and remaining mass at this point have been marked on the figures. Table 5.3 summarizes the data.

TGA analysis can also be used to determine the ignition temperature of a fuel when experiments are performed in air. Each fuel was first analyzed in a nitrogen environment and then analyzed again in an air environment. The TGA traces of the two fuels began similar, but upon ignition, the fuel would oxidize if air was present. Ignition caused the two TGA traces to deviate. The temperature at which this deviation occurred was defined as the ignition temperature. Figure 5.5 presents a trace illustrating fuel ignition. The ignition temperatures of the fuels are also included in Table 5.3. The DTA traces of TXL and WYO look similar. The portions of the trace that are below 0.0 °C/mg are endothermic and the portions above are exothermic. The most significant

endothermic process occurred at approximately 373K. This was the drying process, which is known to be endothermic. Pyrolysis was an exothermic process. This agrees with combustion theory which says that all pyrolysis must be an exothermic process.

5.3 Experimental Parameters

TXL was used as the base case fuel. TXL and WYO were fired as blends with two DB fuels. Each coal was blended with each DB fuel in 100-0, 95-5, 90-10, and 80-20 blends on a mass basis. This created 14 different fuel blends. For each blended fuel, the equivalence ratio was varied from 0.8 to 1.2 in 0.1 increments. The 80-20 blends were too rich in DB to be used in industrial applications, but were used in order to get more data points for the study. In the rich regime (equivalence ratio > 1.0) the HA-PC-DB-SoilS quickly clogged the sampling port due to high ash content. Thus, a full set of data points could not be generated.

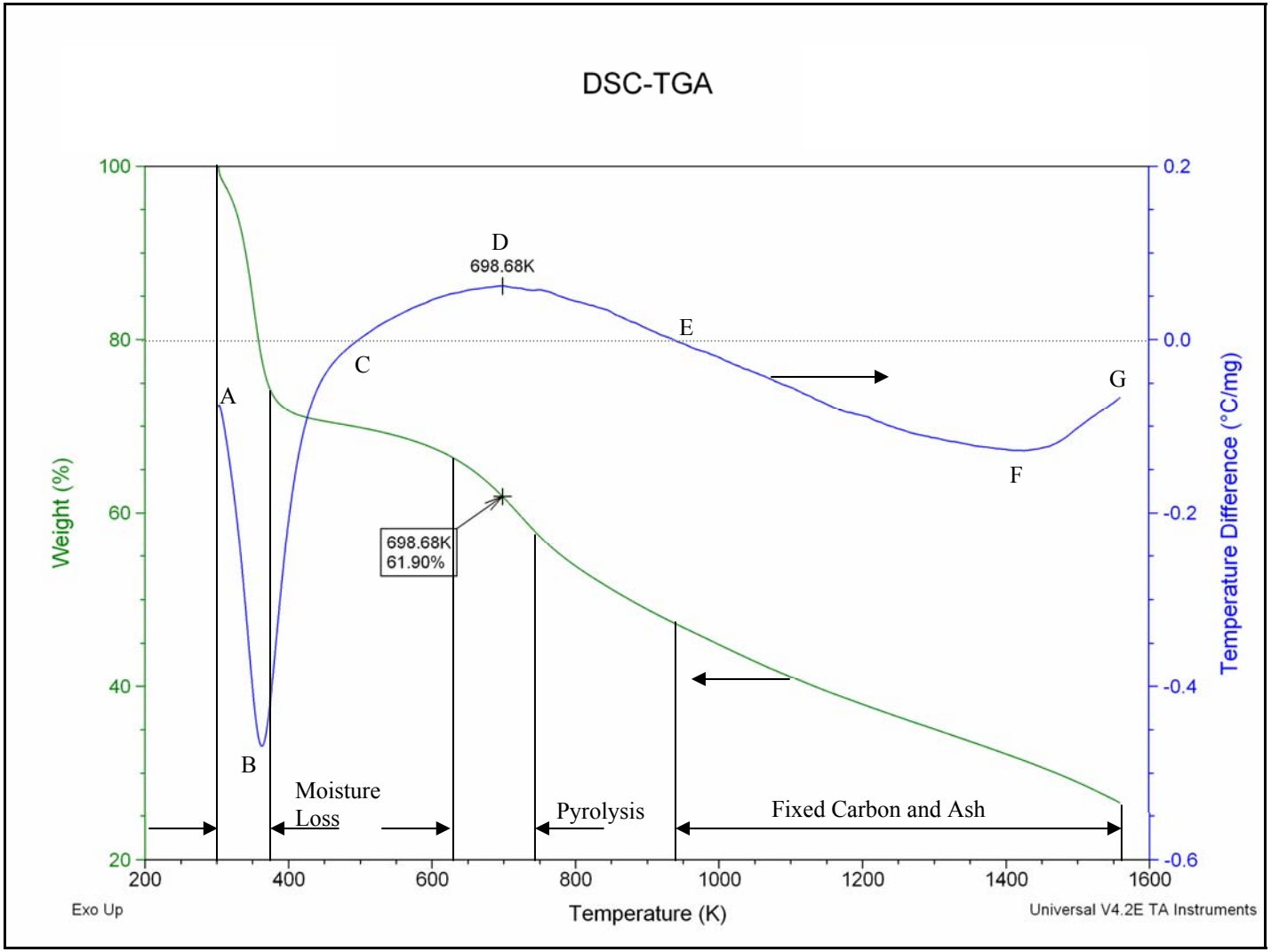

Figure 5.1: TGA and DTA trace of TXL.

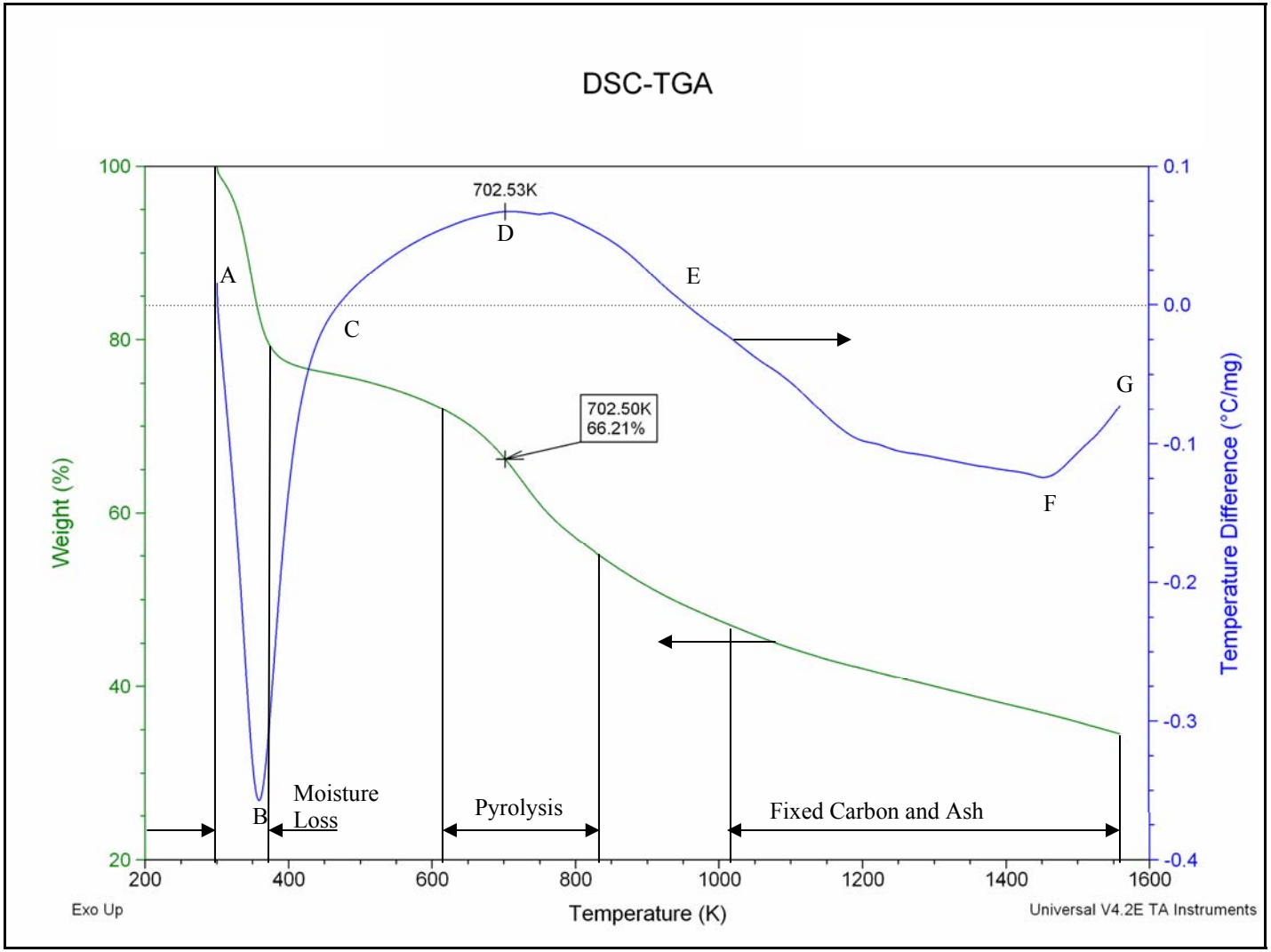

Figure 5.2: TGA and DTA trace of WYO.

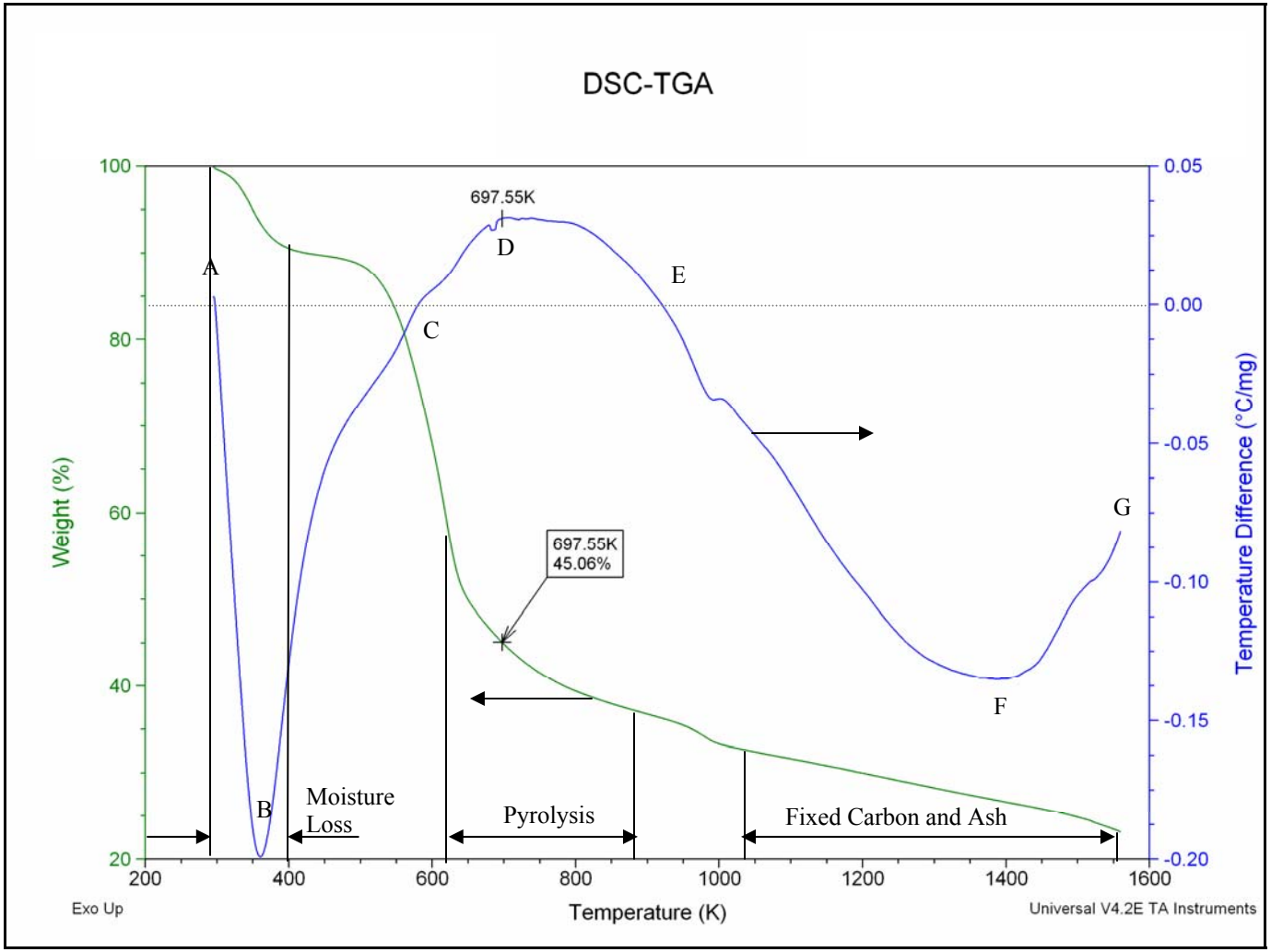

Figure 5.3: TGA and DTA trace of LA-PC-DB-SepS. Note the data labels showing the peak of the DTA curve and the corresponding mass percent at that temperature.

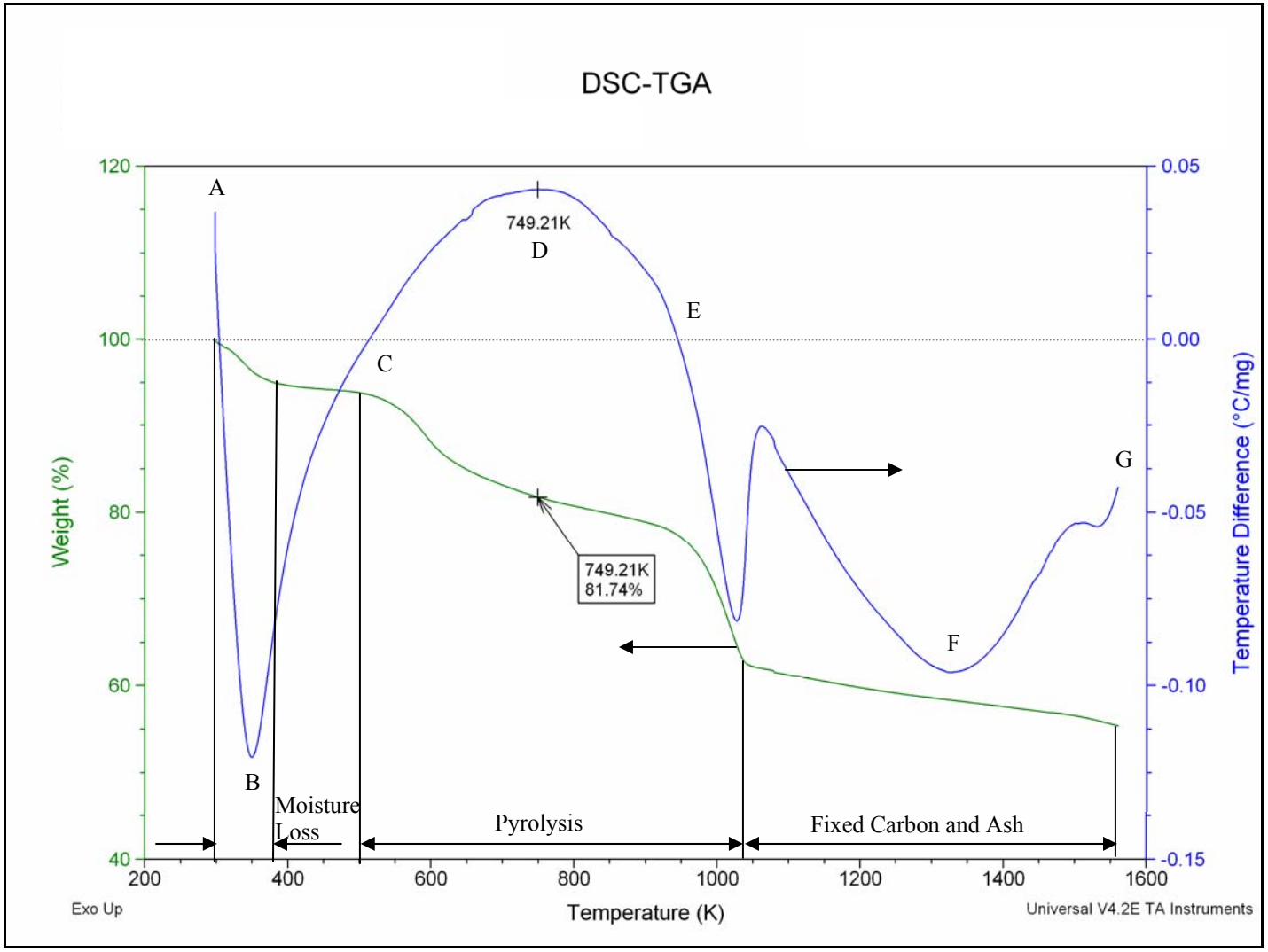

Figure 5.4: TGA and DTA trace of HA-PC-DB-SoilS.

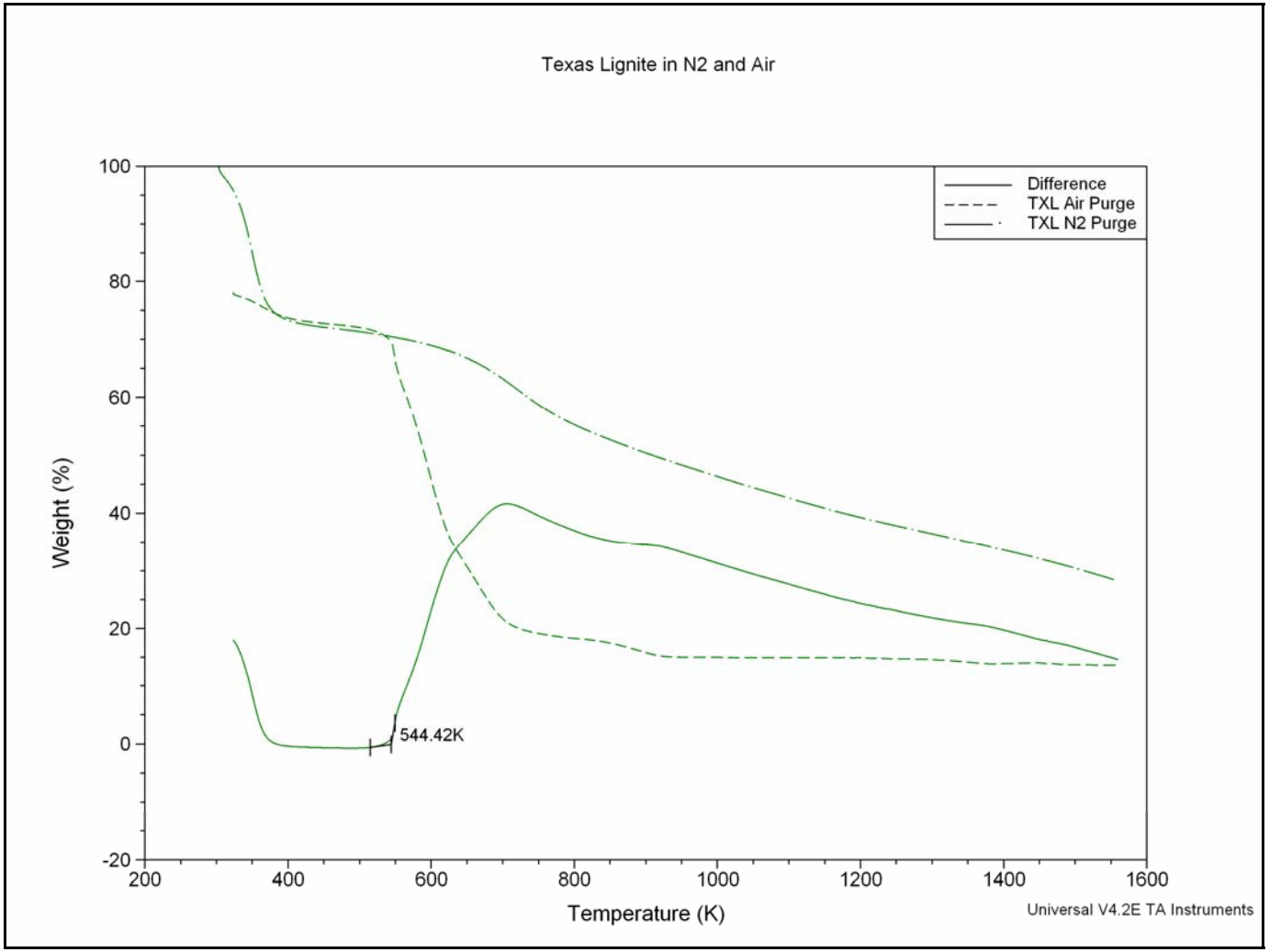

Figure 5.5: Example of ignition of TXL coal. Ignition is the point where the difference curve begins to deviate from 0%.

Table 5.3: TGA analysis of fuels.

Fuel	TXL	WYO	HA-PC-DB-SoilS	LA-PCDB-SepS
Moisture Loss Onset Temperature (K)	373.09	375.71	367.45	386.19
Moisture Mass (%)	24.12	20.92	4.678	8.89
Pyrolysis Loss Onset Temperature (K)	637.93	657.15	529.23	513.6
Pyrolysis Mass (%)	18.95	21.01	32.53	56.01
10% of Pyrolysis Mass (%)	1.895	2.101	3.253	5.601
Mass at 10% of Pyrolysis Mass (%)	73.985	76.979	92.069	85.509
10% Pyrolysis Mass Loss Temperature (K)	661.11	685.44	552.99	536.27
90% of Pyrolysis Mass (%)	17.055	18.909	29.277	50.409
Mass at 90% of Pyrolysis Mass (%)	58.825	60.171	66.045	40.701
90% Pyrolysis Mass Loss Temperature (K)	748.78	759.83	1021.28	766.89
Peak Pyrolysis Mass (%)	61.9	66.21	45.06	81.74
Peak Pyrolysis Temperature (K)	698.68	702.5	697.55	749.21
FC and Ash Mass (%)	56.93	58.07	62.792	35.1
FC and Ash Loss Onset (K)	774.07	786.56	1037.1	990.95
Ignition Temperature (K)	544.42	571.78	509.43	526.06

Primary air was provided from a compressed air line and was used to carry solid fuel to the burner nozzle. The amount of primary air was dictated by the feeder and was constant at 5.95 m^3/hr (15 - 25% of total air). However, secondary air (75 – 85% of total air) was provider by a separate compressed air line and could be adjusted to change the equivalence ratio. Table B.1 in the Appendix gives fuel and air flow rates for TXL and TXL:DB blended fuels. Table B.2 in the Appendix gives the equivalents blends on a heat basis. Table B.3 in the Appendix gives fuel and air flow rates for WYO and WYO:DB blended fuels. Table B.4 in the Appendix gives the equivalent blends on a heat basis. Note that on a heat basis, the percent of heat attributed to each fuel type was much less compared to percent mass basis. For example: for the 80:20 WYO:HA-PC-DB-SoilS fuel, 80% of the mass was WYO, but more than 94% of the heat came from WYO. All fuel and air flow rates were calculated from a program developed by Goughnour (2006). Combustion any leaner than 0.8 created a heavy strain on the compressor and was also useless for industrial applications.

Note that for pure coal and coal:biomass blends, the fuel flow rates and air flow rates remained relatively constant at the same equivalence ratio. This is in agreement with combustion theory. (Annamalai and Puri, 2007) The coal:biomass blends needed slightly more fuel in order to compensate for the lower energy content of biomass. Also note that the HHV on a stoichiometric air basis is roughly constant (except for HA-PC-DB-SoilS).

5.4 Exhaust Gas Analysis

5.4.1 O_2 and Equivalence Ratio

5.4.1.1 TXL and TXL:DB Blended Fuels

The air fuel ratio, and hence the equivalence ratio, can be estimated from measured flow rates of air and fuel. It can also be computed using the measured O_2 percentage in the exhaust for lean mixtures. Appendix Table B.5 presents the oxygen mole fraction measured in the flue gas for TXL and TXL:DB blended fuels. Using O_2 percentage data the equivalence ratio of the exhaust stream was approximated by:

$\phi_{flue} \approx 1 - 4.76 * O_2$; Eq. 5.4.1.1 $\qquad \phi_{flue} < 1.0$ (Annamalai and Puri, 2007)

Equation 5.4.1.1 assumes that all the fuel has been gasified. If large particles are not gasified, the O_2 percentage will increase. This will cause the ϕ based on exhaust gases to decrease. Figure 5.6 plots the ϕ_{flue} computed from flue gas analysis versus the ϕ_{flow} computed from air and fuel flow rates. It is seen that ϕ_{flue} is less than ϕ_{flow}. This indicates that the BF is less than 1.0. Also note that the ϕ_{flow} requires knowledge of the fuel flow rate. Due to limitations of the feeder, only average flow rates could be measured.

5.4.1.2 WYO and WYO:DB Blended Fuels

Appendix Table B.6 gives the oxygen concentration in the exhaust stream for WYO and WYO:DB blended fuels. Figure 5.7 presents the exhaust equivalence ratio for WYO and WYO:DB blended fuels. Ideally, the data points would follow a 45 line, indicating ϕ_{flue} and ϕ_{flow} were in perfect agreement. The real data points lie within the experimental uncertainty of each other. This indicates that the values are valid.

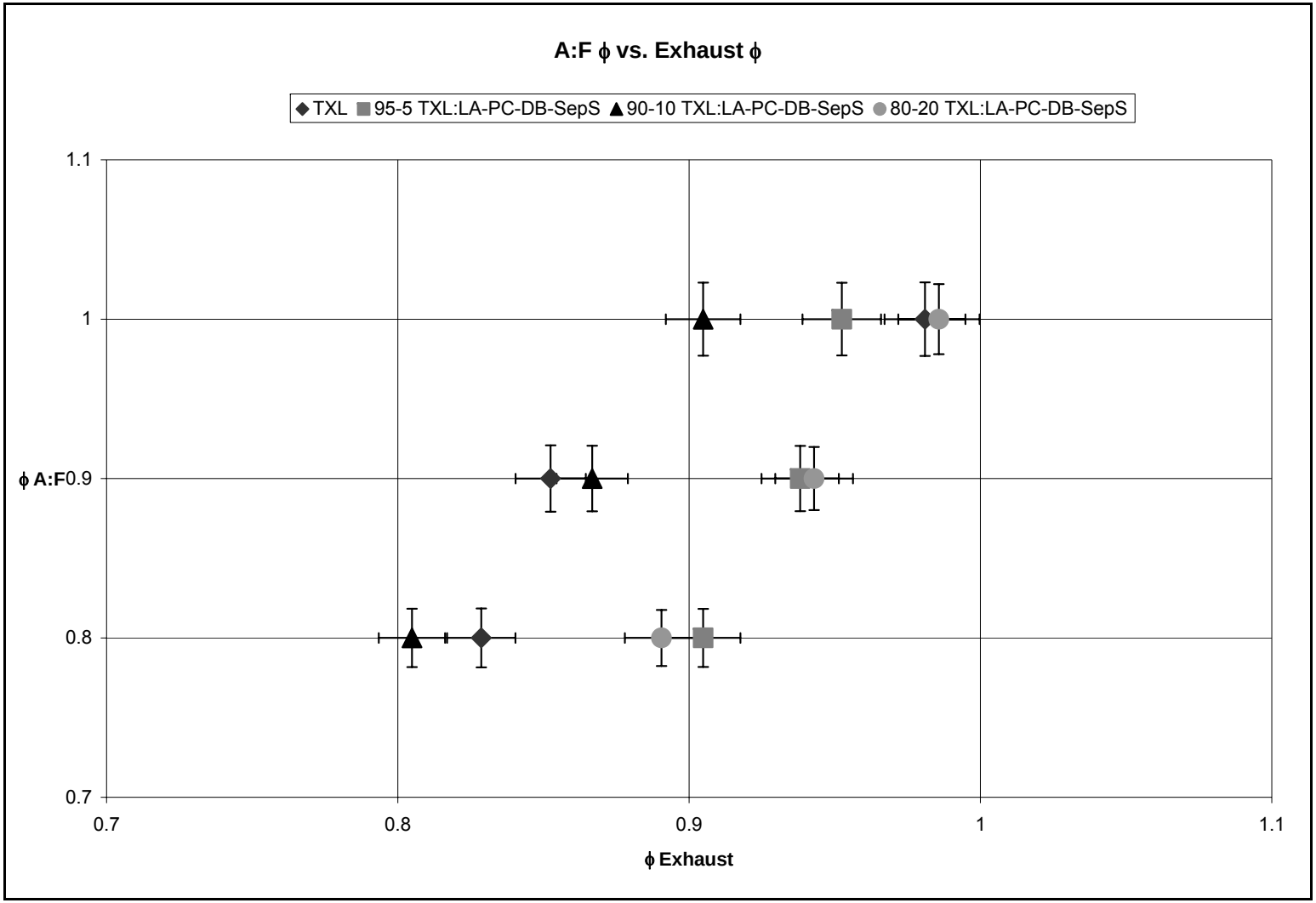

Figure 5.6: Equivalence ratio based on air flow rates and the calibrated fuel flow rate vs. equivalence ratio based on O_2% in exhaust for TXL and TXL:DB blended fuels.

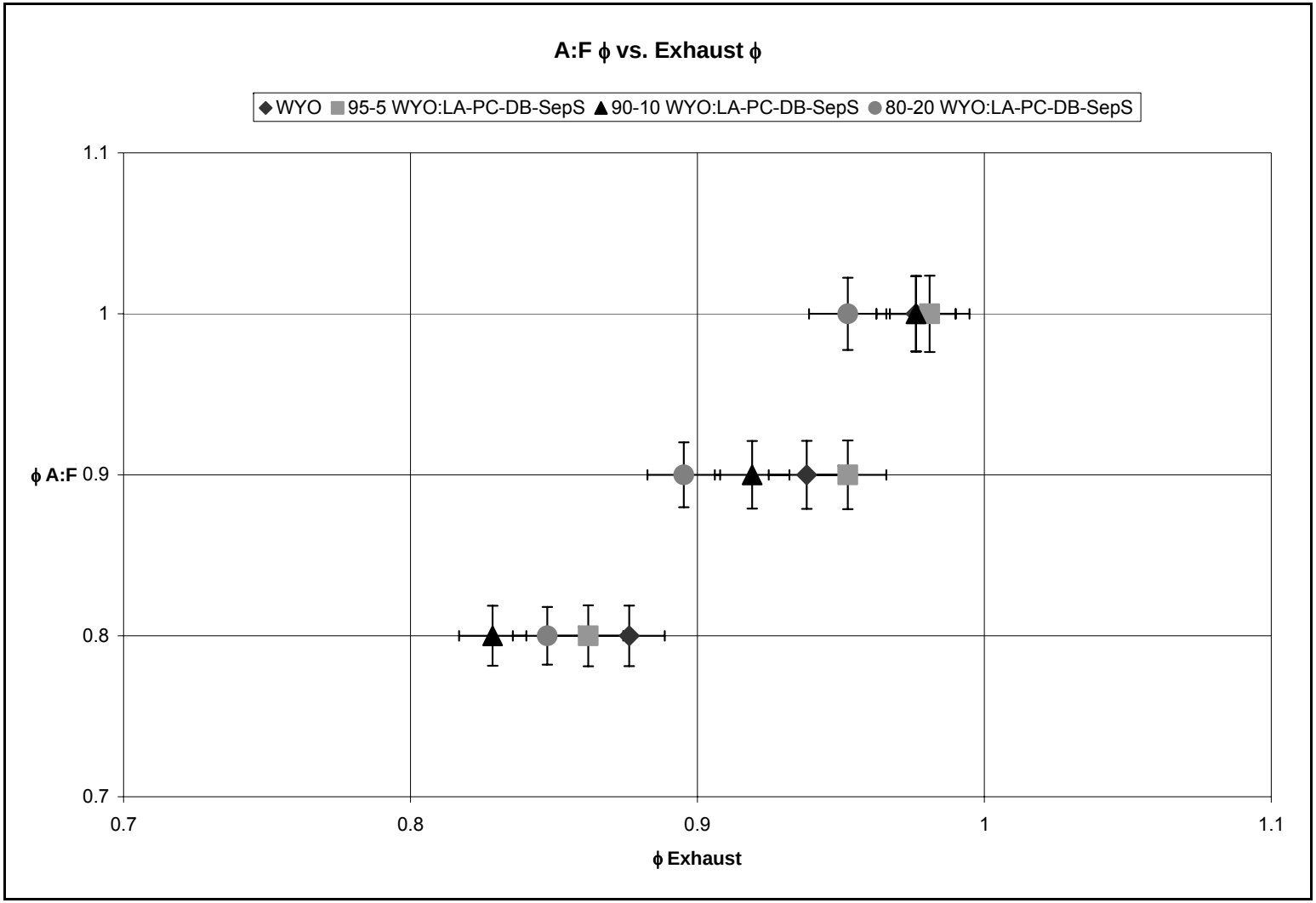

Figure 5.7: Equivalence ratio based on air flow rates and calibrated fuel flow rate vs. equivalence ratio based on O_2% in exhaust for TXL and TXL:DB blended fuels.

5.4.2 CO and CO_2 Emissions

5.4.2.1 TXL and TXL:DB Blended Fuels

Table B.7 in Appendix B lists CO and CO_2 emissions measured from experiments firing pure TXL coal and cofiring TXL:DB fuels. Very little CO was formed in the lean regime. In lean combustion, there is sufficient oxygen for all the carbon to fully oxidize to CO_2. However, once combustion became oxygen deficient (rich) CO begins to be formed. In general, the blended fuels produced more CO because the DB fuels contained more oxygen.

Figures 5.8 and 5.9 present the CO_2 and CO exhaust concentrations for TXL and TXL:DB blended fuels respectively. The equivalence ratio was based upon measured air and calibrated fuel flow rates. It is apparent that CO_2 peaked at approximately the stoichiometric condition. As air flow was increased from the stoichiometric point, the excess air diluted the flue gas concentrations. This dilution affect decreased the CO_2 percentage. On the other hand, if air flow was decreased below the stoichiometric air flow rate, less CO_2 was formed due to insufficient O_2 to oxidize fuel bound carbon. This, explains why the peak in CO_2 was at approximately stoichiometric.

In all future plots, the ϕ represents the equivalence ratio based on measured air flow rates and the calibrated fuel flow rate.

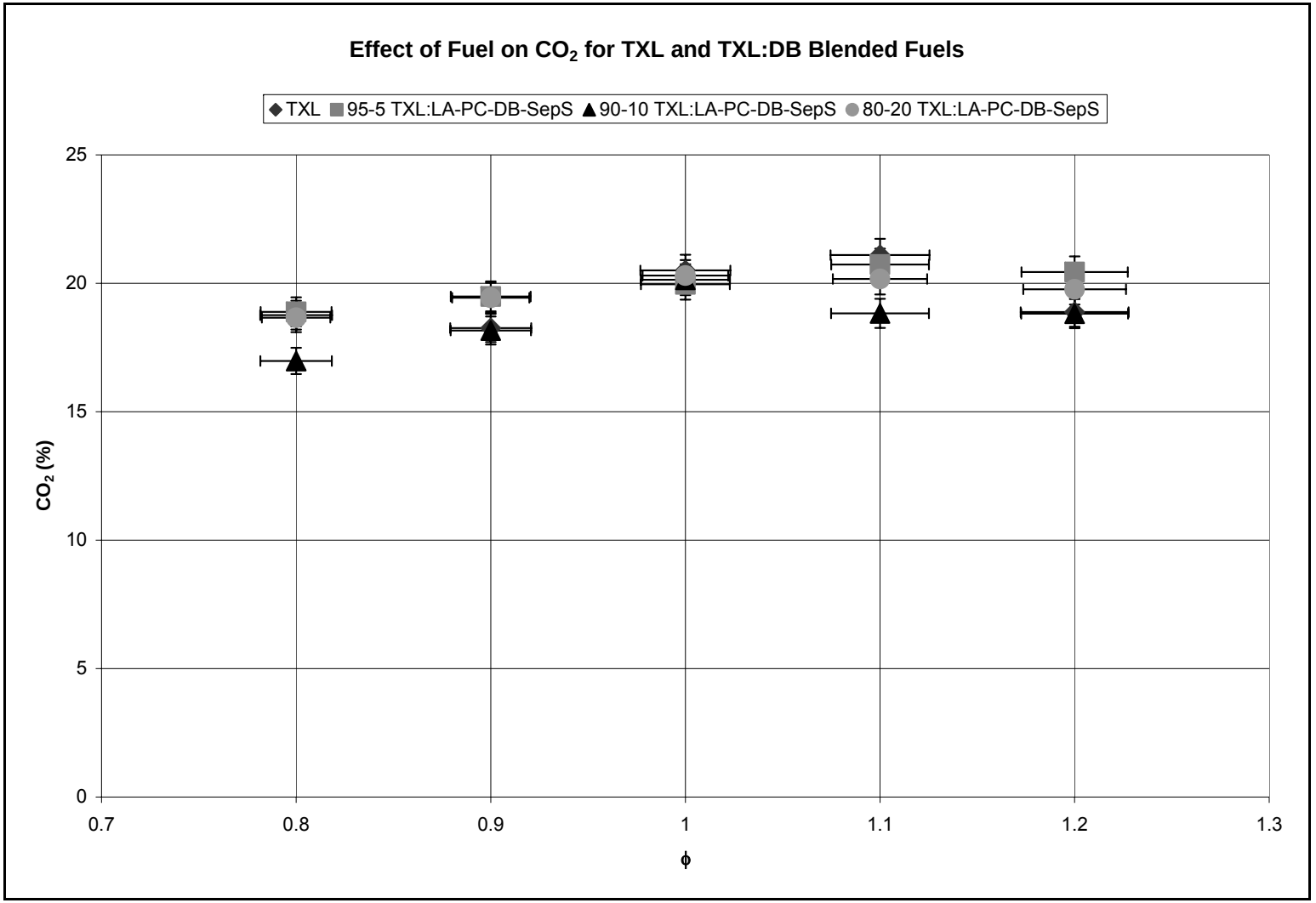

Figure 5.8: Effect of fuel on CO_2 for TXL and TXL:DB blended fuels.

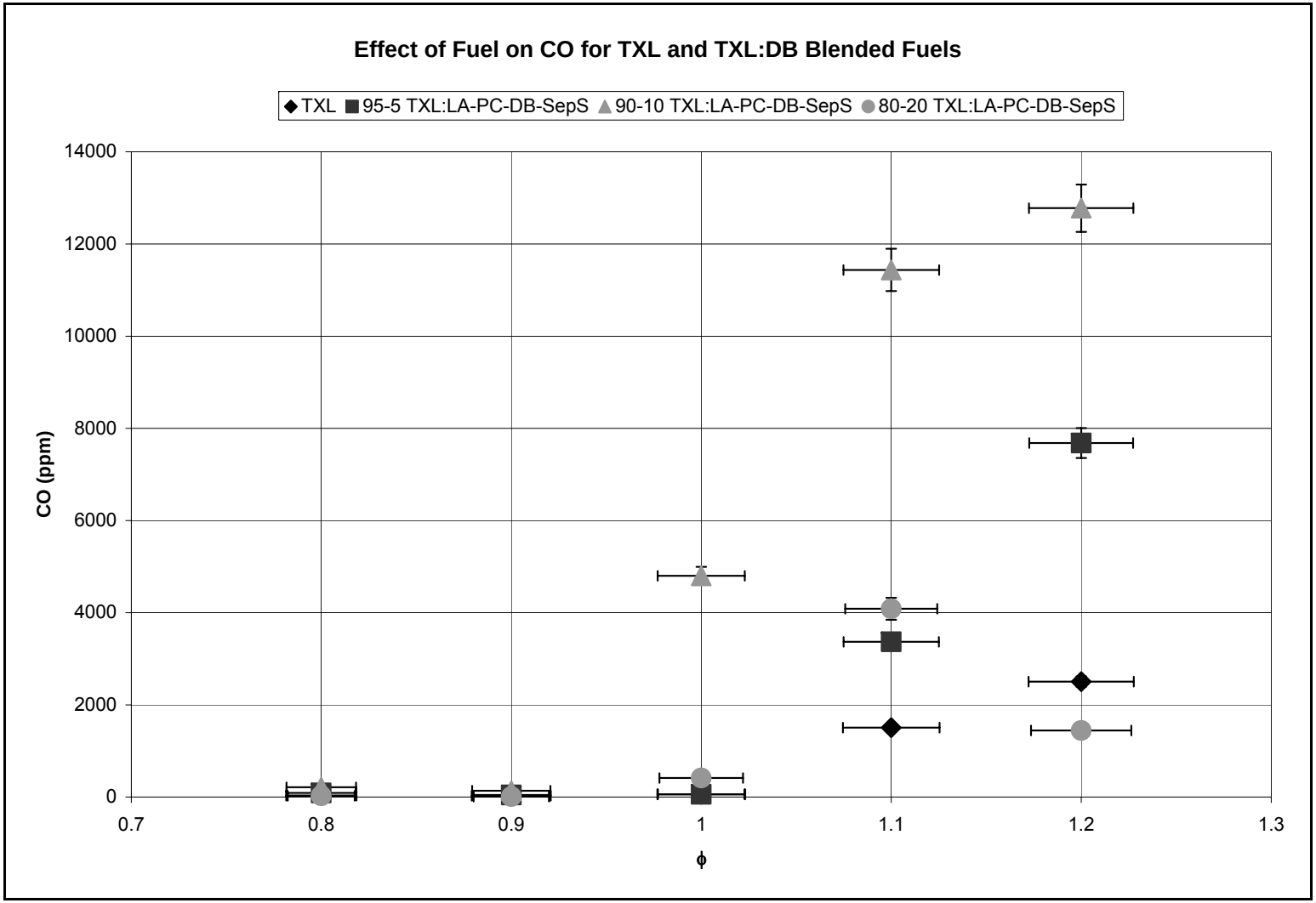

Figure 5.9: Effect of fuel on CO for TXL and TXL:DB blended fuels.

5.4.2.2 WYO and WYO:DB Blended Fuels

Table B.8 in Appendix B presents the CO_2 and CO emissions measured from experiments firing pure WYO coal and cofiring WYO:DB fuels. The trends were similar to those of TXL:DB blends. Figures 5.10 and 5.11 present the CO_2 and CO concentrations for WYO and WYO:DB blended fuels. The wider uncertainty bands for CO were due to the uncertainty in CO measurements being a percentage of the reading. The uncertainty bands overlap too much to draw any conclusions about the effect of blending coal with DB on CO production. The equivalence ratio was based upon air and fuel flow rates.

5.4.3 Burnt Fraction

5.4.3.1 Relation

Recall that O_2 in the exhaust is an indicator of ϕ used in experimentation. Thien (2002) derived an expression for the burnt fraction of a solid fuel can be approximated as:

$$BF \approx \frac{1}{\phi} * \left(1 - \frac{X_{O_2}}{X_{O_{2,A}}} \right); \text{ Eq. 5.6.1.1}$$

Where BF is the burnt fraction, ϕ is the measured equivalence ratio from flow rates, X_{O2} is the mole fraction of oxygen in the exhaust gases (dry basis), and $X_{O2,A}$ is the mole fraction of oxygen in the ambient air (dry basis). This equation can be used for rich or lean mixtures.

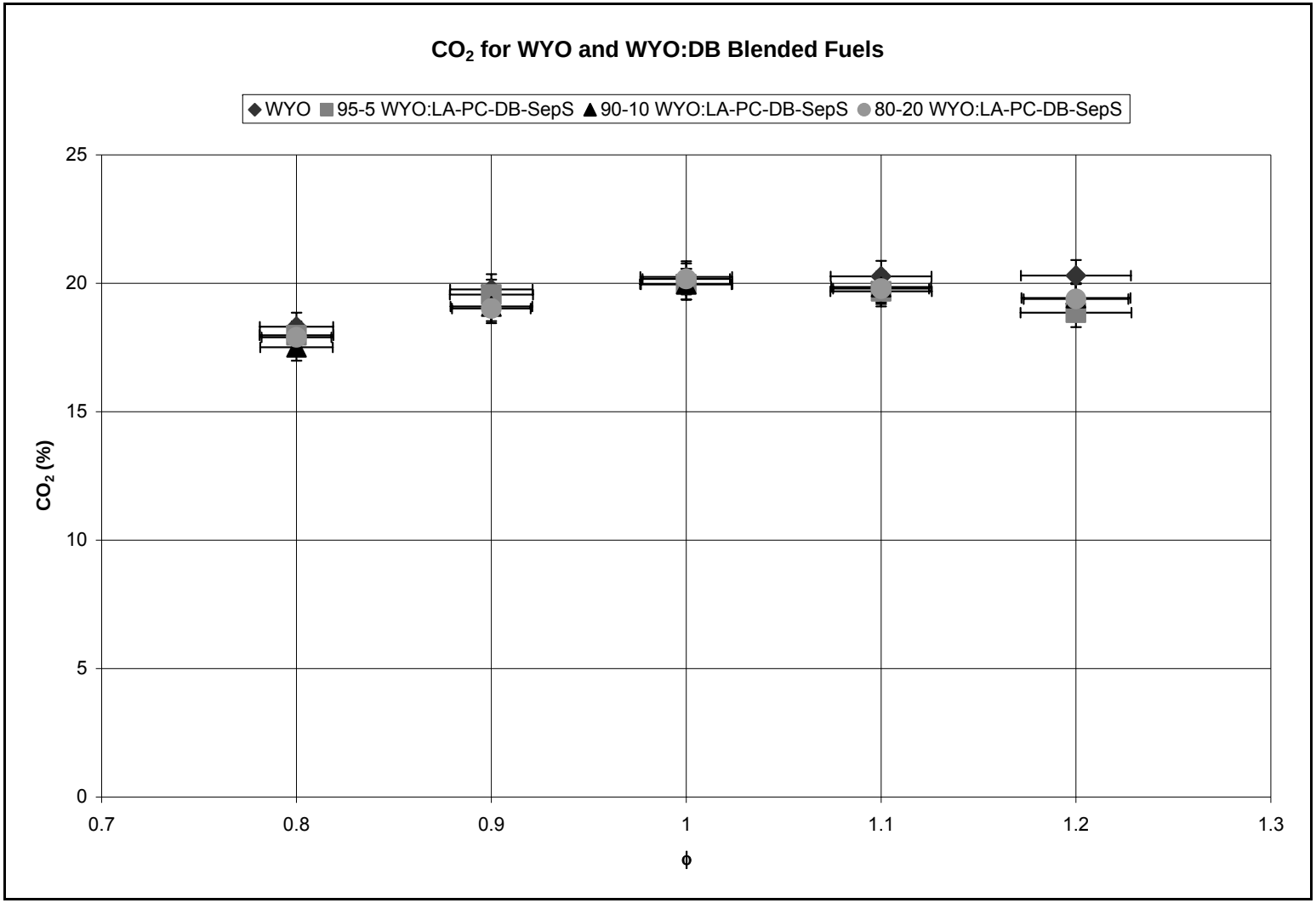

Figure 5.10: Effect of fuel on CO_2 for WYO and WYO:DB blended fuels.

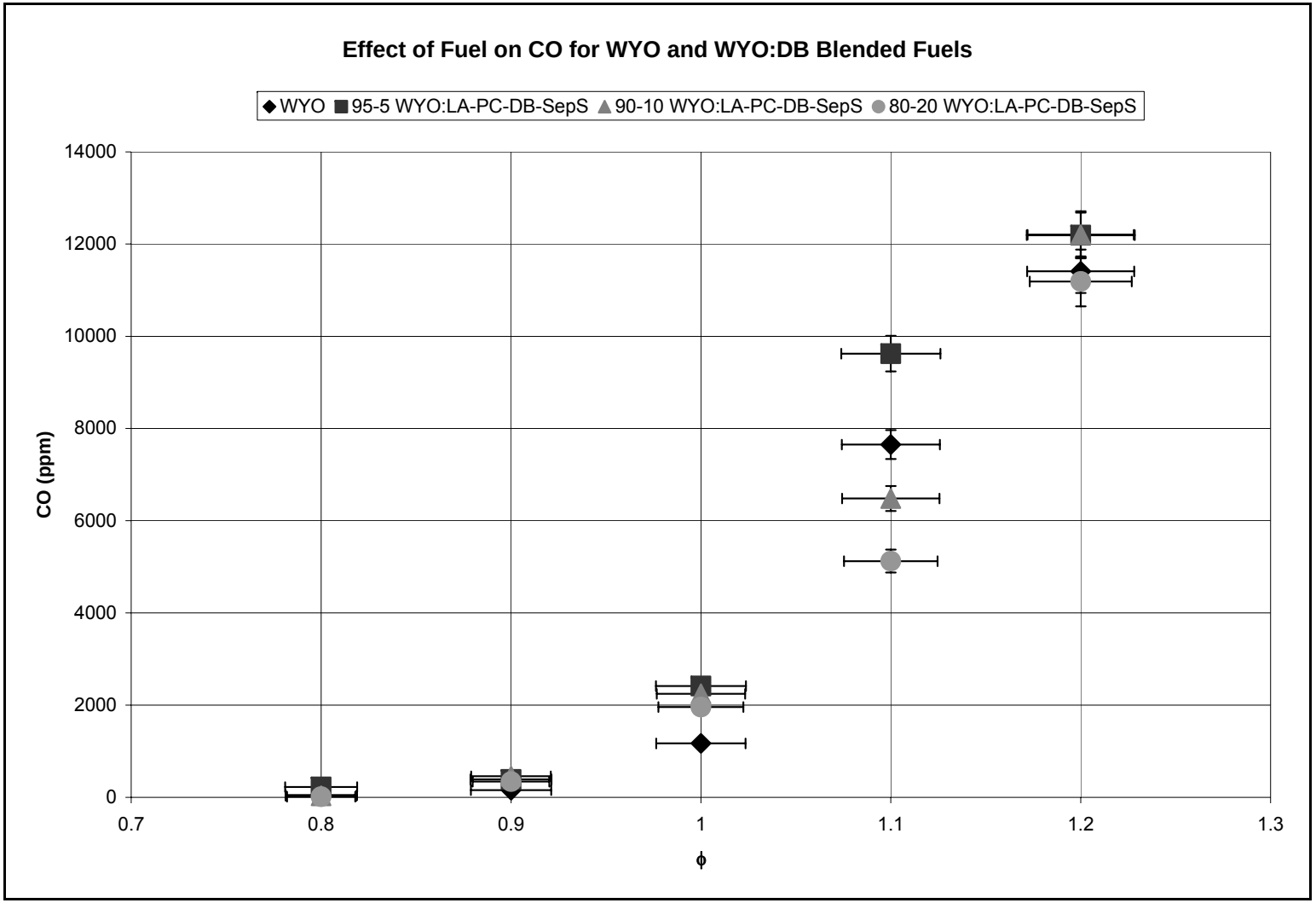

Figure 5.11: Effect of fuel on CO for WYO and WYO:DB blended fuels.

5.4.3.2 Values

Table B.9 in Appendix B gives the values of X_{O2}, $X_{O2,A}$, ϕ, and BF for all experiments conducted using TXL. Table B.10 gives the values of X_{O2}, $X_{O2,A}$, ϕ, and BF for all experiments conducted using WYO. Note that BF is larger than 1 for some of the extremely lean experiments. These values demonstrate the limitations of EQ. 5.6.1.1 as well as experimental uncertainties including fuel compositions. As to be expected, BF decreased with increasing equivalence ratio. In rich combustion, insufficient air was provided to completely oxidize all fuel carbon to CO_2, leaving unburned fuel in the ash. This caused the BF to be less than 1.

Figures 5.12 and 5.13 present the BF for TXL and TXL:DB blended fuels and WYO and WYO:DB blended fuels, respectively. Even in the very rich combustion (ϕ =1.2), approximately 83% of the fuel was burnt.

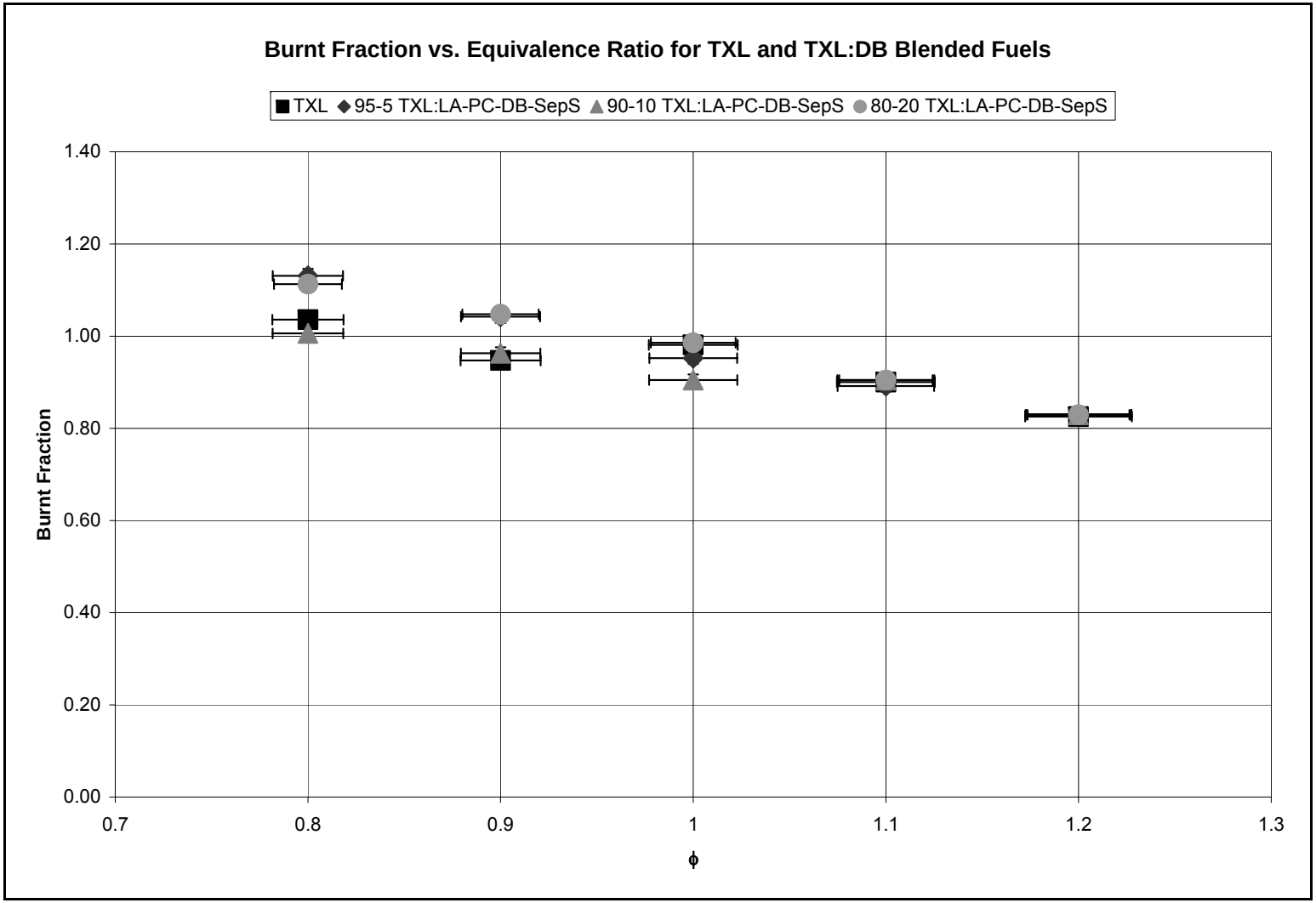

Figure 5.12: Effect of fuel on BF for TXL and TXL:DB blended fuels. Note that in the rich regime, the BF overlaps for all fuels. This indicates that the same percentage of all fuels was burnt.

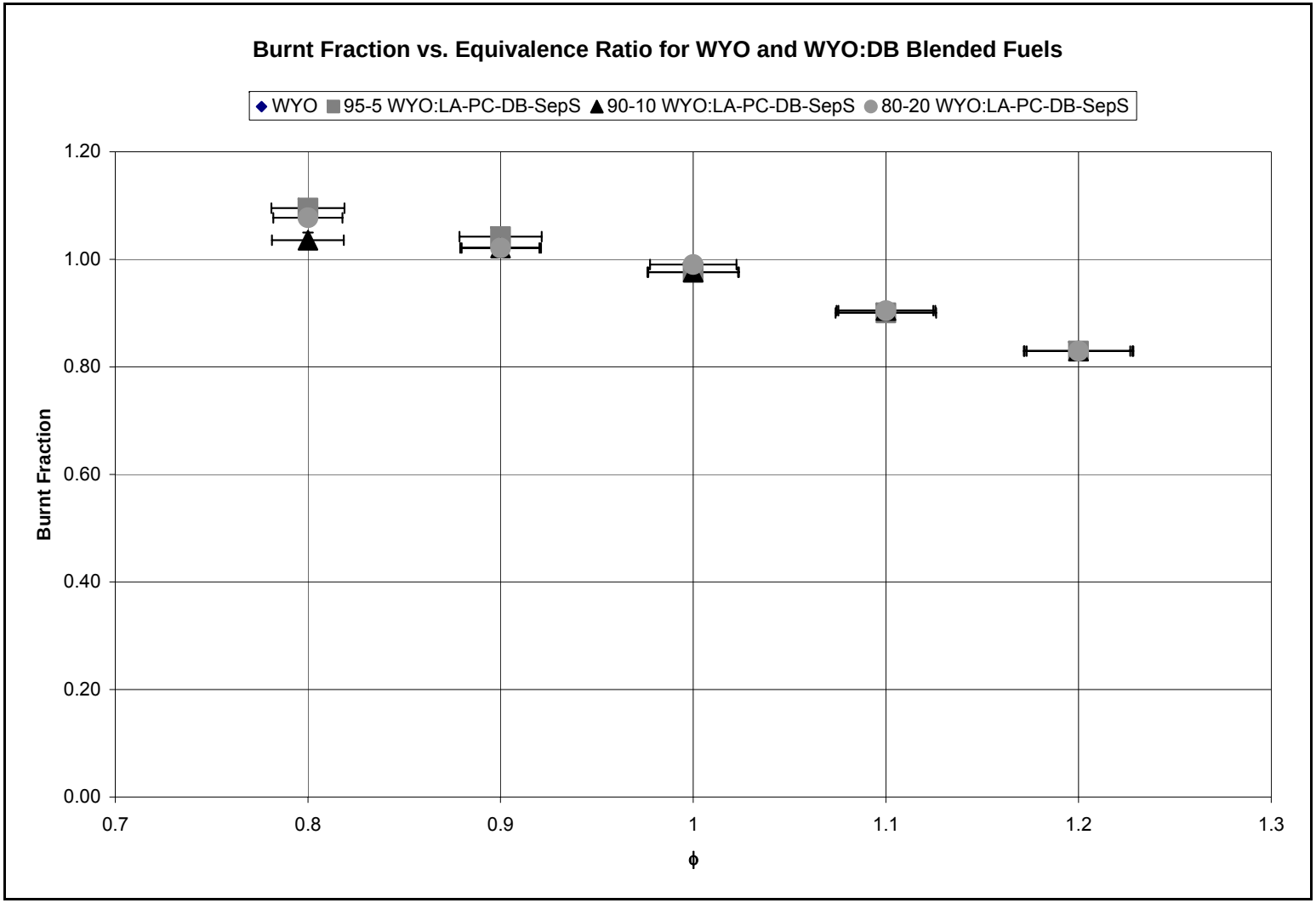

Figure 5.13: Effect of fuel on BF for WYO and WYO:DB blended fuels. Note that the data points come close to overlapping for all equivalence ratios. Thus, BF was independent of fuel type.

5.4.4 NO_x Emissions

5.4.4.1 TXL and TXL:DB Blended Fuels

Appendix Table B.11 lists NO_x emissions measured from experiments firing pure TXL coal and cofiring TXL:DB fuels. With the exception of 95-5 TXL:HA-PC-DB-SoilS, all of the blended fuels produced more NO_x in the lean region than the pure TXL. This is due to the higher amount of fuel bound nitrogen present in the biomass binding with the excess oxygen to form NO_x. But, in the slightly rich region, the blended fuels produced less NO_x than the pure TXL. This is due to the fuel bound nitrogen being forced to form other nitrogen compounds due to the deficiency in oxygen and VM reacting quickly to absorb any available oxygen the might bound with nitrogen.. No experiments with 80:20 TXL:HA-PC-DB-SoilS were possible due to excessive amounts of particulate matter (mostly ash) clogging the flue gas analyzer. The instrument clogged faster than it was able to settle to a stable reading.

Figures 5.14 and 5.15 presents the NO_x emissions for TXL and TXL:DB blended fuels in ppm and corrected to 3% O_2. Correcting to 3% O_2 is a common industry practice to prevent utilities from artificially diluting NO_x emissions with O_2. In the very lean regime, correcting caused the NO_x emissions to increase. However, for all other equivalence ratios, correcting caused the NO_x emissions to decrease because there is less than 3% O_2 in the exhaust prior to correcting.

Another method employed to prevent emission dilution is to report NO_x levels on a heat basis. Figure 5.16 presents the NO_x emissions in kg/GJ of heat input.

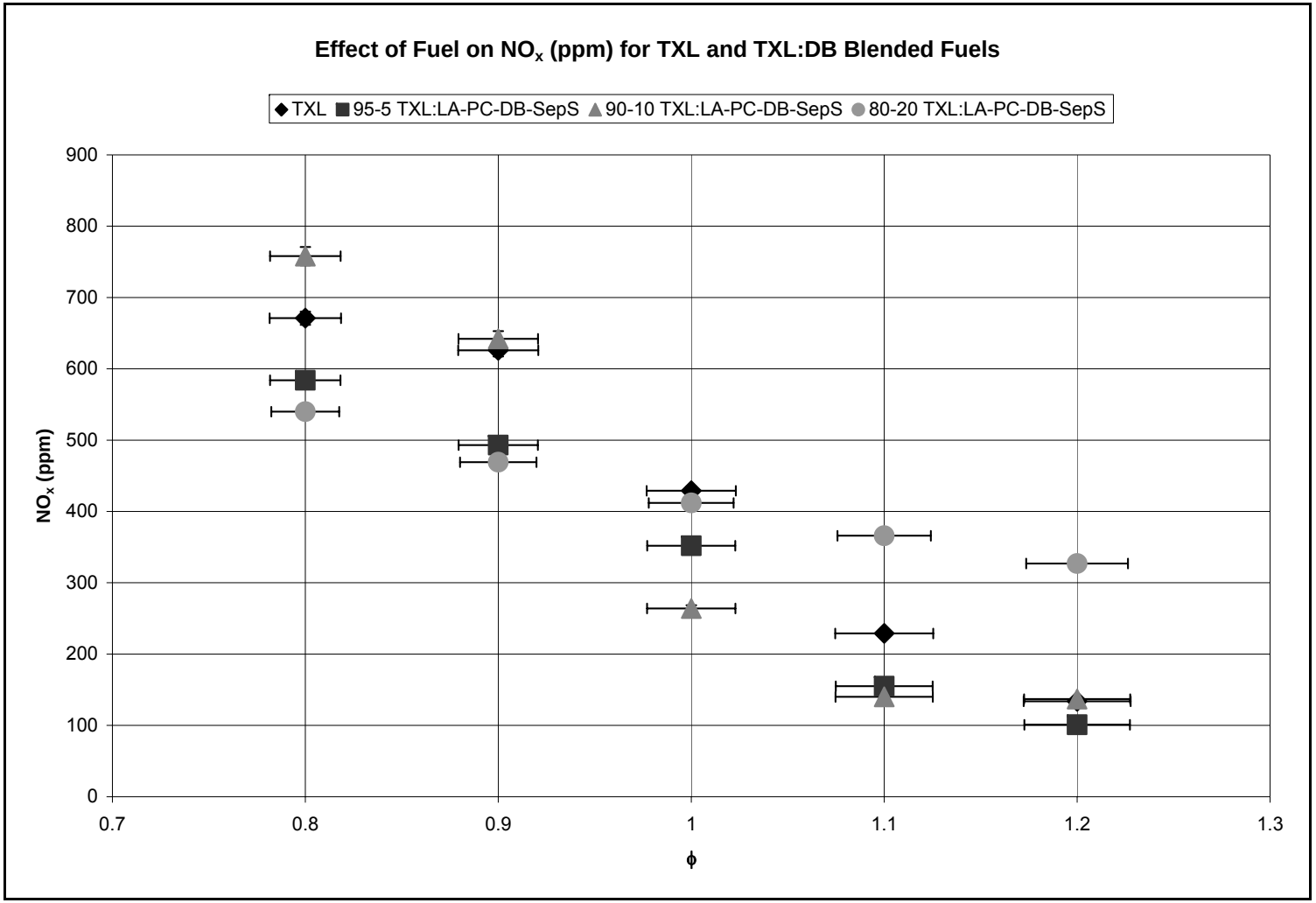

Figure 5.14: Effect of fuel on NO_x for TXL and TXL:DB blended fuels. Note that blended fuels have lower NO_x values at stoichiometric and in rich combustion.

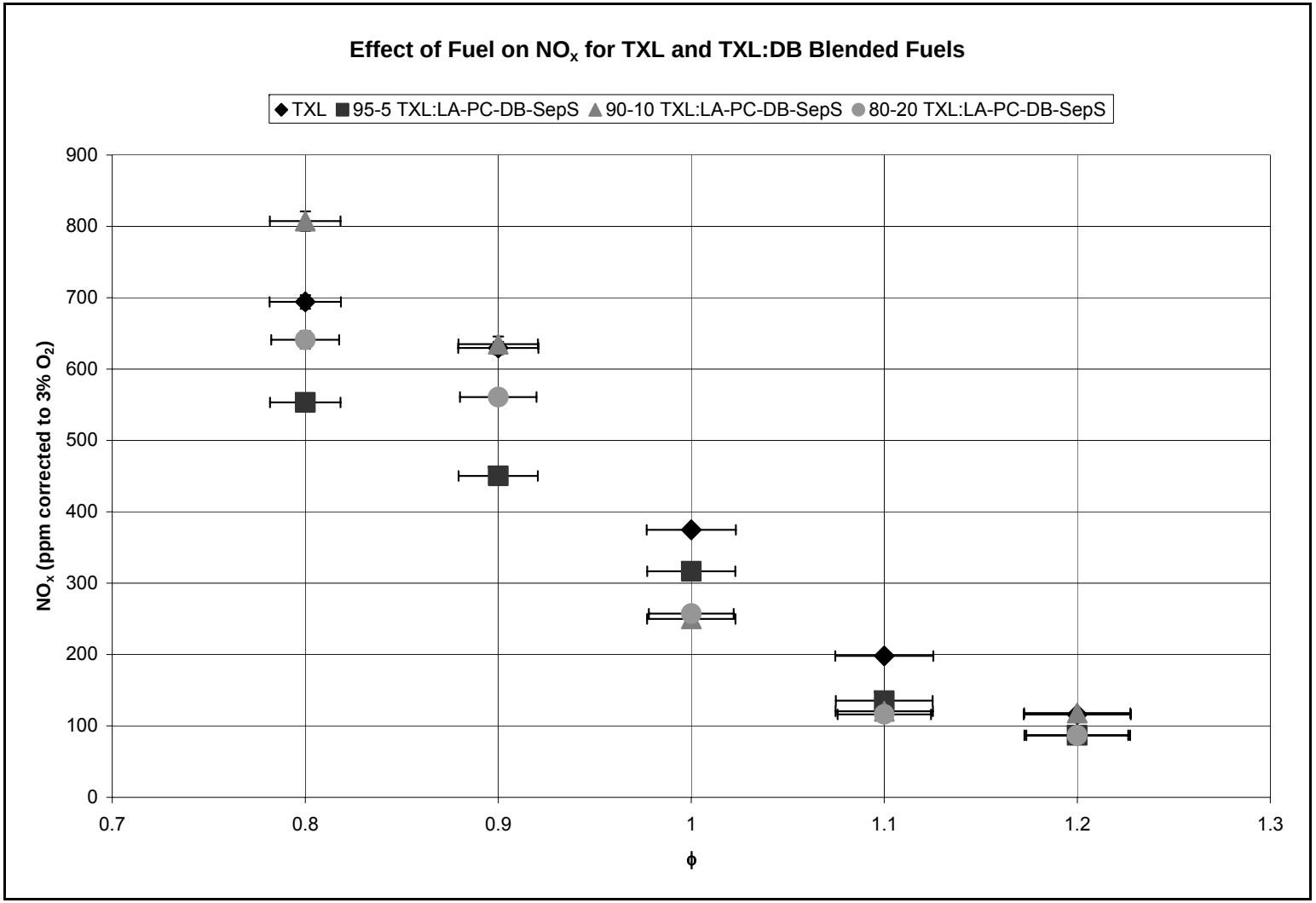

Figure 5.15: Effect of fuel on NO_x for TXL and TXL:DB blended fuels corrected to 3% O_2.

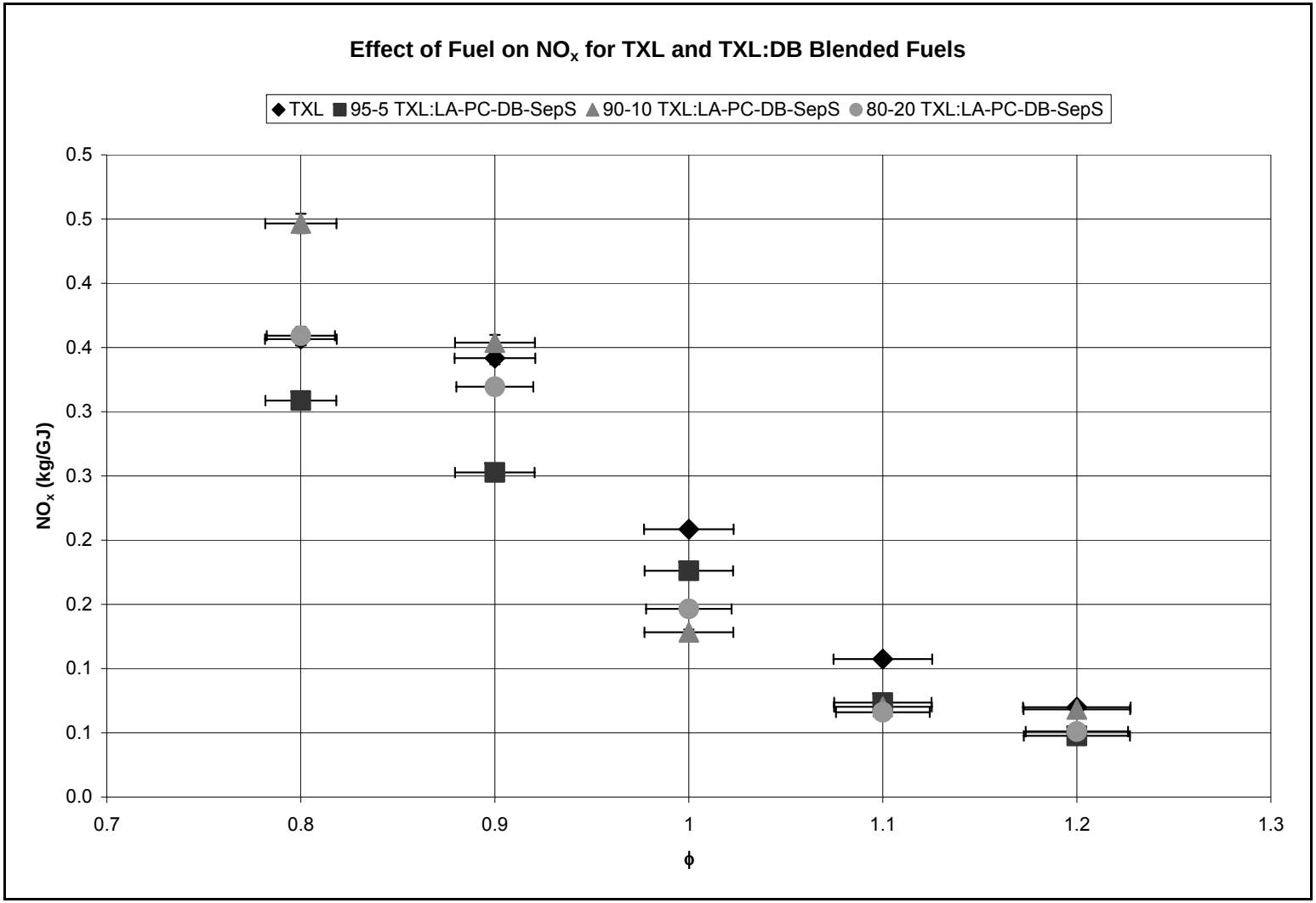

Figure 5.16: Effect of fuel on NO_x for TXL and TXL:DB blended fuels in kg/GJ.

5.4.4.2 WYO and WYO:DB Blended Fuels

Table B.12 in the Appendix lists NO_x emissions measured from experiments firing pure WYO coal and cofiring WYO:DB fuels. Note that in the lean region, the blended fuels produce more NO_x than the pure WYO. In the slightly rich region, the blended fuels produce less NO_x than the pure WYO. The same explanation for TXL applies to the WYO fuels. Experiments in the rich region with 80-20 WYO:HA-PC-DB-SoilS were unsuccessful due to excessive amounts of particulate matter (mostly ash) clogging the flue gas analyzer.

Figures 5.17 and 5.18 present the NO_x emissions from WYO and WYO:DB blended fuels in ppm and corrected to 3% O_2. Figure 5.19 presents the NO_x emissions from WYO and WYO:DB blended fuels in kg/GJ of heat input.

5.4.5 Fuel Nitrogen Conversion Efficiency

5.4.5.1 Expression

In coal combustion, the majority of NO_x comes from fuel bound nitrogen bonding with available oxygen to form NO_x. This reaction is inhibited by carbon radicals bonding with available oxygen to form CO and CO_2. The nitrogen conversion efficiency is defined as the amount of fuel nitrogen that gets converted to NO_x. Annamalai and Puri (2007) showed that overall fuel nitrogen conversion efficiency can be approximated by:

$$N_{CONV} \approx \frac{(c/n)^* X_{NO}}{X_{CO_2} + X_{CO}} \text{ ; Eq. 5.7.1.1}$$

Where c/n is the ratio of the empirical carbon and nitrogen respectively, X_{NO} is the mole fraction of NO_x, X_{CO2} is the mole fraction of CO_2, and X_{CO} is the mole fraction

of CO. All gases were measured in the exhaust stream. Note that the equation assumes that all NO_x originates from fuel nitrogen and hence it presents an upper bound on fuel nitrogen conversion efficiency. Work should be done to investigate the validity of assuming all NO_x comes from the fuel. Burning a fuel that does not produce fuel NO_x (i.e. natural gas) at the same temperature profile as the solid fuel could measure the amount of thermal NO_x produced.

5.4.5.2 Values

Table B.13 in the Appendix presents the fuel nitrogen conversion efficiency calculated from the experimental results for TXL and TXL:DB cofiring experiments. Table B.14 in the Appendix presents the fuel nitrogen conversion efficiency calculated from the experimental results for WYO and WYO:DB cofiring experiments. Note that as equivalence ratio increased, less nitrogen was converted to NO_x. In the extremely rich region, the conversion efficiency was nearly 0%. The largest decrease in conversion occurred when the flame went from stoichiometric to rich. Figures 5.20 and 5.21 present the fuel nitrogen conversion efficiency for TXL and TXL:DB blended fuels and WYO and WYO:DB blended fuels, respectively. Also note that in general, the DB blended fuels converted less nitrogen to NO_x. These fuels produced more NO_x than pure coal because there was more fuel bond nitrogen. If both fuels had the same amount of fuel bound nitrogen, the DB would have produced less NO_x than coal because a lower percentage of nitrogen.

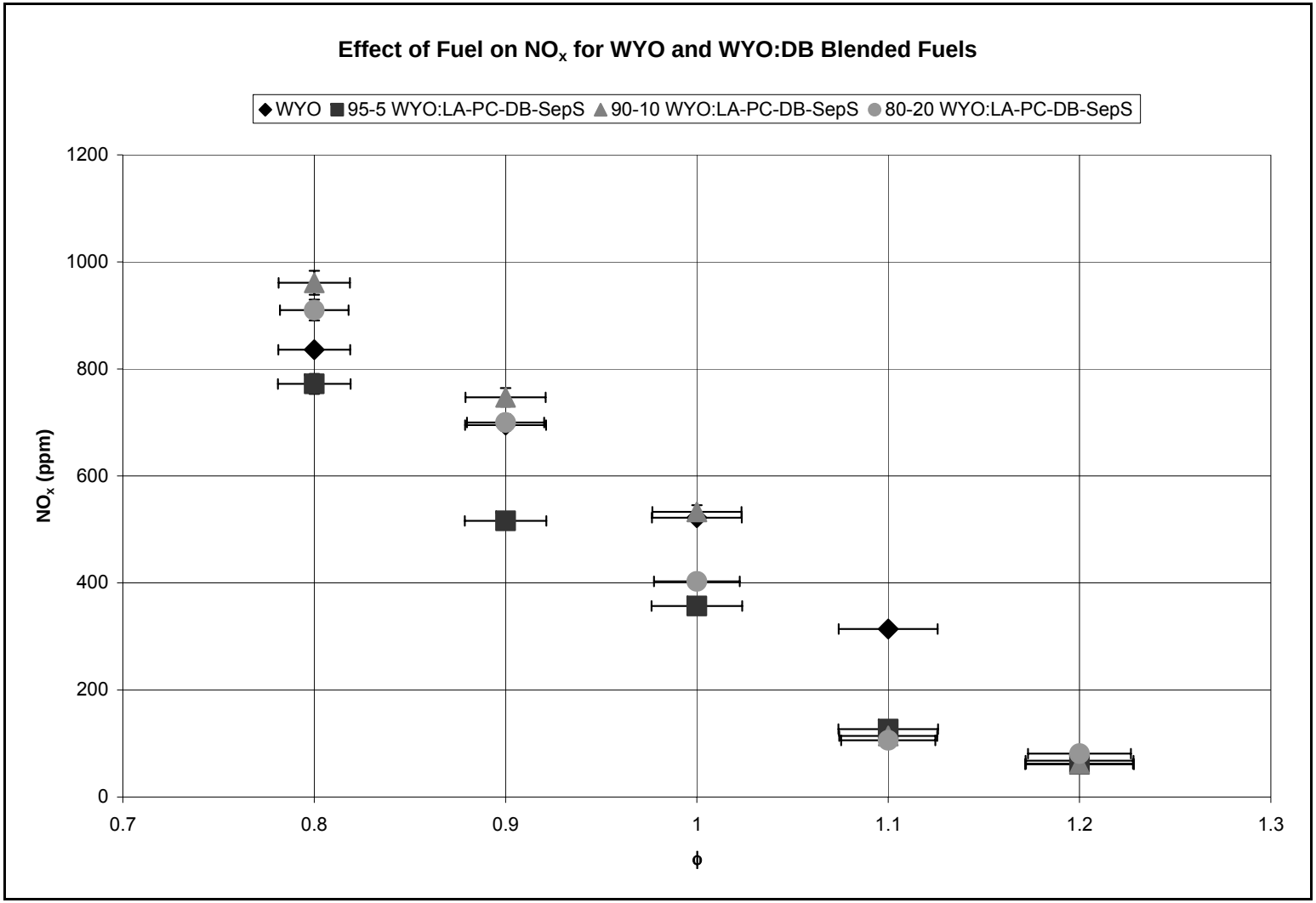

Figure 5.17: Effect of fuel on NO_x for WYO and WYO:DB blended fuels. Note how NO_x decreases in the near lean region for blended fuels.

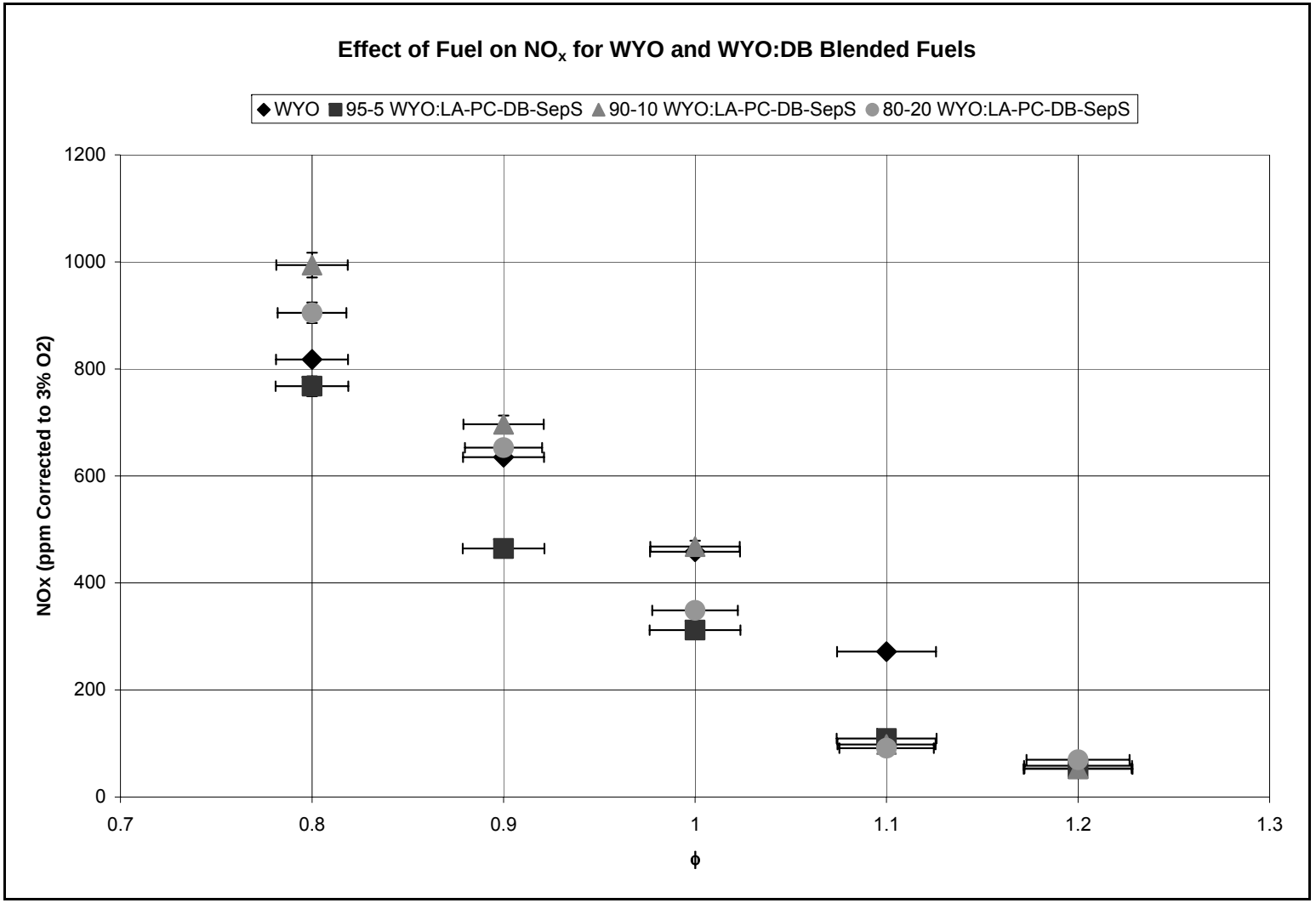

Figure 5.18: Effect of fuel on NO_x for WYO and WYO:DB blended fuels corrected to 3% O_2.

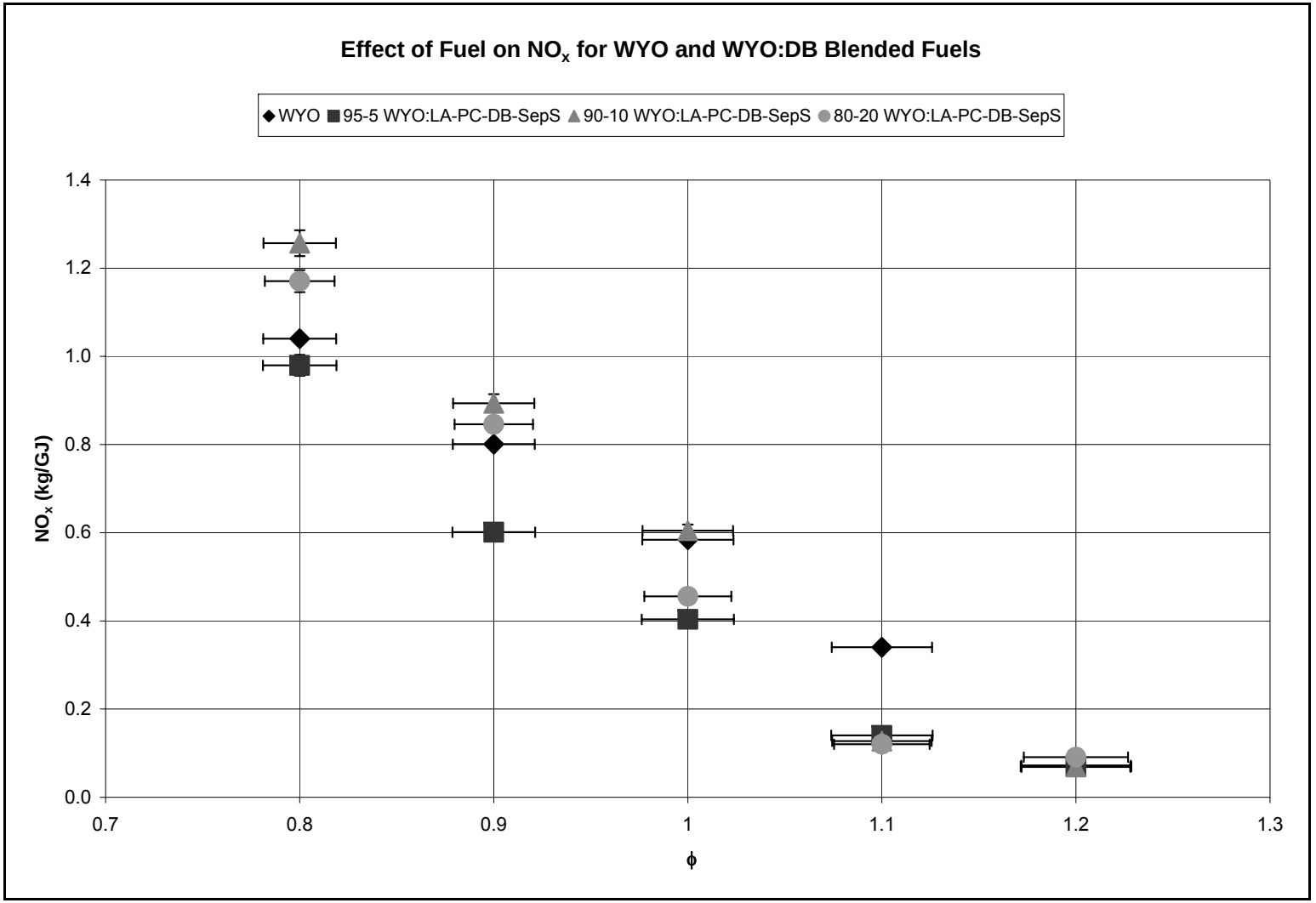

Figure 5.19: Effect of fuel on NO_x for WYO and WYO:DB blended fuels in kg/GJ.

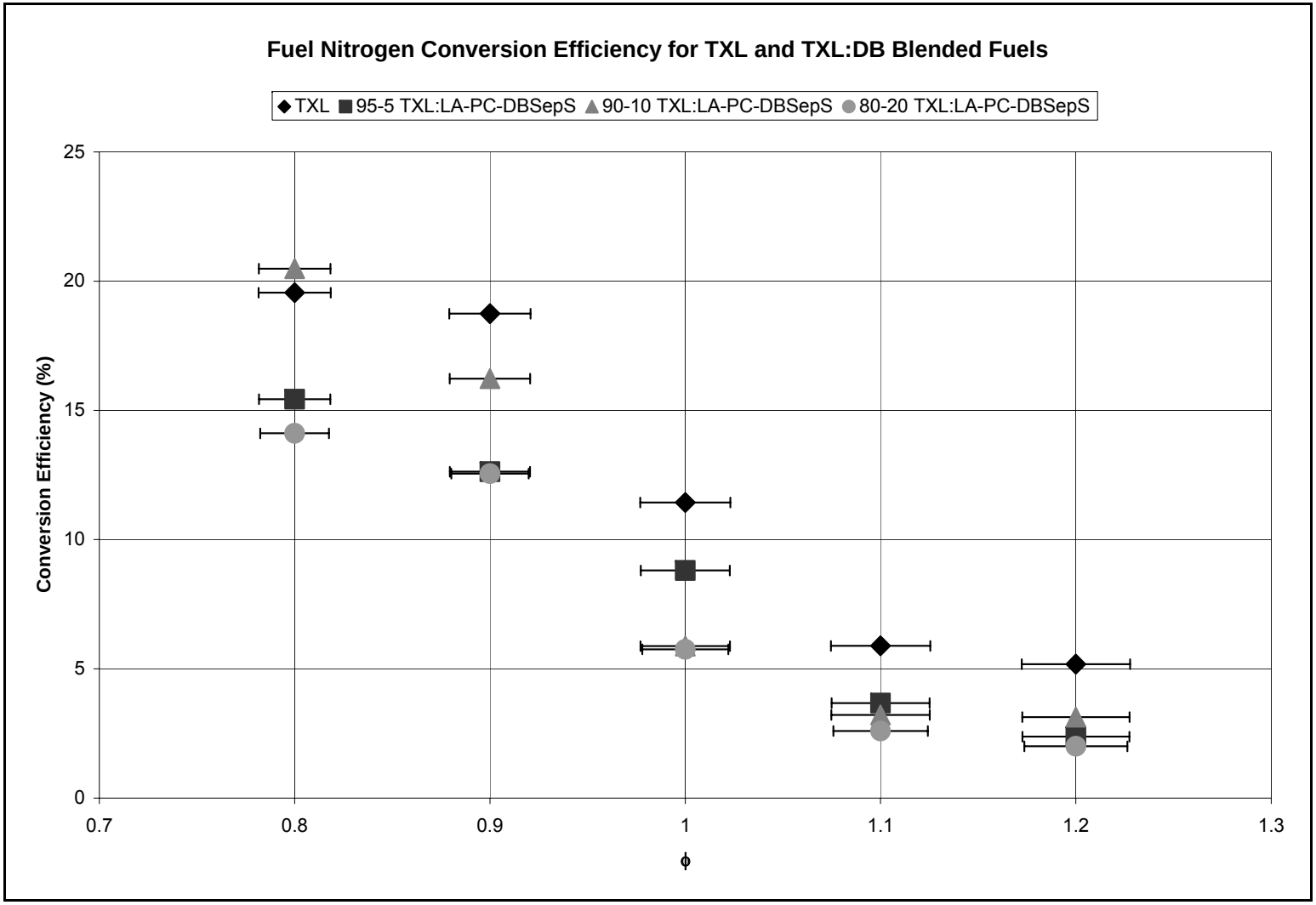

Figure 5.20: Effect of fuel on nitrogen conversion efficiency for TXL and TXL:DB blended fuels. Note that the conversion efficiency is less than coal for almost all TXL:DB blended fuels.

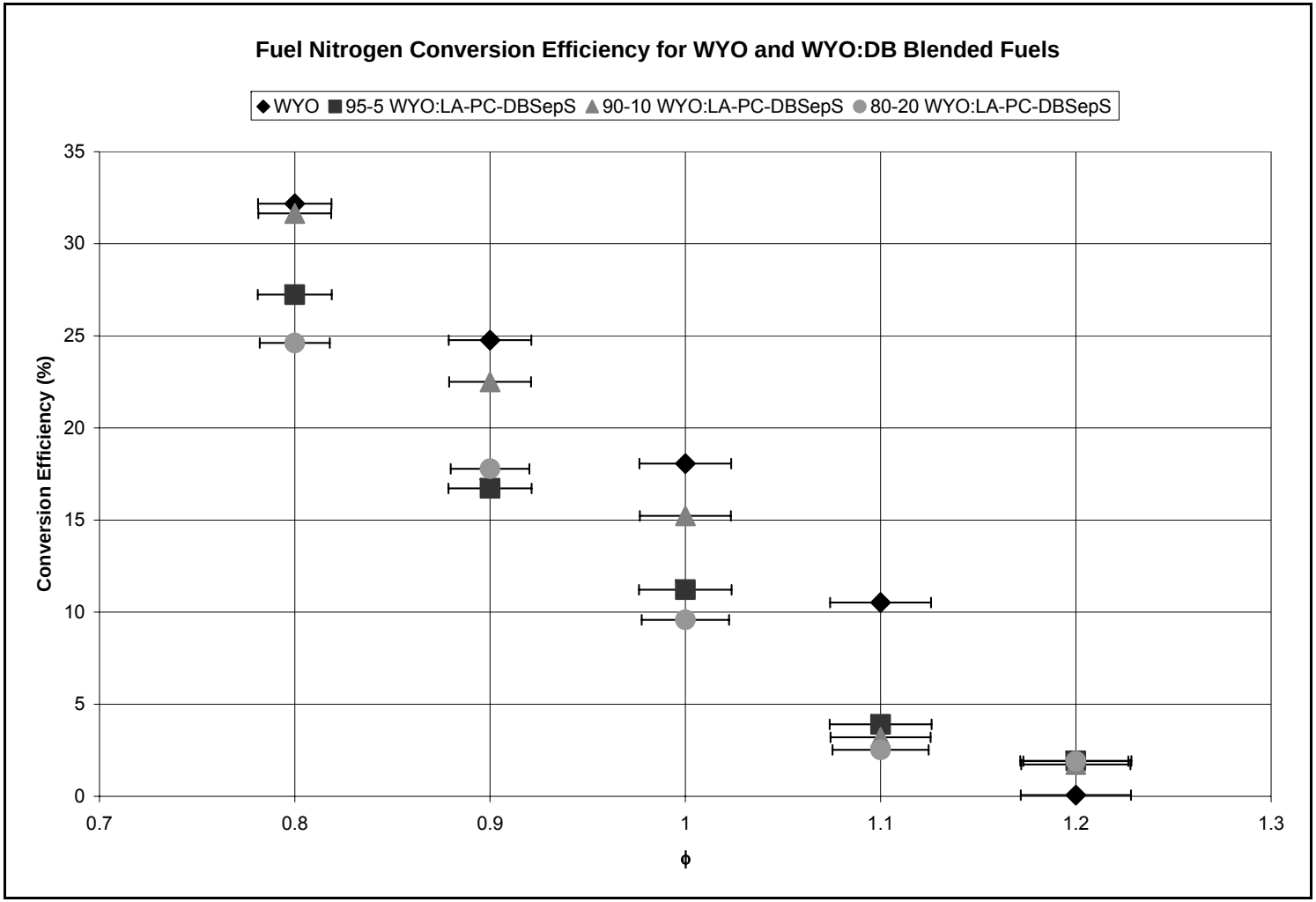

Figure 5.21: Effect of fuel on nitrogen conversion efficiency for WYO and WYO:DB blended fuels. Note that the conversion efficiency is less than coal for almost all WYO:DB blended fuels.

6. SUMMARY AND CONCLUSIONS

The major conclusions of this research are:

1. DB had a lower heat content due to less fixed carbon, more oxygen, and more ash; furthermore it contained more fuel bound nitrogen.
2. DB can be successfully blended with coal and cofired in a furnace.
    - Cofiring has minimal effect on burnt fraction.
    - BF was independent of fuel type. BF was almost unity when operating near stoichiometric.
    - DB fuels converted produced more NO_x due to greater fuel bound nitrogen percentages, however; they converted a lower percentage of fuel bound nitrogen to NO_x.
    - Cofiring increased NO_x in lean combustion, however; NO_x was reduced by blending coal with DB in rich combustion.
3. Blending of fuel by more than 90-10 was beyond practical limitations imposed by the high ash percentage in DB fuel.
4. High ash content of HA-PC-DB-SoilS made it a poor quality fuel.

7. FUTURE WORK

1. More experiments should be conducted that use a wider array of coals.
2. Samples could be collected from different points along the furnace length to investigate the creation of NO_x as the fuel burns.
3. Further research could be conducted by cofiring coal and biomass in a low NO_x burner.
4. The ash from cofiring experiments should be analyzed to determine ash composition. Ash also must be analyzed for combustibles in order to determine the BF. This BF should be compared against the BF calculated from dry gas analysis.
5. Investigate the validity of assuming all NO_x comes from thermal NO_x in the fuel nitrogen conversion efficiency equation.

REFERENCES

Annamalai, K., I. K. Puri, (2007) *Combustion Science and Engineering*, CRC Press, Taylor and Francis Group, Boca Raton, FL.

Annamalai, K., J. Sweeten, S. Mukhtar, B. Thien, G. Wei, S. Priyadarsan, S. Arumugam, K. Heflin, (2003a) Co-firing Coal: Feedlot and Litter Biomass (CFB and CLB) Fuels in Pulverized Fuel and Fixed Bed burners, Final DOE Report , DOE-Pittsburgh Contract # 40810.

Annamalai, K., J. Sweeten, S. Priyadarsan, S. Arumugam, (2006) Energy Conversion *in The Encyclopedia of Energy Engineering and Technology*/Ed. B. Capehart. Taylor and Francis Group, Boca Raton, FL.

Annamalai, K., B. Thien, J. Sweeten, (2003b) Co-firing of coal and cattle feedlot biomass (FB) fuels. Part II. Performance results from 30 kW_t (100,000) BTU/h laboratory scale boiler burner. *Fuel*, **82**(10), 1183-1193.

Arumugam, S., K. Annamalai, B. Thien, J Sweeten, (2005) *Int. National Journal of Green Energy*, **2**, 409-419.

ASTM Standard C136-06. (2006) Director V.A. Miller. **4**(2) ASTM International, Baltimore, MD.

Babcock and Wilcox. (1978) *Steam: It's Generation and Use*. Babcock and Wilcox. New York.

Carlin, N., K. Annamalai, J. Sweeten, S. Mukhtar, (2007) I*nt. National J of Green Energy*, in press.

Di Nola, G., (2007) Biomass Fuel Characterization for NO_x Emissions in Co-firing Applications, Ph.D. dissertation, Delft University of Technology, Delft, The Netherlands.

E-Instruments, (2003) Instruction Manual for Greenline 6000 and Greenline 8000. E-Instruments Group LLC Langhorne, PA.

Frazzitta, S., K. Annamalai, J. Sweeten, (1999) Performance of a burner with coal and coal–bio-solid fuel blends. *Journal of Propulsion and Power* **15**(2), 181-186.

Goughnour, P., (2006) NO_x Reduction with the Use of Feedlot Biomass as a Reburn Fuel, M.S. Thesis, Texas A&M University, College Station, TX.

Heflin, K. and J. Sweeten (2006) Preliminary interpretation of data from proximate, ultimate and ash analysis, results of June 7, 2006 samples taken from feedlot and dairy biomass biofuel feedstocks at TAES/USDA-ARS, Bushland, TX Texas Agricultural Experiment Station, Texas A&M Agricultural Research & Extension Center Amarillo/Bushland/Etter, TX.

Kegel, T.M., (1996) Basic measurement uncertainty. *71st International School of Hydrocarbon Measurement*, April 9-11, Oklahoma City, OK. 1-7.

Kline, S.J., and F.A. McClintock, (1953) Describing uncertainties in single sample experiements. *Mechanical Engineering*. **75**(1), 3-8.

Lundgren, J., Pettersson, E., (2002) Combustion of horse manure for heat production. Technical Report, NIFES.

Miller, B.G., S. F. Miller, A. W. Scaroni, (2002) Utilizing agricultural by-products in industrial boilers: Penn State's experience and coal's role in providing security for our nation's food supply, *Nineteenth Annual International Pittsburgh Coal Conference*, Pittsburgh, PA. 23-27.

NASS, (2002) U.S. Dairy Herd Structure, National Agricultural Statistics Service, Agricultural Statistics Board, U.S. Department of Agriculture, Washington, DC.

Schmidt, D.D., V. S. Pinapati, (2003) "Opportunities For Small Biomass Power Systems." Final Technical Report. Prepared for U.S. Department of Energy Chicago Operations Office. DOE Contract No. DE-FGO2-99EE35 128.

Stokes, S., and M. Gamroth, (1999) Freestall Dairy Facilities in Central Texas, Texas A&M University, Texas Agricultural Extension Service. Available at: http://animalscience.tamu.edu/ansc/publications/dairypubs/15311-fresstalldairies.pdf. Accessed on October 17, 2005.

Sweeten, J.M., (1979) Texas Agricultural Extension Service Publication L-1094, Texas Agricultural Extension Service, Texas A&M University, College Station, TX.

Sweeten, J.M., (1990) Texas Agricultural Extension Service Publication B-1671, Texas Agricultural Extension Service, Texas A&M University, College Station, TX.

Sweeten, J.M., K. Annamalai, B. Thien, L. McDonald, (2003) Co-firing of coal and cattle feedlot biomass (FB) fuels, part I: feedlot biomass (cattle manure) fuel quality and characteristics *Fuel* **10**, 1167-1182.

Thien, B., (2002) Cofiring With Coal – Feedlot Biomass Blends, Ph.D. dissertation, Texas A&M University, College Station, TX.

Tillman. D.A., (2000) Biomass cofiring: the technology, the experience, the combustion consequences, *Biomass and Bioenergy* **19**, 365-384.

Tranchida, T., (2007) Cattle manure production, Available at: www.dpi.qld.gov.au/environment/5166.html.

Volk, T.A., L.P. Abrahamson, E.H. White, E. Neuhauser, E. Gray, et al., (2002) Biomass, Available at: http://en.wikipedia.org/wiki/Biomass.

APPENDIX A: SIZE DISTRIBUSTION ANALYSIS

According to Babcock and Wilcox (1978) solid fuels with less than 69% FC and a HHV less than 11,000 BTU/lb need to be ground to 60% less than ASTM mesh 200 (74 microns). This requirement applies to coal for use in a pulverized coal, water cooled furnace. Coarser ground fuels can be fired in stokers and cyclone furnaces.

All fuels were shook in a CE Tyler Roto-Tap model B. The Rossin-Ramler distribution is a weighted probability distribution that has been approved by ASTM (2006) standard C136-06 for coal, clay, gypsum, and coarse aggregate. This standard was followed for shaking the fuels.

Annamalai and Puri (2007) state that a weighted cumulative size distribution is acceptable to describe the size distribution of coal, biomass, and coal:biomass blended fuels. The weighted cumulative size distribution is of the functional form:

$$CMF = 1 - \exp\left(-b * D_p\right)^n \qquad \text{Eq. A.1.a}$$

With $b=(1/D_{pcharacteristic})^n$, Rewriting:

$$CMF = 1 - \exp\left(\frac{-D_p}{D_{pcharacteristic}}\right)^n \text{; Eq. A.1.b}$$

Where CMF is the cumulative mass fraction that is less than a stated D_p, D_p, is the particle diameter of interest, $D_{pcharacteristic}$ is the diameter larger than 63.2% of the fuel particles, and n is a constant that describes the spread of the size distribution.

Eq. A.1 can be rearranged as:

$$1 - CMF = -e\left(\frac{D_p}{D_{pcharacteristic}}\right)^n \text{; Eq. A.2}$$

Then, taking the negative natural logarithm of both sides yields:

$$\ln\left(-\left(1 - CMF\right)\right) = \left(\frac{D_p}{D_{pcharacteristic}}\right)^n \text{; Eq. A.3}$$

Taking another natural logarithm and applying a rule of logarithms leads to:

$$\ln\left(\ln\left(-\left(1 - CMF\right)\right)\right) = n * \ln D_p - n * \ln D_{pcharacteristic} \text{; Eq. A.4}$$

Eq A.4 is linear with a slope of n and the y intercept determined by n and $D_{pcharacteristic}$. The equation of this line can be found from standard regression software. Table A.1 shows the data obtained from shaking LA-PC-DB-SepS. All logarithms are base e.

Figure A.1 gives a line graph of the linearized parameters used to find a linear regression equation.

From Figure A.1 the linear equation describing the size distribution is:

$$\ln\left(-\left(\ln\left(CMF\right)\right)\right) = .9655 * \ln\left(D_P\right) - 5.1159 \text{; Eq. A.5}$$

From this equation n is equal to .9655 and $D_{pcharacteristic}$ is:

$$D_{pcharacteristic} = e^{-\frac{.9655}{-5.1159}} = 200.08 \text{; Eq. A.6}$$

Figure A.2 shows the linearized size distributions for all the fuel considered.

Table A.1: Data from shaking LA-PC-DB-SepS. As the stated diameter gets smaller, the fraction of particles less than the stated size gets smaller.

Mesh #	Sieve Dia (μm)	bigger than (g)	bigger than (%)	less than (%)	R in sieve	-log (R/100)	log (-log (R/100))	log (Mean Dia)
10	2000	0.182	0.042032721	99.95796728	0.042032721	3.376412496	0.528455499	3.301029996
16	1190	1.125	0.259817643	99.69814964	0.301850364	2.520208297	0.401436437	3.075546961
20	840	3.64	0.840654417	98.85749522	1.142504781	1.942141974	0.288280974	2.924279286
50	300	94.458	21.81498212	77.04251309	22.95748691	0.639075655	-0.194447726	2.477121255
100	150	136.181	31.45086791	45.59164519	54.40835481	0.264334406	-0.577846305	2.176091259
200	75	99.068	22.87965709	22.7119881	77.2880119	0.111887864	-0.951217017	1.875061263
325	45	41.575	9.601705328	13.11028277	86.88971723	0.061031616	-1.21444513	1.653212514
Pan	0	56.767	13.11028277		100			

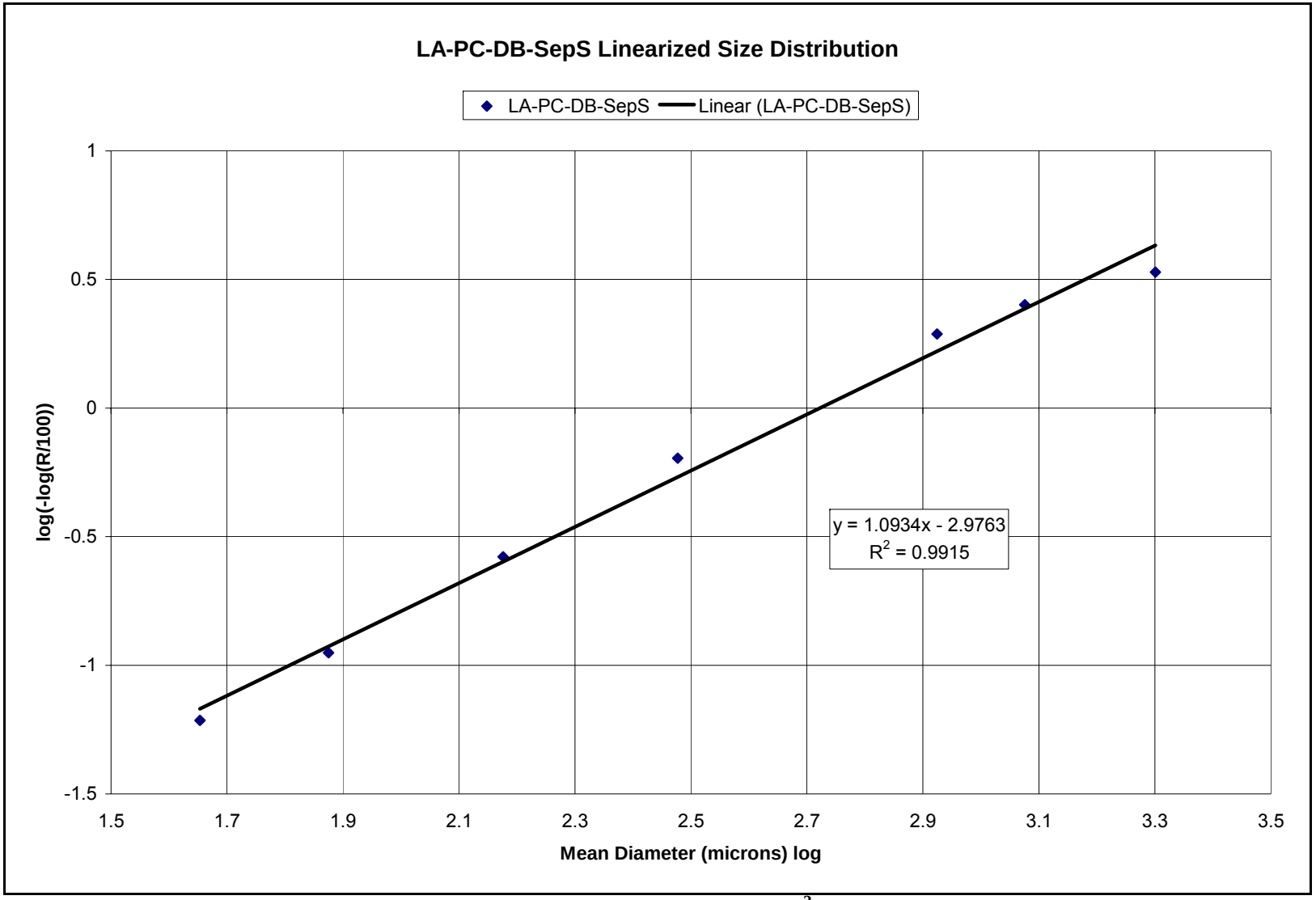

Figure A.1: Linearized size distribution for LA-PC-DB-SepS. Note the R^2 value is very close to unity.

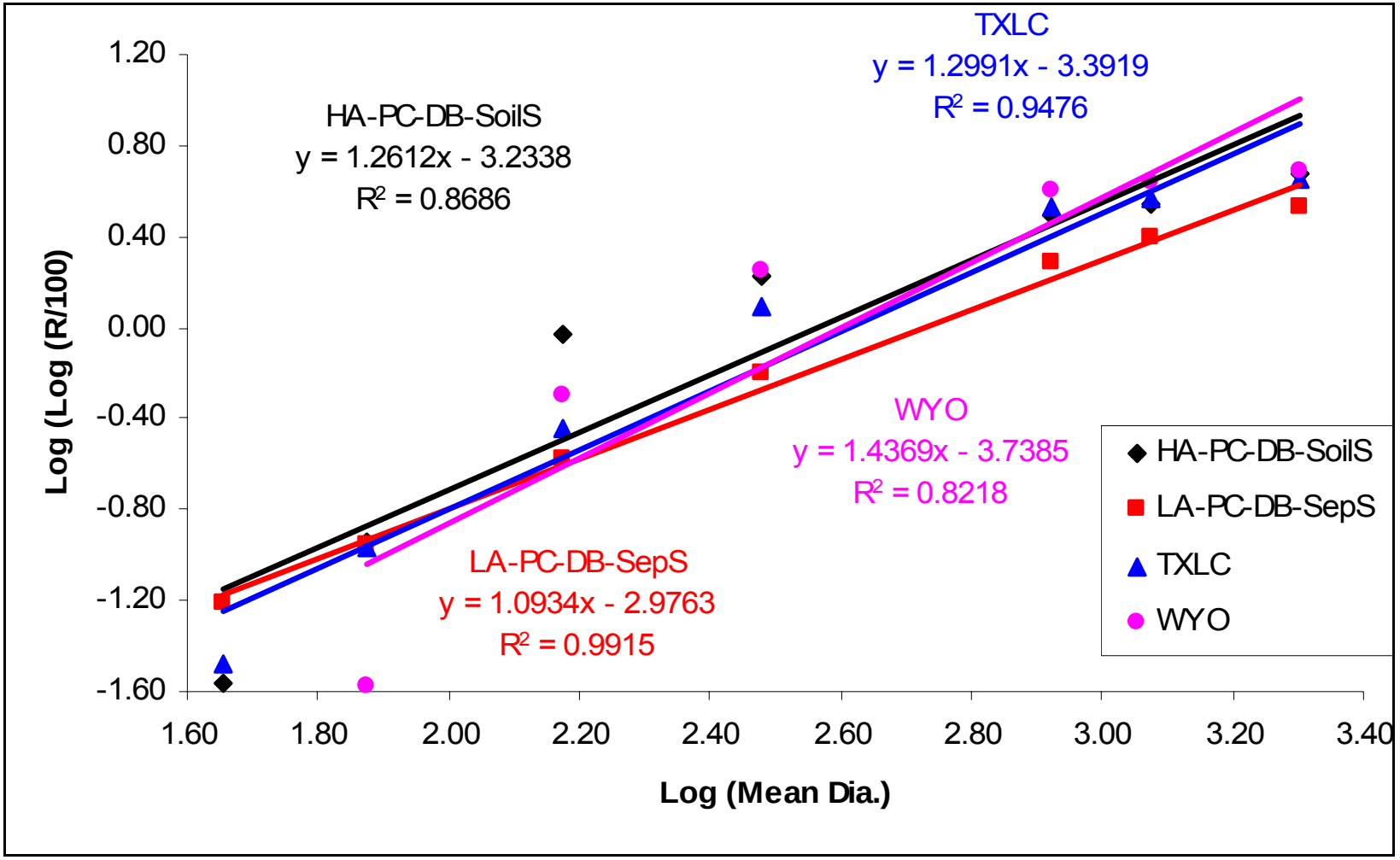

Figure A.2: Linearized size distributions for all fuels.

Another way to present the data is on a log-log axis. Figure A.3 presents Figures A.2 with the particle size diameter on a log scale. The percentage of the sample that was smaller than a specified diameter is also given on a log scale.

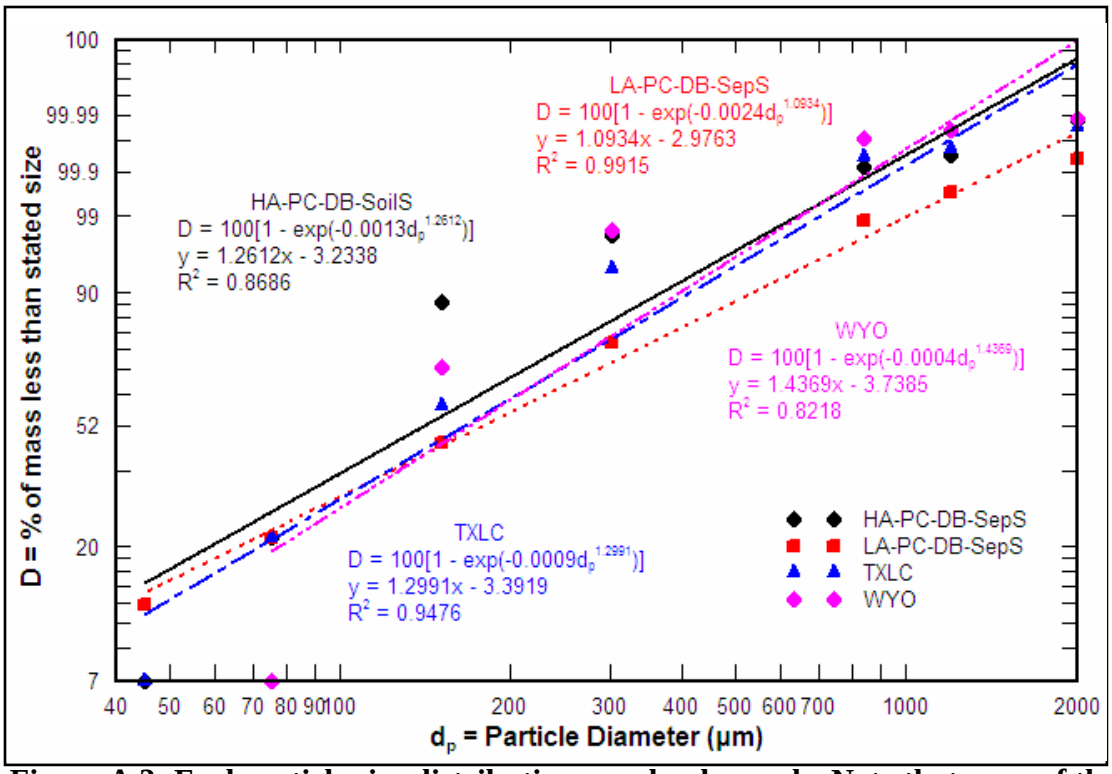

Figure A.3: Fuel particle size distribution on a log-log scale. Note that none of the fuels are ground to 60% less than 74 microns. Feeding difficulties occurred during experiments due to the coarseness of the fuels.

Figure A.4 presents the size distribution plot for the work Thien (2002) did cofiring coal, FB, and LB. Table A.2 presents the Rosin-Rammler parameters he obtained.

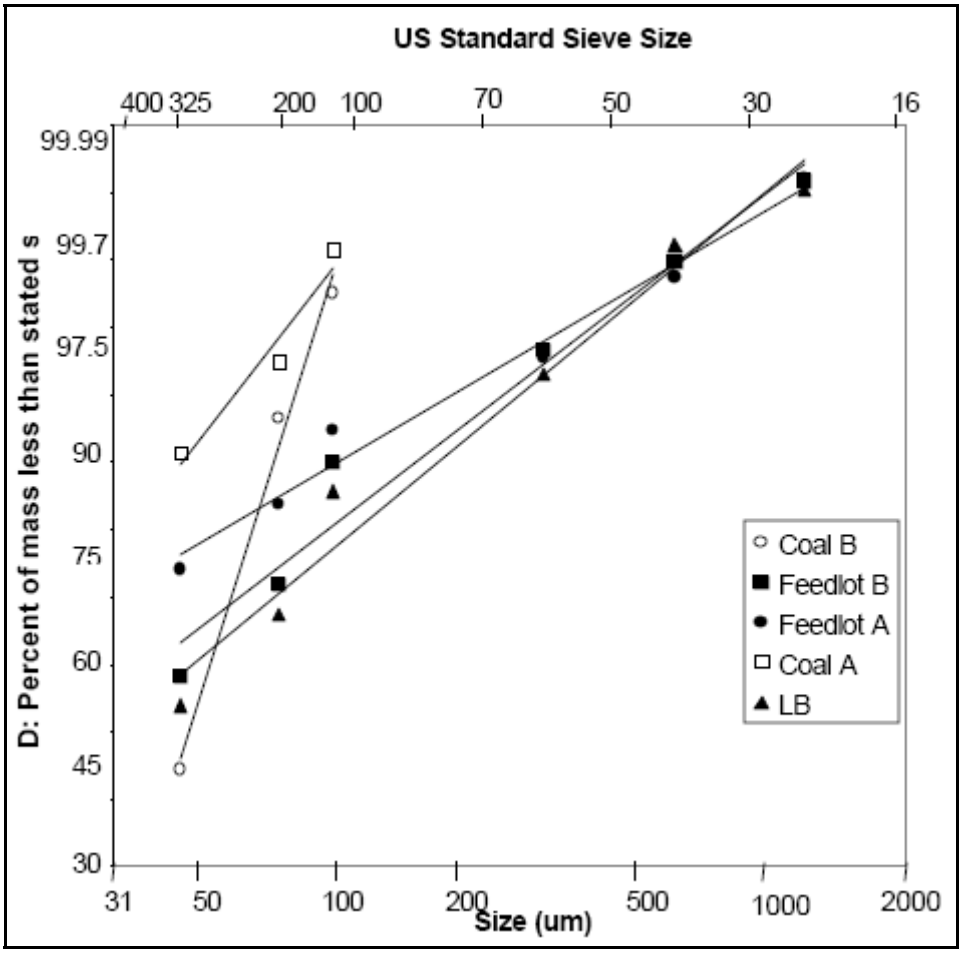

Figure A.4: Fuel particle size distribution for coal, FB, and LB. Adapted from Thien (2002).

Table A.2: Rosin-Rammler parameters for coal, FB, and LB. Adapted from Thien (2002).

Value	Coal A	FB A	Coal B	FB B	LB
n	1.6765	.7683	4.1559	1.0007	1.0751
b	.001544	.026140	1.637E-8	.00601	.0189

APPENDIX B: RESULTS TABLES

B.1 Operating Parameters

Table B.1: Experimental parameters for TXL and TXL:DB blended fuels.

	Equivalence Ratio	Fuel Flow Rate (kg/hr)	Primary Air (m^3/hr)	Secondary Air (m^3/hr)	Total Air (m^3/h	Total Air (kg/hr)	A:F	Secondary / Total (%)
TXL	0.8	7.38	5.95	29.40	35.35	41.85	5.67	83.18
	0.9	7.38	5.95	25.68	31.63	37.45	5.07	81.20
	1	7.38	5.95	22.56	28.51	33.75	4.57	79.14
	1.1	7.38	5.95	20.04	25.99	30.77	4.17	77.12
	1.2	7.38	5.95	18.72	24.67	29.21	3.96	75.89
95-5 TXL:LA-PC-DB-SepS	0.8	7.42	5.95	30.36	36.31	42.99	5.79	83.62
	0.9	7.42	5.95	26.46	32.41	38.37	5.17	81.65
	1	7.42	5.95	23.28	29.23	34.61	4.66	79.65
	1.1	7.42	5.95	20.70	26.65	31.55	4.25	77.68
	1.2	7.42	5.95	18.54	24.49	28.99	3.91	75.72
90-10 TXL:LA-PC-DB-SepS	0.8	7.46	5.95	30.48	36.43	43.13	5.78	83.68
	0.9	7.46	5.95	26.40	32.35	38.30	5.13	81.62
	1	7.46	5.95	23.16	29.11	34.47	4.62	79.57
	1.1	7.46	5.95	20.58	26.53	31.41	4.21	77.58
	1.2	7.46	5.95	18.30	24.25	28.71	3.85	75.47
80-20 TXL:LA-PC-DB-SepS	0.8	7.54	5.95	32.40	38.35	45.41	6.03	84.49
	0.9	7.54	5.95	28.14	34.09	40.36	5.36	82.55
	1	7.54	5.95	24.72	30.67	36.31	4.82	80.61
	1.1	7.54	5.95	21.96	27.91	33.04	4.38	78.69
	1.2	7.54	5.95	19.62	25.57	30.27	4.02	76.74
95-5 TXL:HA-PC-DB-SoilS	0.8	7.94	5.95	29.46	35.41	41.93	5.28	83.20
	0.9	7.94	5.95	25.56	31.51	37.31	4.70	81.13
	1	7.94	5.95	22.38	28.33	33.54	4.23	79.01
	1.1	7.94	5.95	19.80	25.75	30.49	3.84	76.90
	1.2	7.94	5.95	17.64	23.59	27.93	3.52	74.79
90-10 TXL:HA-PC-DB-SoilS	0.8	7.65	5.95	28.98	34.93	41.36	5.41	82.97
	0.9	7.65	5.95	25.14	31.09	36.81	4.81	80.87
	1	7.65	5.95	22.02	27.97	33.12	4.33	78.74
	1.1	7.65	5.95	19.50	25.45	30.13	3.94	76.63
	1.2	7.65	5.95	17.28	23.23	27.50	3.59	74.40

Table B.2: Equivalent heat blends for mass blended TXL and TXL:DB blended fuels.

	% By Mass			HHV (kJ/kg)			% By Heat		
Fuel	TXL	LA-PC-DB-SepS	HA-PC-DB-SoilS	TXL	LA-PC-DB-SepS	HA-PC-DB-SoilS	TXL	LA-PC-DB-SepS	HA-PC-DB-SoilS
TXL	100	0	0	14287	12844	4312	100.00	0.00	
95-5:TXL:LA-PC-DB-SepS	95	5	0	14287	12844	4312	95.48	4.52	
90-10:TXL:LA-PC-DB-SepS	90	10	0	14287	12844	4312	90.92	9.08	
80-20:TXL:LA-PC-DB-SepS	80	20	0	14287	12844	4312	81.65	18.35	
95-5:TXL:HA-PC-DB-SoilS	95	0	5	14287	12844	4312	98.44		1.56
90-10:TXL:HA-PC-DB-SoilS	90	0	10	14287	12844	4312	96.76		3.24
80-20:TXL:HA-PC-DB-SoilS	80	0	20	14287	12844	4312	92.98		7.02

Table B.3: Experimental parameters for WYO and WYO:DB blended fuels.

	Equivalence Ratio	Fuel Flow Rate (kg/hr)	Primary Air (m^3/hr)	Secondary Air (m^3/hr)	Total Air (m^3/hr)	Total Air (kg/hr)	A:F	Secondary / Total (%)
WYO	0.8	5.80	5.95	28.74	34.69	41.07	7.08	82.86
	0.9	5.80	5.95	25.26	31.21	36.95	6.37	80.94
	1	5.80	5.95	22.20	28.15	33.33	5.75	78.87
	1.1	5.80	5.95	19.74	25.69	30.42	5.25	76.85
	1.2	5.80	5.95	17.52	23.47	27.79	4.79	74.66
95-5 WYO:LA-PC-DB-SepS	0.8	5.88	5.95	28.98	34.93	41.36	7.03	82.97
	0.9	5.88	5.95	25.14	31.09	36.81	6.25	80.87
	1	5.88	5.95	21.96	27.91	33.04	5.62	78.69
	1.1	5.88	5.95	19.44	25.39	30.06	5.11	76.58
	1.2	5.88	5.95	17.34	23.29	27.57	4.69	74.46
90-10 WYO:LA-PC-DB-SepS	0.8	5.97	5.95	29.82	35.77	42.35	7.09	83.37
	0.9	5.97	5.95	25.80	31.75	37.59	6.29	81.27
	1	5.97	5.95	22.62	28.57	33.83	5.66	79.18
	1.1	5.97	5.95	20.04	25.99	30.77	5.15	77.12
	1.2	5.97	5.95	17.88	23.83	28.21	4.72	75.04
80-20 WYO:LA-PC-DB-SepS	0.8	6.16	5.95	31.44	37.39	44.27	7.19	84.09
	0.9	6.16	5.95	27.30	33.25	39.37	6.39	82.11
	1	6.16	5.95	23.94	29.89	35.39	5.74	80.10
	1.1	6.16	5.95	21.24	27.19	32.19	5.23	78.13
	1.2	6.16	5.95	18.96	24.91	29.49	4.79	76.12
95-5 WYO:HA-PC-DB-SoilS	0.8	6.03	5.95	29.82	35.77	42.35	7.03	83.37
	0.9	6.03	5.95	25.86	31.81	37.66	6.25	81.30
	1	6.03	5.95	22.68	28.63	33.90	5.62	79.23
	1.1	6.03	5.95	20.04	25.99	30.77	5.10	77.12
	1.2	6.03	5.95	17.88	23.83	28.21	4.68	75.04
90-10 WYO:HA-PC-DB-SoilS	0.8	6.28	5.95	30.24	36.19	42.85	6.83	83.57
	0.9	6.28	5.95	26.22	32.17	38.09	6.07	81.51
	1	6.28	5.95	23.04	28.99	34.32	5.47	79.49
	1.1	6.28	5.95	20.40	26.35	31.20	4.97	77.43
	1.2	6.28	5.95	18.18	24.13	28.57	4.55	75.35
80-20 WYO:HA-PC-DB-SoilS	0.8	6.84	5.95	29.46	35.41	41.93	6.13	83.20
	0.9	6.84	5.95	25.56	31.51	37.31	5.45	81.13
	1	6.84	5.95	22.44	28.39	33.61	4.91	79.05

Table B.4: Equivalent heat blends for mass blended WYO and WYO:DB fuels.

	% By Mass			HHV (kJ/kg)			% By Heat		
Fuel	WYO	LA-PC-DB-SepS	HA-PC-DB-SoilS	WYO	LA-PC-DB-SepS	HA-PC-DB-SoilS	WYO	LA-PC-DB-SepS	HA-PC-DB-SoilS
WYO	100	0	0	18193	12844	4312	100.00	0.00	
95-5:WYO:LA-PC-DB-SepS	95	5	0	18193	12844	4312	96.42	3.58	
90-10:WYO:LA-PC-DB-SepS	90	10	0	18193	12844	4312	92.73	7.27	
80-20:WYO:LA-PC-DB-SepS	80	20	0	18193	12844	4312	85.00	15.00	
95-5:WYO:HA-PC-DB-SoilS	95	0	5	18193	12844	4312	98.77		1.23
90-10:WYO:HA-PC-DB-SoilS	90	0	10	18193	12844	4312	97.43		2.57
80-20:WYO:HA-PC-DB-SoilS	80	0	20	18193	12844	4312	94.41		5.59

B.2: Exhaust Gas Oxygen Analysis

Table B.5: Exhaust O_2 mole fraction and exhaust equivalence ratio for TXL and TXL:DB blended fuels.

	Equivalence Ratio	O_2 (mole fraction)	$O_{2,A}$ (mole fraction)	Equivalence Ratio (Gas Analysis)
TXL	0.8	0.036	0.21	0.82864
	0.9	0.031	0.21	0.85244
	1	0.004	0.21	0.98096
	1.1	0.002	0.21	0.99048
	1.2	0.002	0.21	0.99048
95-5 TXL:LA-PC-DB-SepS	0.8	0.02	0.21	0.9048
	0.9	0.013	0.21	0.93812
	1	0.01	0.21	0.9524
	1.1	0.004	0.21	0.98096
	1.2	0.001	0.21	0.99524
90-10 TXL:LA-PC-DB-SepS	0.8	0.041	0.21	0.80484
	0.9	0.028	0.21	0.86672
	1	0.02	0.21	0.9048
	1.1	0.001	0.21	0.99524
	1.2	0.001	0.21	0.99524
80-20 TXL:LA-PC-DB-SepS	0.8	0.023	0.21	0.89052
	0.9	0.012	0.21	0.94288
	1	0.003	0.21	0.98572
	1.1	0.001	0.21	0.99524
	1.2	0.001	0.21	0.99524
95-5 TXL:HA-PC-DB-SoilS	0.8	0.034	0.21	0.83816
	0.9	0.023	0.21	0.89052
	1	0.009	0.21	0.95716
	1.1	0.004	0.21	0.98096
	1.2	0.001	0.21	0.99524
90-10 TXL:HA-PC-DB-SoilS	0.8	0.033	0.21	0.84292
	0.9	0.012	0.21	0.94288
	1	0.009	0.21	0.95716
	1.1	0.006	0.21	0.97144
	1.2	0.003	0.21	0.98572

Table B.6: Exhaust O_2 mole fraction and exhaust equivalence ratio for WYO and WYO:DB blended fuels.

	Equivalence Ratio	O_2 (mole fraction)	$O_{2,A}$ (mole fraction)	Equivalence Ratio (Gas Analysis)
WYO	0.8	0.026	0.21	0.87624
	0.9	0.013	0.21	0.93812
	1	0.005	0.21	0.9762
	1.1	0.002	0.21	0.99048
	1.2	0.001	0.21	0.99524
95-5 WYO:LA-PC-DB-SepS	0.8	0.029	0.21	0.86196
	0.9	0.01	0.21	0.9524
	1	0.004	0.21	0.98096
	1.1	0.001	0.21	0.99524
	1.2	0.001	0.21	0.99524
90-10 WYO:LA-PC-DB-SepS	0.8	0.036	0.21	0.82864
	0.9	0.017	0.21	0.91908
	1	0.005	0.21	0.9762
	1.1	0.001	0.21	0.99524
	1.2	0.001	0.21	0.99524
80-20 WYO:LA-PC-DB-SepS	0.8	0.029	0.21	0.86196
	0.9	0.017	0.21	0.91908
	1	0.002	0.21	0.99048
	1.1	0.001	0.21	0.99524
	1.2	0.001	0.21	0.99524
95-5 WYO:HA-PC-DB-SoilS	0.8	0.032	0.21	0.84768
	0.9	0.022	0.21	0.89528
	1	0.01	0.21	0.9524
	1.1	0.002	0.21	0.99048
	1.2	0.001	0.21	0.99524
90-10 WYO:HA-PC-DB-SoilS	0.8	0.045	0.21	0.7858
	0.9	0.029	0.21	0.86196
	1	0.007	0.21	0.96668
	1.1	0.003	0.21	0.98572
	1.2	0.001	0.21	0.99524
80-20 WYO:HA-PC-DB-SoilS	0.8	0.045	0.21	0.7858
	0.9	0.02	0.21	0.9048
	1	0.005	0.21	0.9762

B.3: Exhaust Gas CO and CO_2 Analysis

Table B.7: CO and CO_2 emissions from TXL and TXL:DB blended fuels.

	Equivalence Ratio	CO (ppm)	X_{CO2}	X_{CO2} (%)
TXL	0.8	29	0.1876	18.76
	0.9	27	0.1826	18.26
	1	60	0.205	20.5
	1.1	1505	0.211	21.1
	1.2	2504	0.1888	18.88
95-5 TXL:LA-PC-DB-SepS	0.8	89	0.1889	18.89
	0.9	45	0.1949	19.49
	1	59	0.1996	19.96
	1.1	3368	0.2073	20.73
	1.2	7681	0.2044	20.44
90-10 TXL:LA-PC-DB-SepS	0.8	211	0.1698	16.98
	0.9	136	0.1816	18.16
	1	4800	0.2014	20.14
	1.1	11437	0.1883	18.83
	1.2	12777	0.1882	18.82
80-20 TXL:LA-PC-DB-SepS	0.8	28	0.1866	18.66
	0.9	9	0.1944	19.44
	1	414	0.203	20.3
	1.1	4084	0.2017	20.17
	1.2	1445	0.1977	19.77
95-5 TXL:HA-PC-DB-SoilS	0.8	68	0.1795	17.95
	0.9	758	0.1964	19.64
	1	1072	0.1953	19.53
	1.1	6593	0.1966	19.66
	1.2	8512	0.2006	20.06
90-10 TXL:HA-PC-DB-SoilS	0.8	305	0.1783	17.83
	0.9	624	0.1793	17.93
	1	4942	0.1989	19.89
	1.1	2886	0.2029	20.29
	1.2	7512	0.1879	18.79

Table B.8: CO and CO_2 emissions from WYO and WYO:DB blended fuels.

	Equivalence Ratio	CO (ppm)	X_{CO2}	X_{CO2} (%)
WYO	0.8	49	0.1831	18.31
	0.9	156	0.1976	19.76
	1	1169	0.2025	20.25
	1.1	7652	0.2027	20.27
	1.2	11409	0.203	20.3
95-5 WYO:LA-PC-DB-SepS	0.8	225	0.1798	17.98
	0.9	389	0.1956	19.56
	1	2415	0.1997	19.97
	1.1	9624	0.1969	19.69
	1.2	12195	0.1886	18.86
90-10 WYO:LA-PC-DB-SepS	0.8	34	0.1751	17.51
	0.9	457	0.191	19.1
	1	2246	0.1996	19.96
	1.1	6483	0.1986	19.86
	1.2	12202	0.1943	19.43
80-20 WYO:LA-PC-DB-SepS	0.8	14	0.179	17.9
	0.9	341	0.1902	19.02
	1	1960	0.2017	20.17
	1.1	5124	0.1979	19.79
	1.2	11190	0.1939	19.39
95-5 WYO:HA-PC-DB-SoilS	0.8	414	0.1784	17.84
	0.9	750	0.1861	18.61
	1	3030	0.1933	19.33
	1.1	8280	0.1961	19.61
	1.2	11793	0.1901	19.01
90-10 WYO:HA-PC-DB-SoilS	0.8	90	0.1648	16.48
	0.9	254	0.1806	18.06
	1	2021	0.1966	19.66
	1.1	5871	0.1989	19.89
	1.2	7979	0.20	20.00

B.4: Burnt Fraction Analysis

B.4.1: Derivation of Burnt Fraction

Beginning with a stoichiometric reaction:

$CH_hO_o + (1 + h/4 - o/2)\ (O_2 + 3.76\ N_2\ ) \rightarrow\ CO_2 + (h/2)\ H_2O$; Eq. B.1

Introduce a variable for the equivalence ratio:

Let ϕ = stoich O_2 /actual O_2= 1/(1+ Excess O_{2Fr}) = (1 + h/4 –o/2)/a; Eq.B.2

Solving for a

$a= (1 + h/4 –o/2) (1+ E_{O2, fr})$ or $(1 + h/4 –o/2)= a/(1+ E_{O2, fr}) = a\phi$; Eq.B.3

Solving for X02:

$X_{O2} = (a – z(1 + h/4 –o/2))/\{z + (a – z(1 + h/4 –o/2))+ 3.76\ a\}= \{a – z\ a\ \phi\}/\{z + a – z\ a\phi+ 3.76\ a\}=\{1– z\ \phi\}/\{z/a + 1 – z\phi+ 3.76\ \}$; Eq.B.4

Solving for z and introducing:

$X_{O2a} = 1/(1 + 3.76)$; Eq.B.5

Yeilds:

$X_{O2}\ \{z/a + 1/ X_{O2,a} – z\phi\} = \{1– z\ \phi\}$; Eq.B.6

With further rearrangement:

$z = [1- \{X_{O2}/ X_{O2,a}\}]/\{\ \phi + X_{O2}/a-\ \phi X_{O2}\}$; Eq.B.7

Look at:

$\phi + X_{O2}/a-\ \phi X_{O2} = \phi\ [1+ X_{O2}/a\phi-\ X_{O2}] = \phi\ [1+ X_{O2}/a\phi-\ X_{O2}] = \phi\ \{ 1+ X_{O2}\ [(1 + h/4 –o/2)-1]\}= \phi\ \{ 1+ X_{O2}\ (h/4 –o/2)\}$; Eq.B.8

Then:

$z = [1- \{X_{O2}/ X_{O2,a}\}]/[\phi\ \{ 1+ X_{O2}\ (h/4 –o/2)\}]$; Eq.B.9

Applying the approximation:

$\phi\ \{ 1+ X_{O2}\ (h/4 –o/2)\} \approx \phi$ because $X_{O2} \approx 0.03$; Eq.B.10

For many solid fuels:

$h/4\text{-}O/2 \approx 0.2$; Eq.B.11

Thus:

$X_{O2} * 0.2 = 0.006 << 1$; Eq.B.12

Leads to the final result:

$Z \approx [1/\phi] [1- \{X_{O2}/ X_{O2,a}\}]$; Eq.B.13

B.4.2: Tables

Table B.9: Burnt fraction from TXL and TXL:DB blended fuels.

	Equivalence Ratio	O_2 (mole fraction)	$O_{2,A}$ (mole fraction)	Burnt Fraction
TXL	0.8	0.036	0.21	1.04
	0.9	0.031	0.21	0.95
	1	0.004	0.21	0.98
	1.1	0.002	0.21	0.90
	1.2	0.002	0.21	0.83
95-5 TXL:LA-PC-DB-SepS	0.8	0.02	0.21	1.13
	0.9	0.013	0.21	1.04
	1	0.01	0.21	0.95
	1.1	0.004	0.21	0.89
	1.2	0.001	0.21	0.83
90-10 TXL:LA-PC-DB-SepS	0.8	0.041	0.21	1.01
	0.9	0.028	0.21	0.96
	1	0.02	0.21	0.90
	1.1	0.001	0.21	0.90
	1.2	0.001	0.21	0.83
80-20 TXL:LA-PC-DB-SepS	0.8	0.023	0.21	1.11
	0.9	0.012	0.21	1.05
	1	0.003	0.21	0.99
	1.1	0.001	0.21	0.90
	1.2	0.001	0.21	0.83
95-5 TXL:HA-PC-DB-SoilS	0.8	0.034	0.21	1.05
	0.9	0.023	0.21	0.99
	1	0.009	0.21	0.96
	1.1	0.004	0.21	0.89
	1.2	0.001	0.21	0.83
90-10 TXL:HA-PC-DB-SoilS	0.8	0.033	0.21	1.05
	0.9	0.012	0.21	1.05
	1	0.009	0.21	0.96
	1.1	0.006	0.21	0.88
	1.2	0.003	0.21	0.82

Table B.10: Burnt fraction from WYO and WYO:DB blended fuels.

	Equivalence Ratio	O_2 (mole fraction)	$O_{2,A}$ (mole fraction)	Burnt Fraction
WYO	0.8	0.026	0.21	1.10
	0.9	0.013	0.21	1.04
	1	0.005	0.21	0.98
	1.1	0.002	0.21	0.90
	1.2	0.001	0.21	0.83
95-5 WYO:LA-PC-DB-SepS	0.8	0.029	0.21	1.08
	0.9	0.01	0.21	1.06
	1	0.004	0.21	0.98
	1.1	0.001	0.21	0.90
	1.2	0.001	0.21	0.83
90-10 WYO:LA-PC-DB-SepS	0.8	0.036	0.21	1.04
	0.9	0.017	0.21	1.02
	1	0.005	0.21	0.98
	1.1	0.001	0.21	0.90
	1.2	0.001	0.21	0.83
80-20 WYO:LA-PC-DB-SepS	0.8	0.029	0.21	1.08
	0.9	0.017	0.21	1.02
	1	0.002	0.21	0.99
	1.1	0.001	0.21	0.90
	1.2	0.001	0.21	0.83
95-5 WYO:HA-PC-DB-SoilS	0.8	0.032	0.21	1.06
	0.9	0.022	0.21	0.99
	1	0.01	0.21	0.95
	1.1	0.002	0.21	0.90
	1.2	0.001	0.21	0.83
90-10 WYO:HA-PC-DB-SoilS	0.8	0.045	0.21	0.98
	0.9	0.029	0.21	0.96
	1	0.007	0.21	0.97
	1.1	0.003	0.21	0.90
	1.2	0.001	0.21	0.83
80-20 WYO:HA-PC-DB-SoilS	0.8	0.045	0.21	0.98
	0.9	0.02	0.21	1.01
	1	0.005	0.21	0.98

B.5: Exhaust Gas NO_X Analysis

Table B.11: NO_x emissions from TXL and TXL:DB blended fuels.

	Equivalence Ratio	NO_x (ppm)	NO_x (g/kg)	NOx (kg/GJ)	NOx (lb/mmBTU)	NO_x (Corrected to 3% O_2)
TXL	0.8	671	5.09	0.36	0.82924	694
	0.9	626	4.88	0.34	0.79482	629
	1	429	2.98	0.21	0.48511	375
	1.1	229	1.53	0.11	0.24988	198
	1.2	134	1.00	0.07	0.16242	116
95-5 TXL:LA-PC-DB-SepS	0.8	584	4.39	0.31	0.71826	553
	0.9	493	3.59	0.25	0.58781	450
	1	352	2.50	0.18	0.40979	317
	1.1	155	1.05	0.07	0.17102	135
	1.2	101	0.68	0.05	0.11069	87
90-10 TXL:LA-PC-DB-SepS	0.8	758	6.32	0.45	1.03884	807
	0.9	642	5.00	0.35	0.82310	635
	1	264	1.81	0.13	0.29831	250
	1.1	140	0.99	0.07	0.16332	121
	1.2	137	0.97	0.07	0.15883	118
80-20 TXL:LA-PC-DB-SepS	0.8	666	5.03	0.36	0.83557	641
	0.9	617	4.47	0.32	0.74311	561
	1	296	2.05	0.15	0.34072	257
	1.1	135	0.92	0.07	0.15361	116
	1.2	101	0.71	0.05	0.11875	87
95-5 TXL:HA-PC-DB-SoilS	0.8	760	5.72	0.43	1.00075	777
	0.9	572	3.92	0.29	0.68600	551
	1	247	1.70	0.13	0.29741	221
	1.1	151	1.00	0.08	0.17572	132
	1.2	115	0.74	0.06	0.13004	99
90-10 TXL:HA-PC-DB-SoilS	0.8	388	3.01	0.22	0.50852	395
	0.9	266	2.05	0.15	0.34607	242
	1	207	1.41	0.10	0.23771	185
	1.1	110	0.74	0.05	0.12513	97
	1.2	115	0.82	0.06	0.13776	100

Table B.12: NO_x emissions from WYO and WYO:DB blended fuels.

	Equivalence Ratio	NO_x (ppm)	NO_x (g/kg)	NOx (kg/GJ)	NOx (lb/mmBTU)	NO_x (Corrected to 3% O_2)
WYO	0.8	836	8.13	0.45	1.03996	818
	0.9	695	6.26	0.34	0.80070	635
	1	522	4.57	0.25	0.58393	458
	1.1	314	2.66	0.15	0.34009	272
	1.2	68	0.57	0.03	0.07226	59
95-5 WYO:LA-PC-DB-SepS	0.8	772	7.55	0.42	0.97953	768
	0.9	516	4.63	0.26	0.60138	464
	1	357	3.11	0.17	0.40346	312
	1.1	127	1.08	0.06	0.14046	109
	1.2	61	0.53	0.03	0.06939	53
90-10 WYO:LA-PC-DB-SepS	0.8	961	9.54	0.54	1.25671	994
	0.9	747	6.78	0.38	0.89358	697
	1	533	4.59	0.26	0.60477	468
	1.1	114	0.97	0.05	0.12731	98
	1.2	62	0.52	0.03	0.06876	53
80-20 WYO:LA-PC-DB-SepS	0.8	910	8.62	0.50	1.17067	905
	0.9	700	6.23	0.36	0.84604	653
	1	403	3.35	0.20	0.45570	349
	1.1	106	0.89	0.05	0.12024	91
	1.2	81	0.67	0.04	0.09095	70
95-5 WYO:HA-PC-DB-SoilS	0.8	707	6.83	0.39	0.90787	715
	0.9	583	5.39	0.31	0.71644	558
	1	458	4.03	0.23	0.53565	412
	1.1	219	1.85	0.11	0.24604	190
	1.2	101	0.86	0.05	0.11487	87
90-10 WYO:HA-PC-DB-SoilS	0.8	856	8.68	0.52	1.20206	934
	0.9	647	5.98	0.36	0.82837	643
	1	393	3.31	0.20	0.45816	348
	1.1	287	2.34	0.14	0.32453	250
	1.2	90	0.72	0.04	0.10020	78
80-20 WYO:HA-PC-DB-	0.8	797	7.50	0.49	1.13104	869
	0.9	563	4.65	0.30	0.70149	533
	1	216	1.66	0.11	0.25090	190

B.6: Fuel Nitrogen Conversion Efficiency Analysis

Table B.13: Fuel nitrogen conversion from TXL and TXL:DB blended fuels.

	Equivalence Ratio	X_{NO}	X_{CO}	X_{CO2}	c/n	N_{CONV} (%)
TXL	0.8	0.000671	0.000029	0.1876	54.68	19.55
	0.9	0.000626	0.000027	0.1826	54.68	18.74
	1	0.000429	0.00006	0.205	54.68	11.44
	1.1	0.000229	0.001505	0.211	54.68	5.89
	1.2	0.000134	0.002504	0.1388	54.68	5.19
95-5 TXL:LA-PC-DBSepS	0.8	0.000584	0.000089	0.1889	49.94	15.43
	0.9	0.000493	0.000045	0.1949	49.94	12.63
	1	0.000352	0.000059	0.1996	49.94	8.80
	1.1	0.000155	0.003368	0.2073	49.94	3.67
	1.2	0.000101	0.007681	0.2044	49.94	2.38
90-10 TXL:LA-PC-DBSepS	0.8	0.000758	0.000211	0.1698	45.94	20.48
	0.9	0.000642	0.000136	0.1816	45.94	16.23
	1	0.000264	0.0048	0.2014	45.94	5.88
	1.1	0.00014	0.011437	0.1883	45.94	3.22
	1.2	0.000137	0.012777	0.1882	45.94	3.13
80-20 TXL:LA-PC-DBSepS	0.8	0.000666	0.000028	0.1866	39.55	14.12
	0.9	0.000617	0.000009	0.1944	39.55	12.55
	1	0.000296	0.000414	0.203	39.55	5.76
	1.1	0.000135	0.004084	0.2017	39.55	2.59
	1.2	0.000101	0.001445	0.1977	39.55	2.01
95-5 TXL:HA-PC-DB-SoilS	0.8	0.000388	0.000305	0.1795	51.49	11.11
	0.9	0.000266	0.000624	0.1964	51.49	6.95
	1	0.000207	0.004942	0.1953	51.49	5.32
	1.1	0.00011	0.002886	0.1966	51.49	2.84
	1.2	0.000115	0.007512	0.2006	51.49	2.85
90-10 TXL:HA-PC-DB-SoilS	0.8	0.00076	0.000068	0.1783	48.51	20.67
	0.9	0.000572	0.000758	0.1793	48.51	15.41
	1	0.000247	0.001072	0.1989	48.51	5.99
	1.1	0.000151	0.006593	0.2029	48.51	3.50
	1.2	0.000115	0.008512	0.1879	48.51	2.84

Table B.14: Fuel nitrogen conversion from WYO and WYO:DB blended fuels.

	Equivalence Ratio	X_{NO}	X_{CO}	X_{CO2}	c/n	N_{CONV} (%)
WYO	0.8	0.000836	0.000049	0.1831	70.48	32.17
	0.9	0.000695	0.000156	0.1976	70.48	24.77
	1	0.000522	0.001169	0.2025	70.48	18.07
	1.1	0.000314	0.007652	0.2027	70.48	10.52
	1.2	0.000002	0.011409	0.203	70.48	0.07
95-5 WYO:LA-PC-DBSepS	0.8	0.000772	0.000225	0.1798	63.52	27.24
	0.9	0.000516	0.000389	0.1956	63.52	16.72
	1	0.000357	0.002415	0.1997	63.52	11.22
	1.1	0.000127	0.009624	0.1969	63.52	3.91
	1.2	0.000061	0.012195	0.1886	63.52	1.93
90-10 WYO:LA-PC-DBSepS	0.8	0.000961	0.000034	0.1751	57.67	31.65
	0.9	0.000747	0.000457	0.191	57.67	22.50
	1	0.000533	0.002246	0.1996	57.67	15.23
	1.1	0.000114	0.006483	0.1986	57.67	3.21
	1.2	0.000062	0.012202	0.1943	57.67	1.73
80-20 WYO:LA-PC-DBSepS	0.8	0.00091	0.000014	0.179	48.42	24.62
	0.9	0.0007	0.000341	0.1902	48.42	17.79
	1	0.000403	0.00196	0.2017	48.42	9.58
	1.1	0.000106	0.005124	0.1979	48.42	2.53
	1.2	0.000081	0.01119	0.1939	48.42	1.91
90-0 WYO:HA-PC-DB-SoilS	0.8	0.000707	0.000414	0.1784	65.88	26.05
	0.9	0.000583	0.00075	0.1861	65.88	20.56
	1	0.000458	0.00303	0.1933	65.88	15.37
	1.1	0.000219	0.00828	0.1961	65.88	7.06
	1.2	0.000101	0.011793	0.1901	65.88	3.30
95-5 WYO:HA-PC-DB-SoilS	0.8	0.000856	0.00009	0.1648	61.60	31.98
	0.9	0.000647	0.000254	0.1806	61.60	22.04
	1	0.000393	0.002021	0.1966	61.60	12.19
	1.1	0.000287	0.005871	0.1989	61.60	8.63
	1.2	0.00009	0.007979	0.2	61.60	2.67
80-20 WYO SoilSurf-DB	0.8	0.000797	0.00006	0.1662	53.86	25.82
	0.9	0.000563	0.000161	0.1892	53.86	16.01
	1	0.000216	0.003425	0.1997	53.86	5.73

APPENDIX C: UNCERTAINTY ANALYSIS

C.1 Introduction

This analysis follows the example of Kegel (1996) which is based upon Kline and McClintock. (1953) Equivalence ratio and emission concentration are both measured values and thus have a degree of uncertainty associated with them. The equivalence ratio is a ratio of the stoichiometric air to the provided air, both of which are ratios of air to fuel. All of these are measured values and will have uncertainty. The emission concentration is measured by the flue gas analyzer and thus the analyzer sets the uncertainty interval. Table C.1 presents all the instruments used in experiments and the uncertainty parameters associated with each instrument from the instruction manual (2003) that accompanies the instrument. The total instrument uncertainty is the root sum squared of the resolution and random uncertainty.

Table C.1 Instrument uncertainty parameters.

Instrument	Resolution	Units	Random	Units	Total Instrument Unceratinty
Primary Air Flow Meter	2.5	SCFH	4	SCFH	4.72
Secondary Air Flow Meter	0.5	SLPM	15	SLPM	15.01
O_2 Analyzer	0.1	%	0.1	%	Varies
CO_2 Analyzer	0.01	%	3	%	Varies
CO Analyzer	1	ppm	4	%	Varies
NO_x Analyzer	0.1	ppm	4	ppm	4.00

C.2 Equivalence Ratio Uncertainty

Beginning with the definition of equivalence ratio:

$$\phi = \frac{A:F_{ST}}{A:F_{PROVIDED}} = \frac{\left(\frac{A}{F}\right)_{ST}}{\left(\frac{A}{F}\right)_{PROVIDED}} = ; \text{ Eq.C.2.1}$$

Deleting the fuel flow rate because it is constant for both A:F:

$$\frac{A_{ST}}{A_{PROVIDED}} = \frac{\left(A_E + A_M + A_{SEC}\right)_{ST}}{\left(A_E + A_M + A_{SEC}\right)_{PROVIDED}} ; \text{ Eq.C.2.2}$$

To determine the uncertainty, the partial derivative of equivalence ratio to each independent variable must be calculated:

$$\frac{\partial \phi}{\partial A_{E:ST}} = \frac{1}{\left(A_E + A_M + A_{SEC}\right)_{PROVIDED}} ; \text{ Eq.C.2.3}$$

$$\frac{\partial \phi}{\partial A_{M:ST}} = \frac{1}{\left(A_E + A_M + A_{SEC}\right)_{PROVIDED}} ; \text{ Eq.C.2.4}$$

$$\frac{\partial \phi}{\partial A_{SEC:ST}} = \frac{1}{\left(A_E + A_M + A_{SEC}\right)_{PROVIDED}} ; \text{ Eq.C.2.5}$$

$$\frac{\partial \phi}{\partial A_{E:PRO}} = -\frac{\left(A_E + A_M + A_{SEC}\right)_{ST}}{\left(A_E + A_M + A_{SEC}\right)^2_{PROVIDED}} ; \text{ Eq.C.2.6}$$

$$\frac{\partial \phi}{\partial A_{M:PRO}} = -\frac{\left(A_E + A_M + A_{SEC}\right)_{ST}}{\left(A_E + A_M + A_{SEC}\right)^2_{PROVIDED}} ; \text{ Eq.C.2.7}$$

$$\frac{\partial \phi}{\partial A_{SEC:PRO}} = -\frac{\left(A_E + A_M + A_{SEC}\right)_{ST}}{\left(A_E + A_M + A_{SEC}\right)^2_{PROVIDED}} ; \text{ Eq.C.2.8}$$

Table C.2 presents the nominal values and pertinent uncertainty values for a sample calculation.

Table C.2: Complete uncertainty analysis for 80-20 WYO:HA-PC-DB-SoilS at an equivalence ratio of 1.0. Note that the uncertainty is plus or minus 2.31% of the nominal value.

	Instrument	Value	$\delta f/\delta x_i$	x_i/ϕ	$s_{xi}=(\delta\phi/\delta x_i)*(x_i/\phi)$	u_{xi}	$s_{xi}*u_{xi}$	$(s_{xi}*u_{xi})^2$	Contribution
x_1	Eductor Stoich Air	110	0.00171	110.00	0.19	0.02487	0.00468	0.0000219	4.12
x_2	Motive Stoich Air	100	0.00171	100.00	0.17	0.02736	0.00468	0.0000219	4.12
x_3	Secondary Stoich Air	374	0.00171	374.00	0.64	0.02327	0.01491	0.0002222	41.75
x_4	Eductor Provided Air	110	0.00171	110.00	0.19	0.02487	0.00468	0.0000219	4.12
x_5	Motive Provided Air	100	0.00171	100.00	0.17	0.02736	0.00468	0.0000219	4.12
x_6	Secondary Provided Air	374	0.00171	374.00	0.64	0.02327	0.01491	0.0002222	41.75
ϕ	Equivalence Ratio	1.00					Sum	0.0005321	100

Table C.3 presents the uncertainty of equivalence ratio for the TXL fuels.

Table C.3: Percentage uncertainty in equivalence ratio for TXL and TXL:DB blended fuels.

	Equivalence Ratio	Uncertainty (%)	Average (%)
TXL	0.8	2.03	2.31
	0.9	2.15	
	1	2.30	
	1.1	2.48	
	1.2	2.60	
95-5 TXL:LA-PC-DB-SepS	0.8	1.99	2.28
	0.9	2.10	
	1	2.25	
	1.1	2.43	
	1.2	2.63	
90-10 TXL:LA-PC-DB-SepS	0.8	1.99	2.29
	0.9	2.11	
	1	2.26	
	1.1	2.44	
	1.2	2.65	
80-20 TXL:LA-PC-DB-SepS	0.8	1.91	2.20
	0.9	2.02	
	1	2.17	
	1.1	2.34	
	1.2	2.54	
95-5 TXL:HA-PC-DB-SoilS	0.8	2.06	2.37
	0.9	2.18	
	1	2.33	
	1.1	2.52	
	1.2	2.74	
80-20 TXL:HA-PC-DB-SoilS	0.8	2.04	2.34
	0.9	2.15	
	1	2.31	
	1.1	2.50	
	1.2	2.71	

Table C.4 presents the uncertainty of equivalence ratio for the WYO fuels.

Table C.4: Percentage uncertainty in equivalence ratio for WYO and WYO:DB blended fuels.

	Equivalence Ratio	Uncertainty (%)	Average (%)
WYO	0.8	2.06	2.35
	0.9	2.17	
	1	2.32	
	1.1	2.50	
	1.2	2.72	
95-5 WYO:LA-PC-DB-SepS	0.8	2.06	2.37
	0.9	2.18	
	1	2.34	
	1.1	2.52	
	1.2	2.73	
90-10 WYO:LA-PC-DB-SepS	0.8	2.02	2.33
	0.9	2.14	
	1	2.30	
	1.1	2.48	
	1.2	2.69	
80-20 WYO:LA-PC-DB-SepS	0.8	1.95	2.24
	0.9	2.06	
	1	2.21	
	1.1	2.39	
	1.2	2.60	
95-5 WYO:HA-PC-DB-SoilS	0.8	2.02	2.32
	0.9	2.14	
	1	2.29	
	1.1	2.48	
	1.2	2.69	
90-10 WYO:HA-PC-DB-SoilS	0.8	2.00	2.30
	0.9	2.12	
	1	2.27	
	1.1	2.45	
	1.2	2.66	
80-20 WYO:HA-PC-DB-SoilS	0.8	2.03	2.16
	0.9	2.15	
	1	2.31	

C.3 NO_x Uncertainty

NO_x is measured by the flue gas analyzer. Thus, the instrument is the sole contributor to the uncertainty. As Table C.1 shows, NO_x uncertainty is always plus or minus 4 ppm. Table C.5 presents the uncertainty bands on NO_x as a percentage of the

measured value for TXL and TXL:DB blended fuels. Table C.6 presents the uncertainty bands on NO_x for WYO and WYO:DB blended fuels.

Table C.5: Percentage uncertainty in NO_x for TXL and TXL:DB blended fuels.

	Equivalence Ratio	NO_x (ppm)	Uncertainty (%)	Average (%)
TXL	0.8	671	0.60	1.38
	0.9	626	0.64	
	1	429	0.93	
	1.1	229	1.75	
	1.2	134	2.99	
95-5 TXL:LA-PC-DB-SepS	0.8	584	0.68	1.83
	0.9	493	0.81	
	1	352	1.14	
	1.1	155	2.58	
	1.2	101	3.96	
90-10 TXL:LA-PC-DB-SepS	0.8	758	0.53	1.69
	0.9	642	0.62	
	1	264	1.52	
	1.1	140	2.86	
	1.2	137	2.92	
80-20 TXL:LA-PC-DB-SepS	0.8	666	0.60	1.90
	0.9	617	0.65	
	1	296	1.35	
	1.1	135	2.96	
	1.2	101	3.96	
95-5 TXL:HA-PC-DB-SoilS	0.8	388	1.03	2.32
	0.9	266	1.50	
	1	207	1.93	
	1.1	110	3.64	
	1.2	115	3.48	
90-10 TXL:HA-PC-DB-SoilS	0.8	760	0.53	1.79
	0.9	572	0.70	
	1	247	1.62	
	1.1	151	2.65	
	1.2	115	3.48	

Table C.6: Percentage uncertainty in NO_x WYO and WYO:DB blended fuels.

	Equivalence Ratio	NO_x (ppm)	Uncertainty (%)	Average (%)
WYO	0.8	836	0.48	0.77
	0.9	695	0.58	
	1	522	0.77	
	1.1	314	1.27	
	1.2	2	200.00	
95-5 WYO:LA-PC-DB-SepS	0.8	772	0.52	2.42
	0.9	516	0.78	
	1	357	1.12	
	1.1	127	3.15	
	1.2	61	6.56	
90-10 WYO:LA-PC-DB-SepS	0.8	961	0.42	2.33
	0.9	747	0.54	
	1	533	0.75	
	1.1	114	3.51	
	1.2	62	6.45	
80-20 WYO:LA-PC-DB-SepS	0.8	910	0.44	2.14
	0.9	700	0.57	
	1	403	0.99	
	1.1	106	3.77	
	1.2	81	4.94	
95-5 WYO:HA-PC-DB-SoilS	0.8	707	0.57	1.58
	0.9	583	0.69	
	1	458	0.87	
	1.1	219	1.83	
	1.2	101	3.96	
90-10 WYO:HA-PC-DB-SoilS	0.8	856	0.47	1.59
	0.9	647	0.62	
	1	393	1.02	
	1.1	287	1.39	
	1.2	90	4.44	
80-20 WYO:HA-PC-DB-SoilS	0.8	797	0.50	1.02
	0.9	563	0.71	
	1	216	1.85	

C.4 CO Uncertainty

The flue gas analyzer has a random uncertainty that is a percentage of the reading. Thus, unlike NO_x, the uncertainty in CO changes depending upon the reading. Table C.7 presents the uncertainty in the CO measurements as a percentage of the measurement for TXL and TXL:DB blended fuels.

Table C.7: Percentage uncertainty in CO for TXL and TXL:DB blended fuels. Note that the uncertainty of 80-20 TXL:LA-PC-DB-SepS ϕ = 0.9 is more than double the uncertainty for any other experiment.

	Equivalence Ratio	CO (ppm)	4% of Reading (ppm)	Total Uncertainty	Total Uncertainty (% of Reading)	Average (%)
TXL	0.8	29	1.16	1.53	5.28	4.61
	0.9	27	1.08	1.47	5.45	
	1	60	2.40	2.60	4.33	
	1.1	1505	60.20	60.21	4.00	
	1.2	2504	100.16	100.16	4.00	
95-5 TXL:LA-PC-DB-SepS	0.8	89	3.56	3.70	4.15	4.22
	0.9	45	1.80	2.06	4.58	
	1	59	2.36	2.56	4.34	
	1.1	3368	134.72	134.72	4.00	
	1.2	7681	307.24	307.24	4.00	
90-10 TXL:LA-PC-DB-SepS	0.8	211	8.44	8.50	4.03	4.02
	0.9	136	5.44	5.53	4.07	
	1	4800	192.00	192.00	4.00	
	1.1	11437	457.48	457.48	4.00	
	1.2	12777	511.08	511.08	4.00	
80-20 TXL:LA-PC-DB-SepS	0.8	28	1.12	1.50	5.36	5.84
	0.9	9	0.36	1.06	11.81	
	1	414	16.56	16.59	4.01	
	1.1	4084	163.36	163.36	4.00	
	1.2	1445	57.80	57.81	4.00	
90-10 TXL:HA-PC-DB-SoilS	0.8	305	12.20	12.24	4.01	4.00
	0.9	624	24.96	24.98	4.00	
	1	4942	197.68	197.68	4.00	
	1.1	2886	115.44	115.44	4.00	
	1.2	7512	300.48	300.48	4.00	
95-5 TXL:HA-PC-DB-SoilS	0.8	68	2.72	2.90	4.26	4.05
	0.9	758	30.32	30.34	4.00	
	1	1072	42.88	42.89	4.00	
	1.1	6593	263.72	263.72	4.00	
	1.2	8512	340.48	340.48	4.00	

Table C.8 presents the uncertainty in the CO measurements as a percentage of the measurement for WYO and WYO:DB blended fuels.

Table C.8: Percentage uncertainty in CO for WYO and WYO:DB blended fuels.

	Equivalence Ratio	CO (ppm)	4% of Reading (ppm)	Total Uncertainty	Total Uncertainty (% of Reading)	Average (%)
WYO	0.8	49	1.96	2.20	4.49	4.11
	0.9	156	6.24	6.32	4.05	
	1	1169	46.76	46.77	4.00	
	1.1	7652	306.08	306.08	4.00	
	1.2	11409	456.36	456.36	4.00	
95-5 WYO LA-PC-DB-SepS	0.8	225	9.00	9.06	4.02	4.01
	0.9	389	15.56	15.59	4.01	
	1	2415	96.60	96.61	4.00	
	1.1	9624	384.96	384.96	4.00	
	1.2	12195	487.80	487.80	4.00	
90-10 WYO LA-PC-DB-SepS	0.8	34	1.36	1.69	4.96	4.19
	0.9	457	18.28	18.31	4.01	
	1	2246	89.84	89.85	4.00	
	1.1	6483	259.32	259.32	4.00	
	1.2	12202	488.08	488.08	4.00	
80-20 WYO LA-PC-DB-SepS	0.8	14	0.56	1.15	8.19	4.84
	0.9	341	13.64	13.68	4.01	
	1	1960	78.40	78.41	4.00	
	1.1	5124	204.96	204.96	4.00	
	1.2	11190	447.60	447.60	4.00	
95-5 WYO HA-PC-DB-SoilS	0.8	414	16.56	16.59	4.01	4.00
	0.9	750	30.00	30.02	4.00	
	1	3030	121.20	121.20	4.00	
	1.1	8280	331.20	331.20	4.00	
	1.2	11793	471.72	471.72	4.00	
90-10 WYO LA-PC-DB-SoilS	0.8	90	3.60	3.74	4.15	4.03
	0.9	254	10.16	10.21	4.02	
	1	2021	80.84	80.85	4.00	
	1.1	5871	234.84	234.84	4.00	
	1.2	7979	319.16	319.16	4.00	
80-20 WYO: HA-PC-DB-SoilS	0.8	60	2.40	2.60	4.33	4.13
	0.9	161	6.44	6.52	4.05	
	1	3425	137.00	137.00	4.00	

APPENDIX D: EXPERIMENT REPETITION

D.1 Introduction

The 90-10 TXL:LA-PC-DB-SepS, 80-20 TXL:LA-PC-DB-SepS, WYO, and 80-20 WYO:LA-PC-DB-SepS experiments were repeated to investigate how the combustion performance can vary with day to day fluctuations. Time constraints and equipment failure made more repetition experiments impossible. All experimental parameters mirrored those of the original. Full statistical analysis was not done on the repetition data. Thus, these results should be used to draw qualitative conclusions only. The results will be presented in the same order as they were presented in Chapter 5.

D.1 O_2 and Equivalence Ratio

Figure D.1 presents the data of the TXL:DB blended fuels equivalence ratio repetition experiments. The figure shows that there was fluctuation between the original data and the repetition data. As the flame got closer to stoichiometric, the span of the data fluctuations decreased. The largest difference was found in the 90:10 TXL:LA-PC-DB-SepS experiments with the equivalence ratio of 1.0.

Figure D.2 presents the data of the WYO and WYO:DB blended fuels equivalence ratio repetition experiments. The figure shows that these fuels had better repeatability. All repeat data points lie within the uncertainty intervals of the original data points. The best agreement was found in the pure WYO experiments with the equivalence ratio of 1.0.

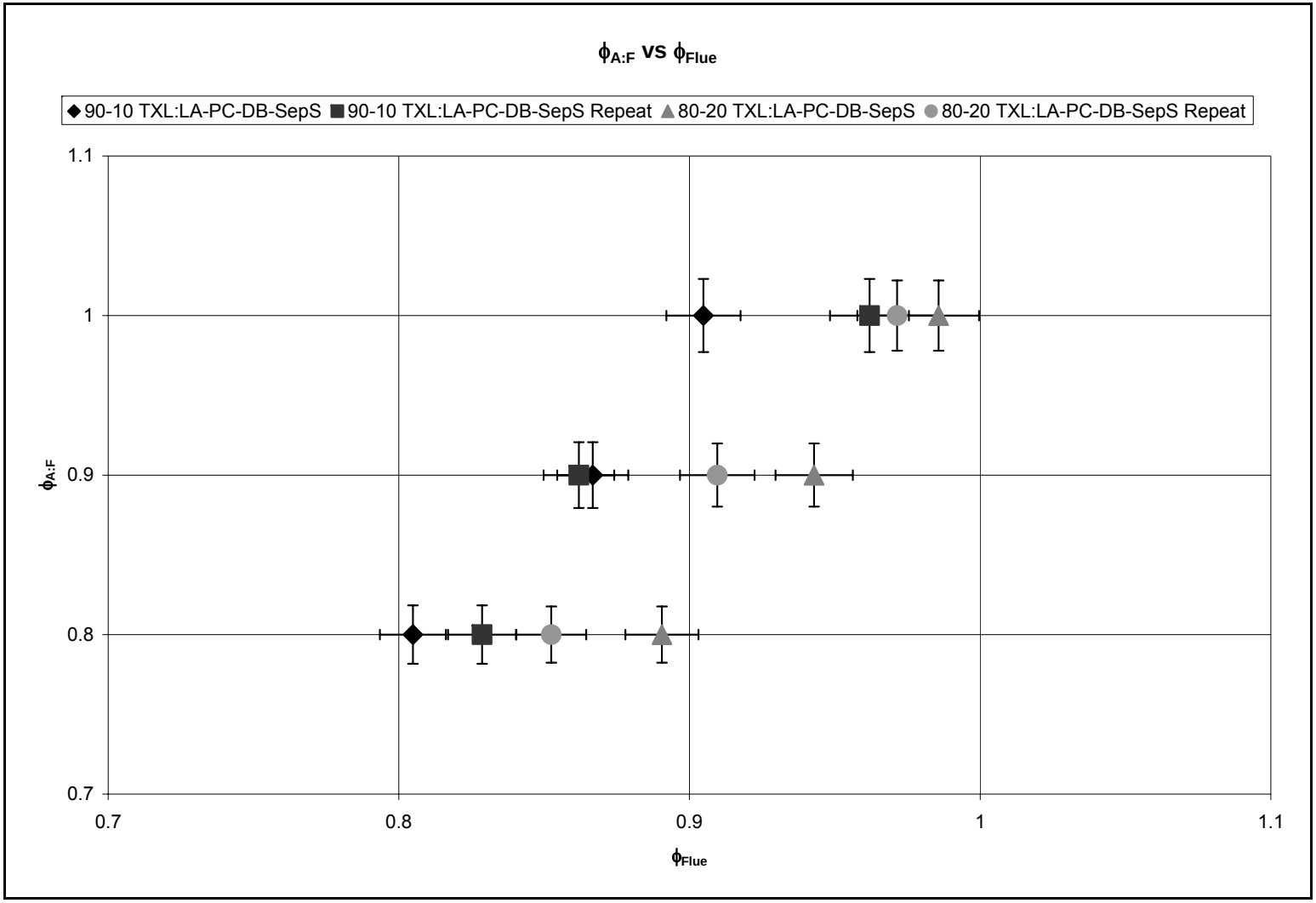

Figure D.1: Repetition of equivalence ratio experiments for TXL:DB blended fuels. Note that some repetition data points were far from their corresponding original data points.

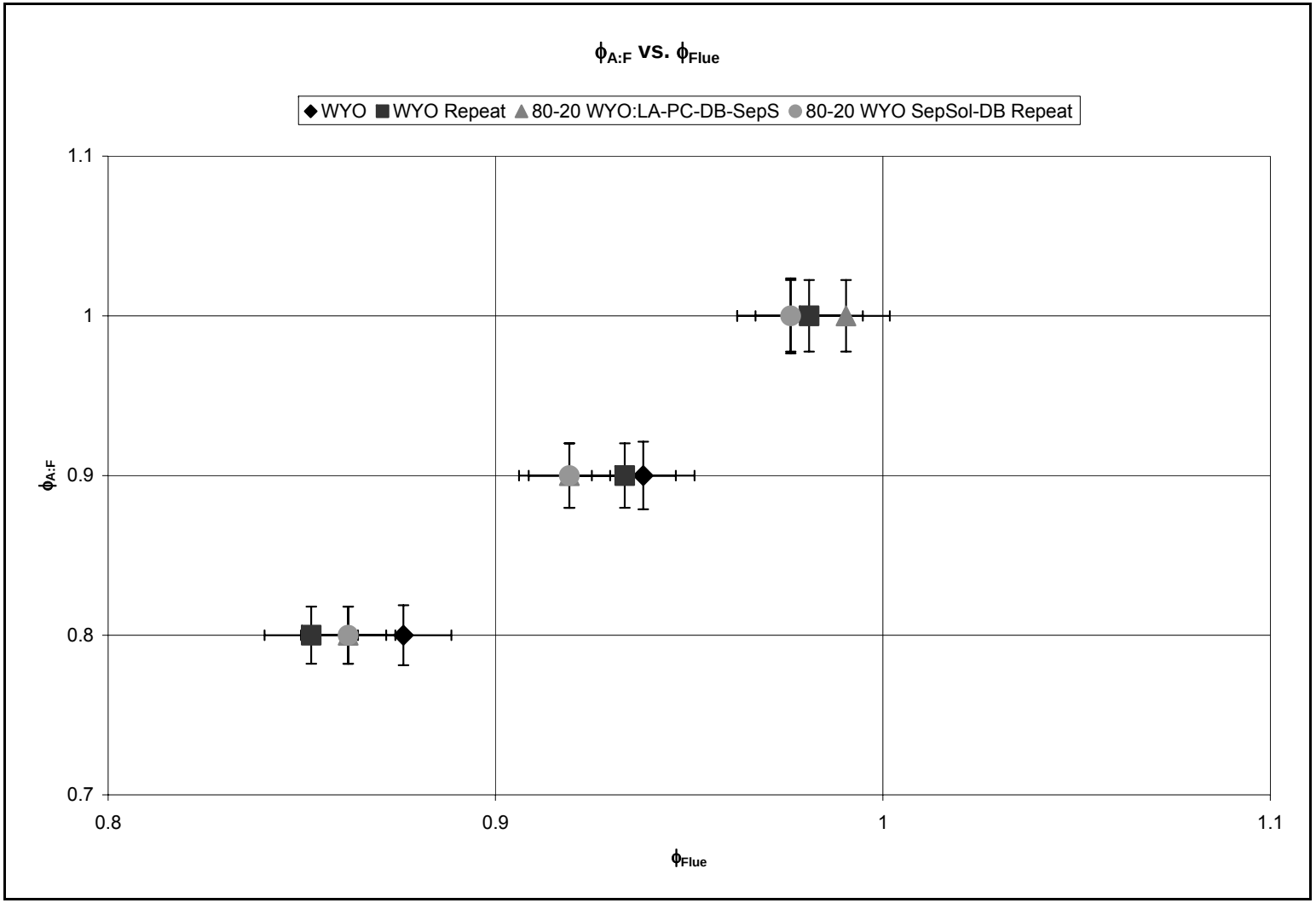

Figure D.2: Repetition of equivalence ratio experiments for WYO and WYO:DB blended fuels. Note that the data points overlapped better for these fuels than for TXL:DB blended fuels.

D.3 CO_2 and CO Emissions

Figures D.3 and D.4 present the CO_2 and CO emissions from repeating the TXL:DB blended fuels experiments. Figure D.3 shows that there was little variation in the emission of CO_2. Most fluctuations were within the uncertainty limits of the data points. The most fluctuation occurred at the very lean and very rich limit. At stoichiometric combustion all of the data points overlapped. Figure D.4 shows that the original data and the repetition data agreed very well in the lean and stoichiometric regimes. In the rich regime, there was fluctuation between the original and repetition data.

Figures D.5 and D.6 present the CO_2 and CO emissions from repeating the WYO and WYO:DB blended fuels experiments. As in the case with the TXL:DB blended fuels, the CO_2 emissions agreed pretty well between the original data and the repetition data. There was slightly more spread than the TXL:DB blended fuels showed, but data points were still within the uncertainty bounds of the data points. Similarly, the CO emissions in the lean regime were in good agreement between the original data and the repetition data. In stoichiometric combustion, the data points did not overlap quite as well as they did for TXL:DB blended fuels. In the slightly rich regime, the data points had significant fluctuation. In the very rich regime, the repetition data points overlapped reasonably well with the original data points.

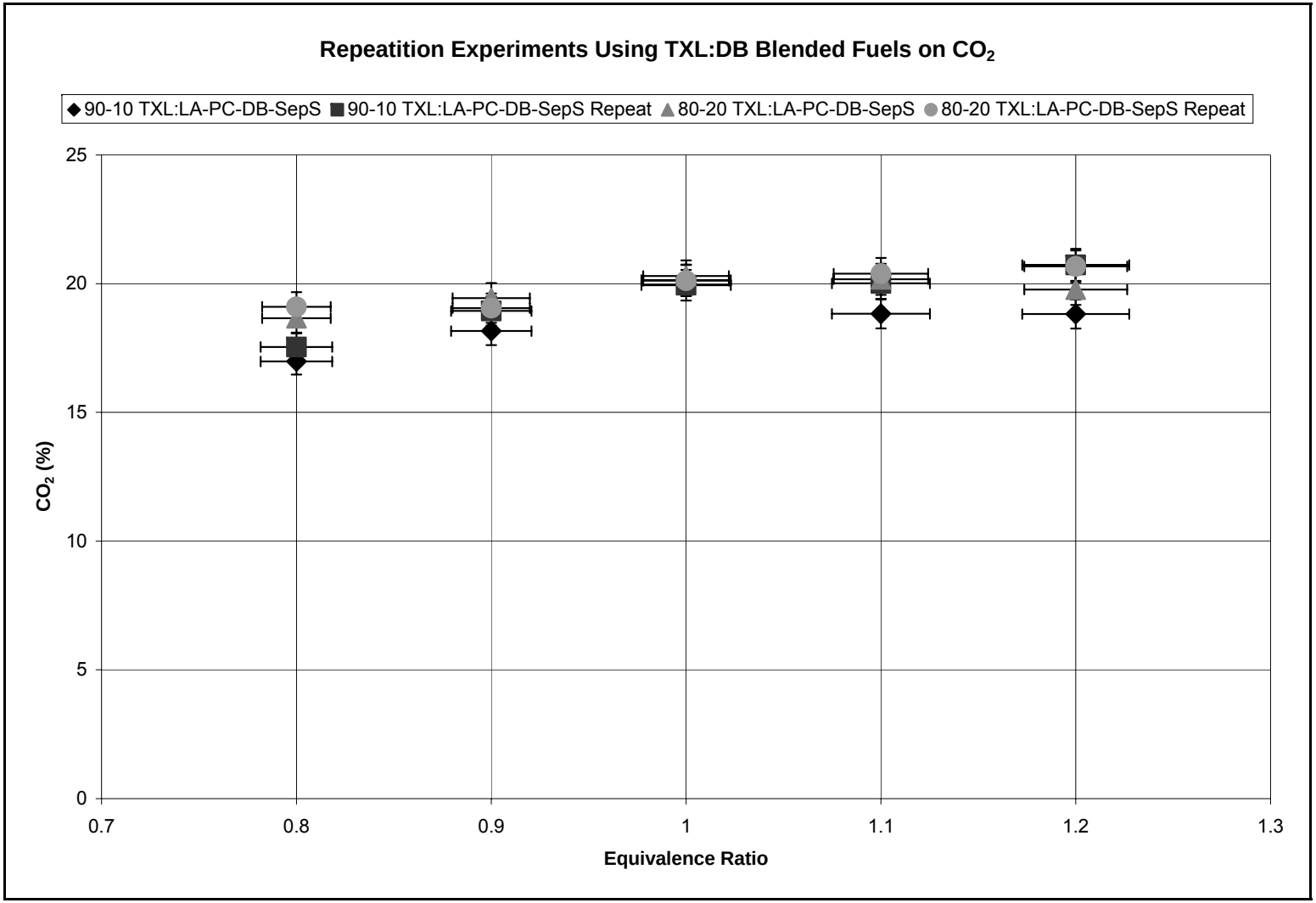

Figure D.3: Repetition of CO_2 emissions experiments for TXL:DB blended fuels. Note that in general the data points overlapped within the uncertainty bounds of the data points.

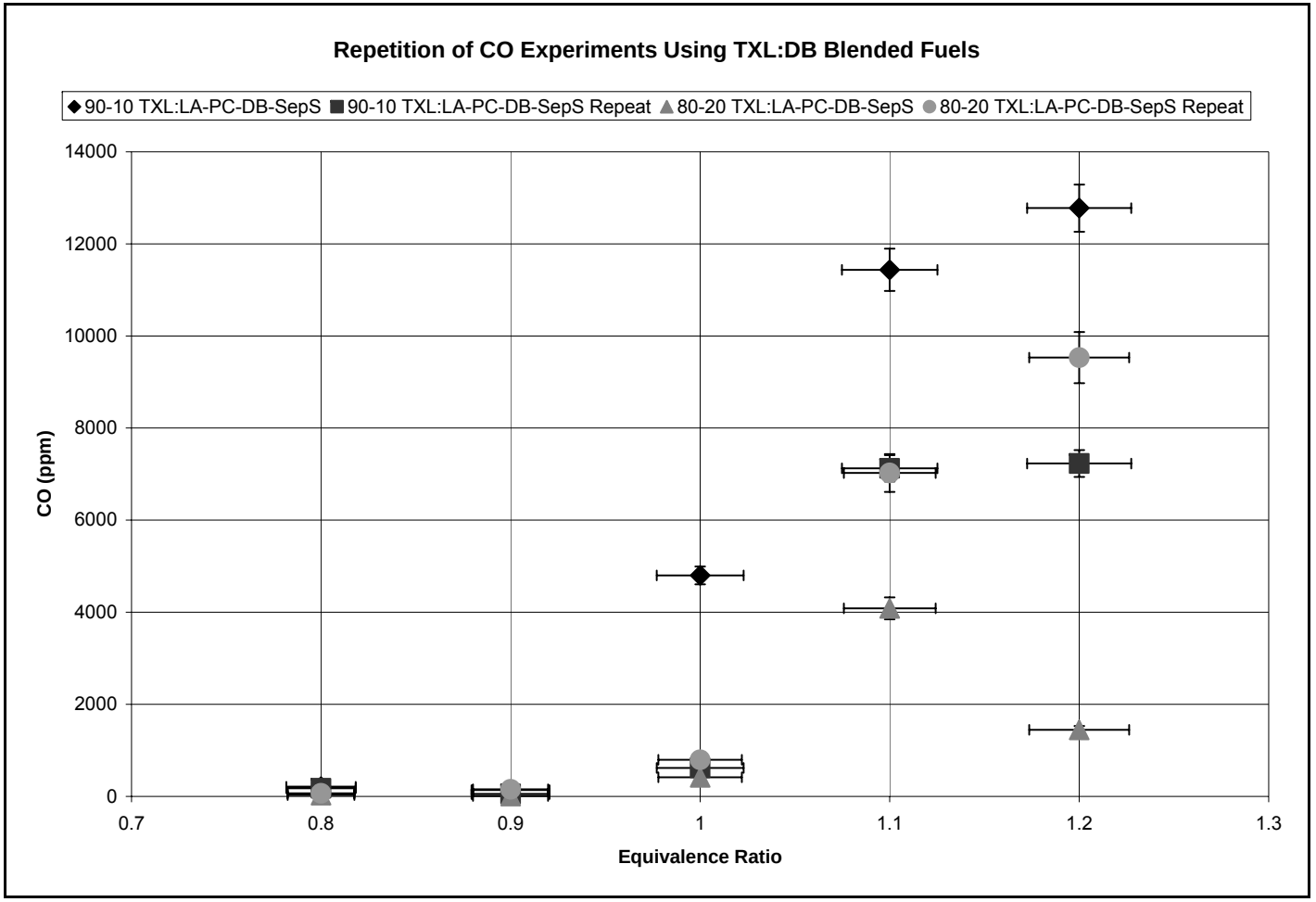

Figure D.4: Repetition of CO emissions experiments for TXL:DB blended fuels. In the lean regime, the repeated experiments matched well with the original data. In general, the data points matched well in stoichiometric combustion. The original 90:10 TXL:LA-PC-DB-SepS data point was different in stoichiometric combustion. In the rich regime, there was variation between the original data and the repeated experiments.

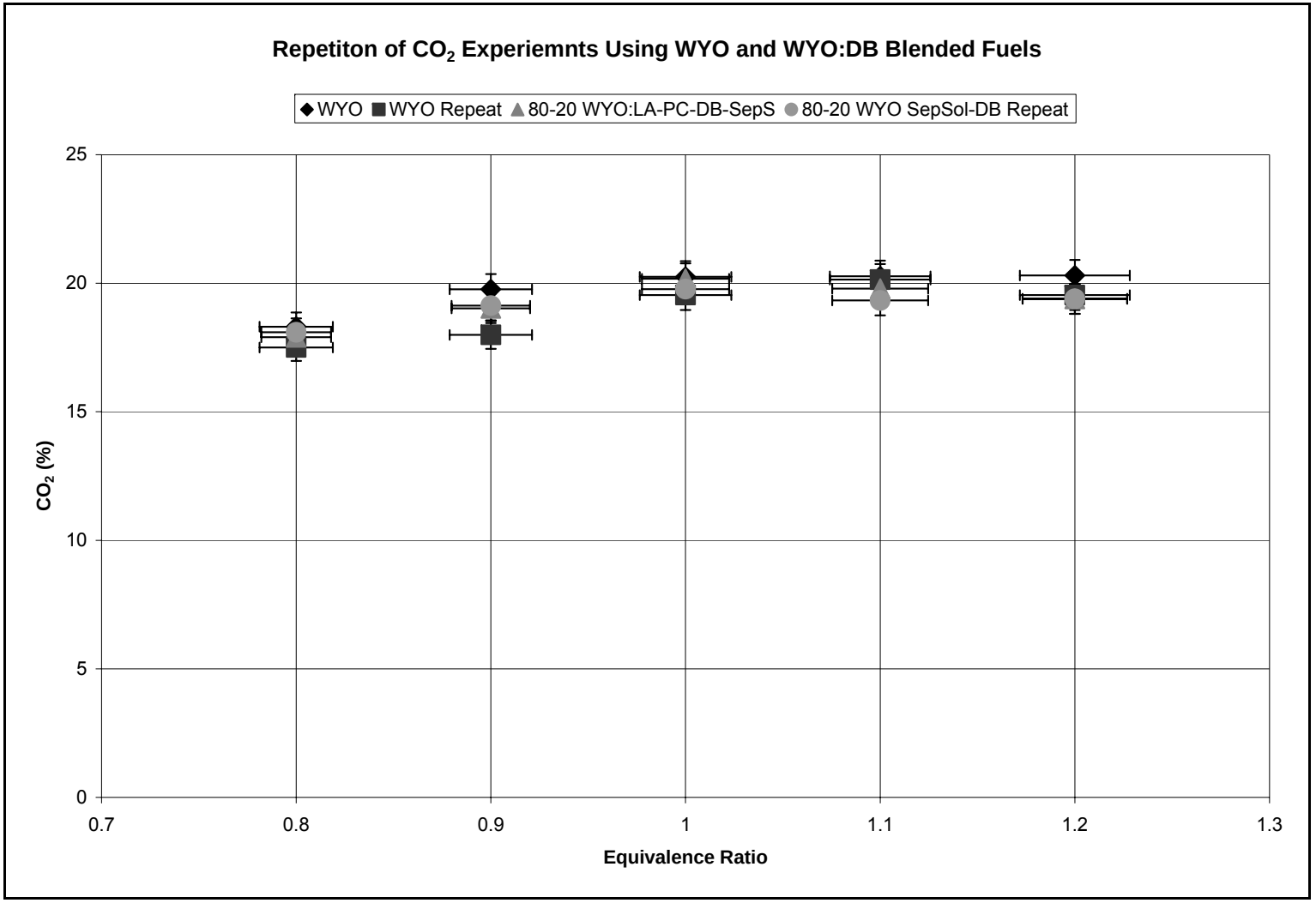

Figure D.5: Repetition of CO_2 emissions experiments for WYO and WYO:DB blended fuels. Note that the original data points overlapped fairly well with the repetition data points.

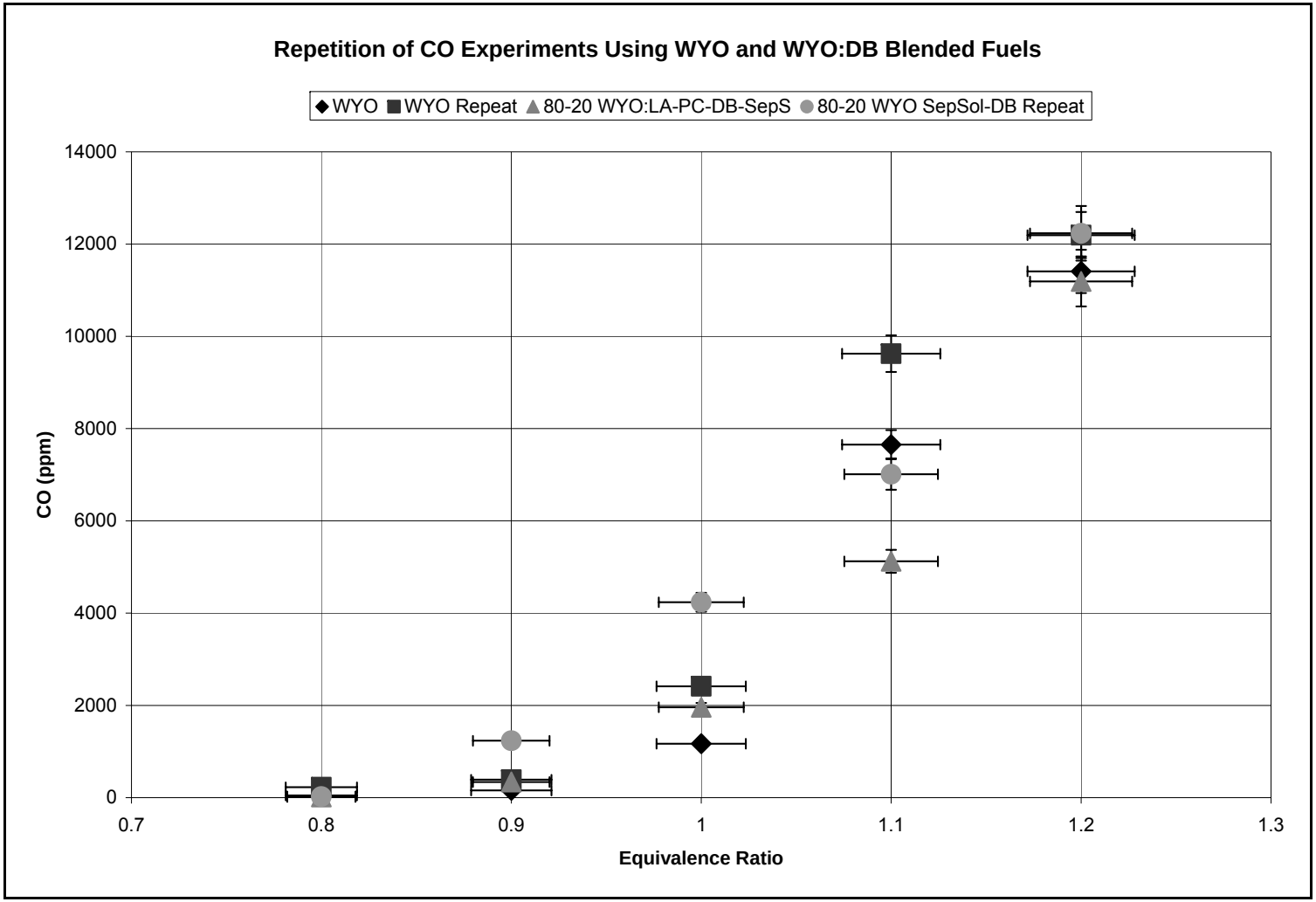

Figure D.6: Repetition of CO emissions experiments for WYO and WYO:DB blended fuels. In the lean regime, the original and repetition data points overlapped well. In the stoichiometric and rich regimes, fluctuations began to appear.

D.4 Burnt Fraction

Figures D.7 and D.8 present the burnt fractions from repetition experiments using TXL:DB blended fuels and WYO and WYO:DB blended fuels, respectively. As Figure D.7 shows, there was some variation in the lean regime. As the flame became closer to stoichiometric, these fluctuations decreased in magnitude. Once the flame became rich, all of the data points agreed. As Figure D.7 shows, the TXL:DB blended fuels did show slightly more fluctuation between the original and repetition data, but even these fluctuations were rather small.

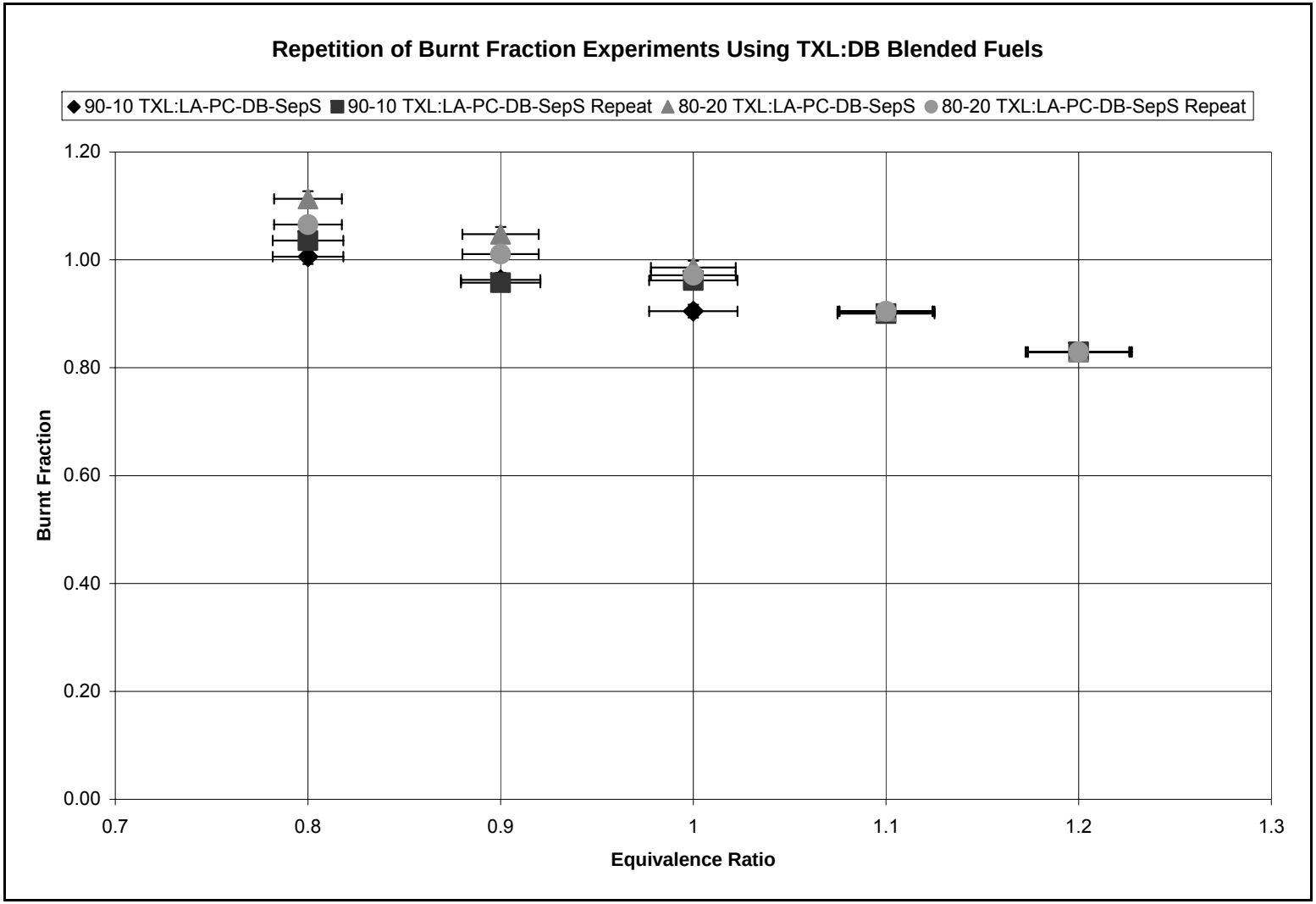

Figure D.7: Repetition of burnt fraction experiments for TXL:DB blended fuels. The original and repetition data points agreed reasonably well.

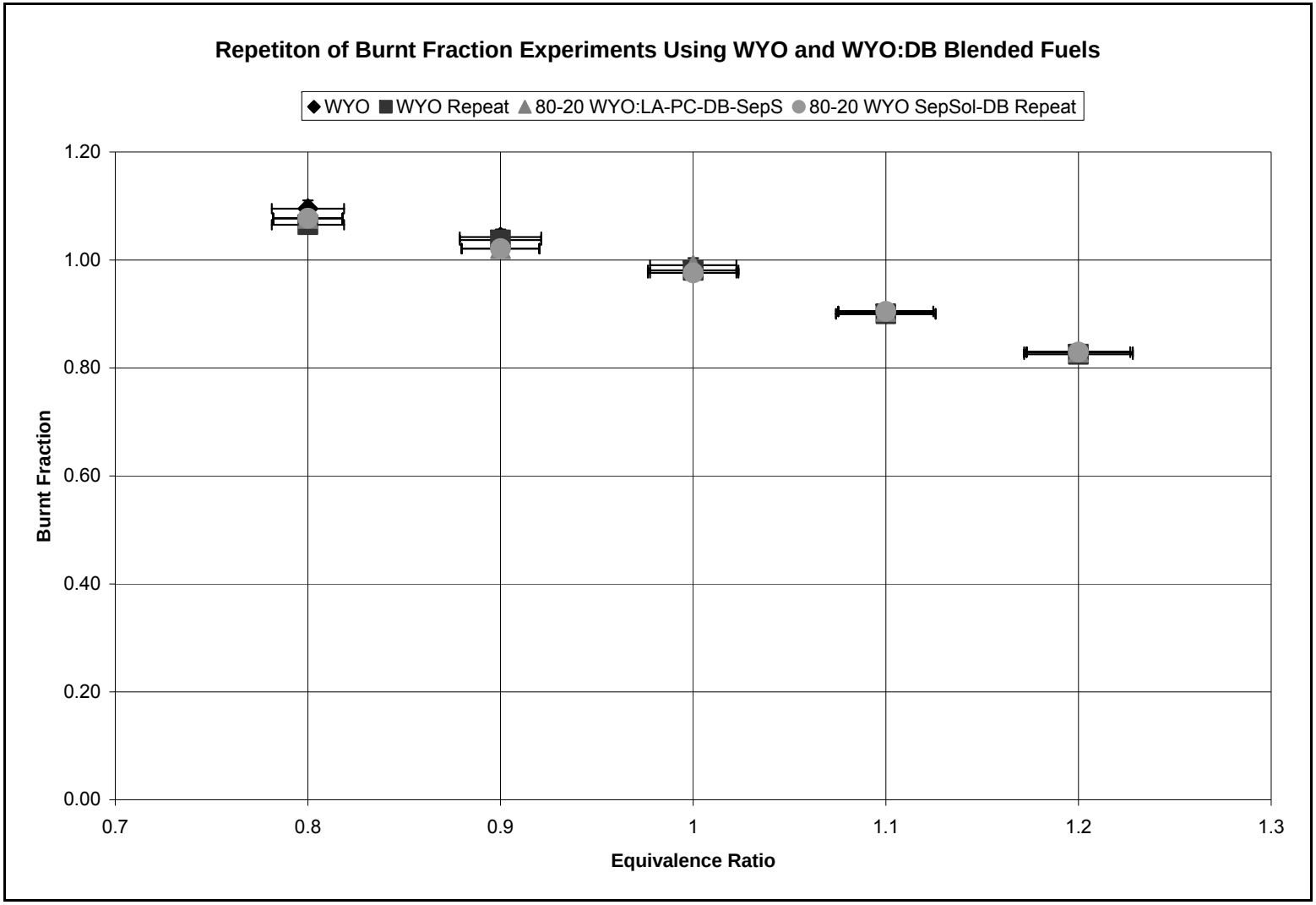

Figure D.8: Repetition of burnt fraction experiments for WYO and WYO:DB blended fuels. The original and repetition data points agreed even better than the TXL:DB blended fuels experiments.

D.5 NO_x Emissions

Figure D.9 presents the NO_x emissions data from repetition experiments using TXL:DB blended fuels. Figure D.10 presents the NO_x data corrected to 3% O_2. As the figures show, there was some fluctuation in the amount of NO_x produced in the lean regime. But, the fluctuation was rather small. In the rich regime, there was very little fluctuation between the original data and the repetition data. As Figure D.10 shows, the fluctuation between the data points did get slightly enhanced by correcting NO_x to 3% O_2.

Figures D.11 and D.12 present the NO_x emissions (uncorrected and corrected) from repetition experiments using WYO and WYO:DB blended fuels. In general, the WYO and WYO:DD blended fuels showed more fluctuation between the original and repetition data than the TXL:DB blended fuels. The WYO and WYO:DB blended fuels did not overlap in the rich regime as well as the TXL:DB blended fuels. Correcting the NO_x to 3% O_2 caused the fluctuations to slightly increase.

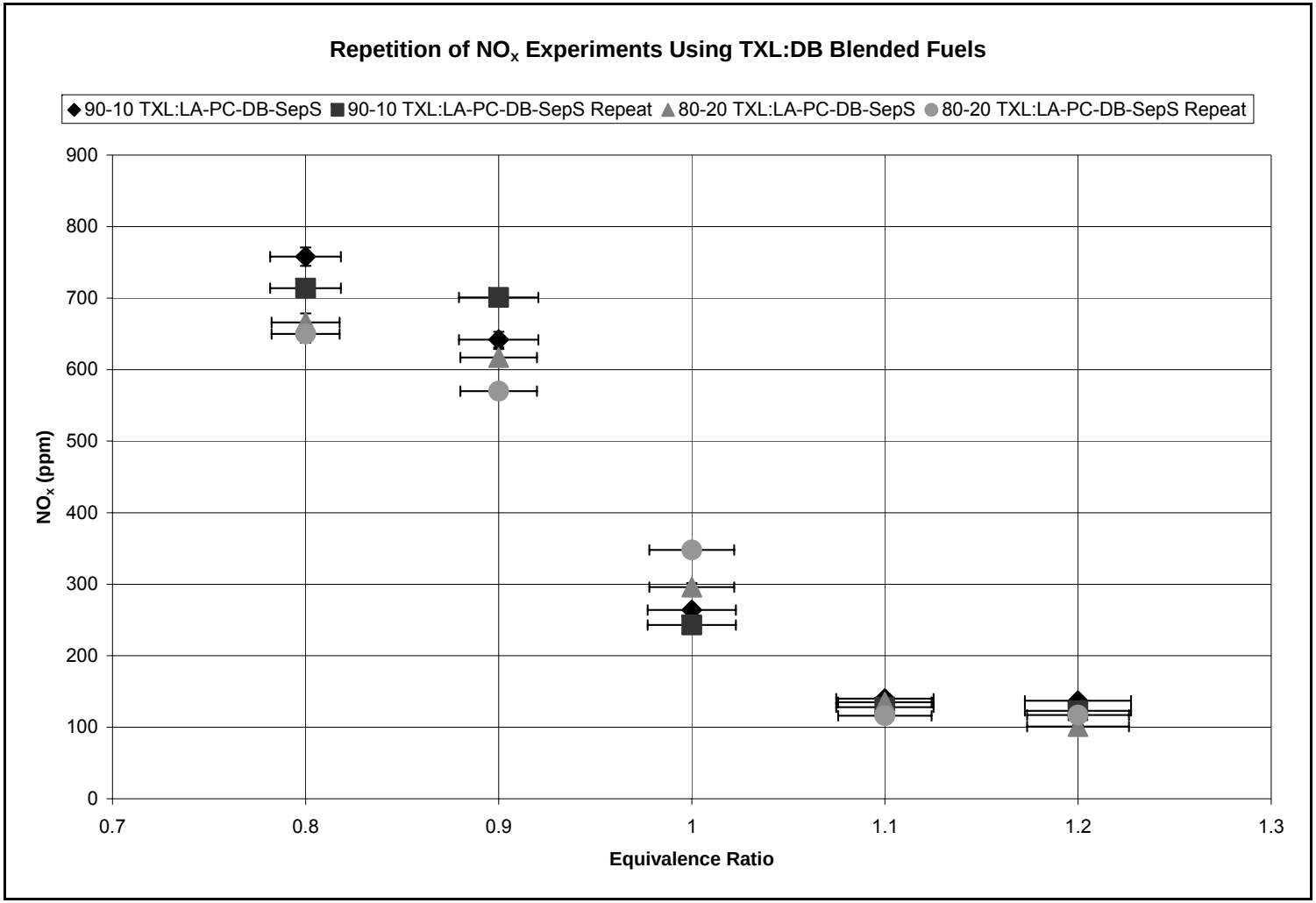

Figure D.9: Repetition of NO_x experiments for TXL:DB blended fuels. In the lean regime, there were some fluctuations between the original data and repetition data. These fluctuations were relatively small. In the rich regime, these fluctuations decreased to almost zero.

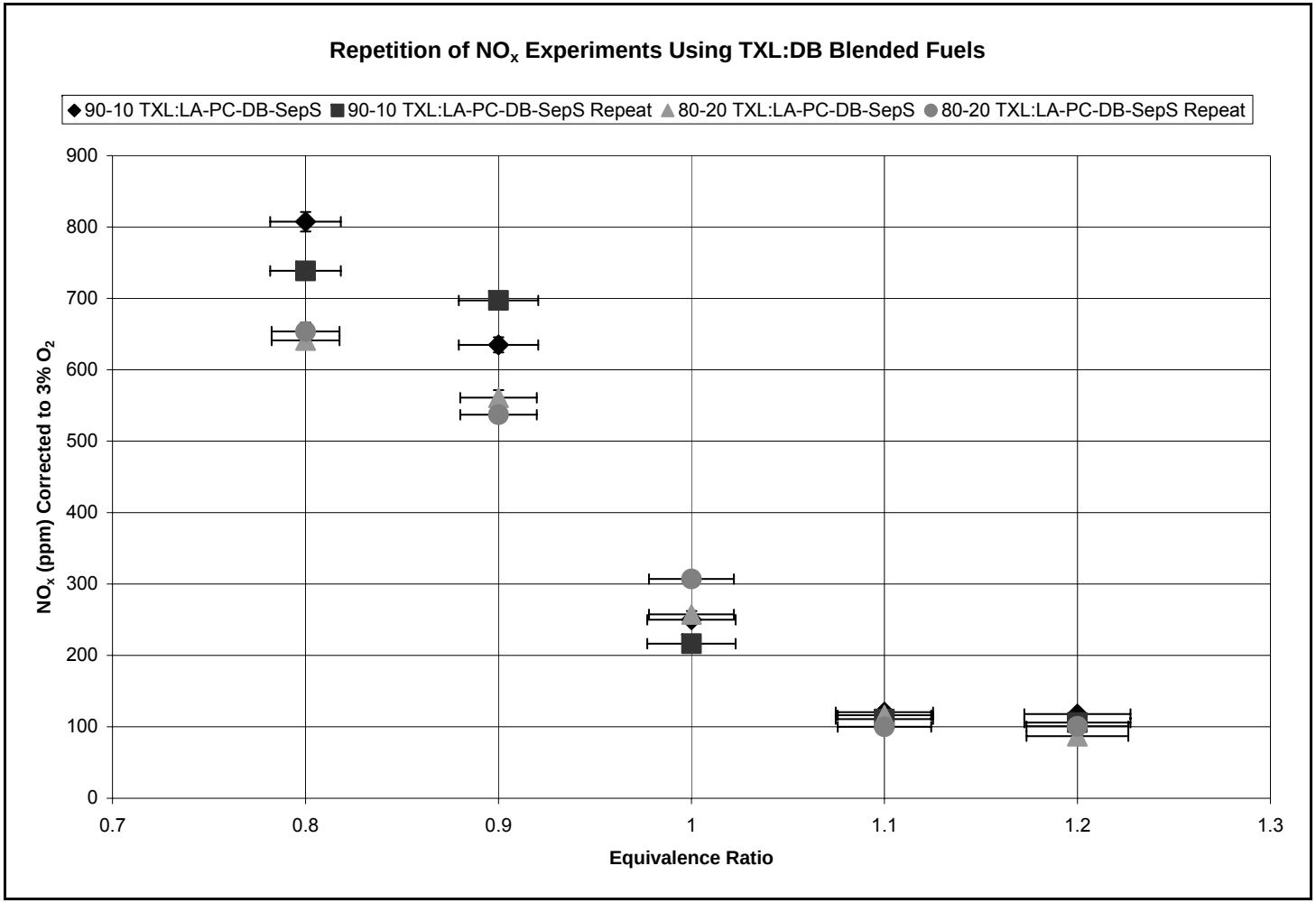

Figure D.10: Repetition of NO_x experiments for TXL:DB blended fuels corrected to 3% O_2. Correcting the NO_x emissions did slightly increase the fluctuation between the original data and the repetition data.

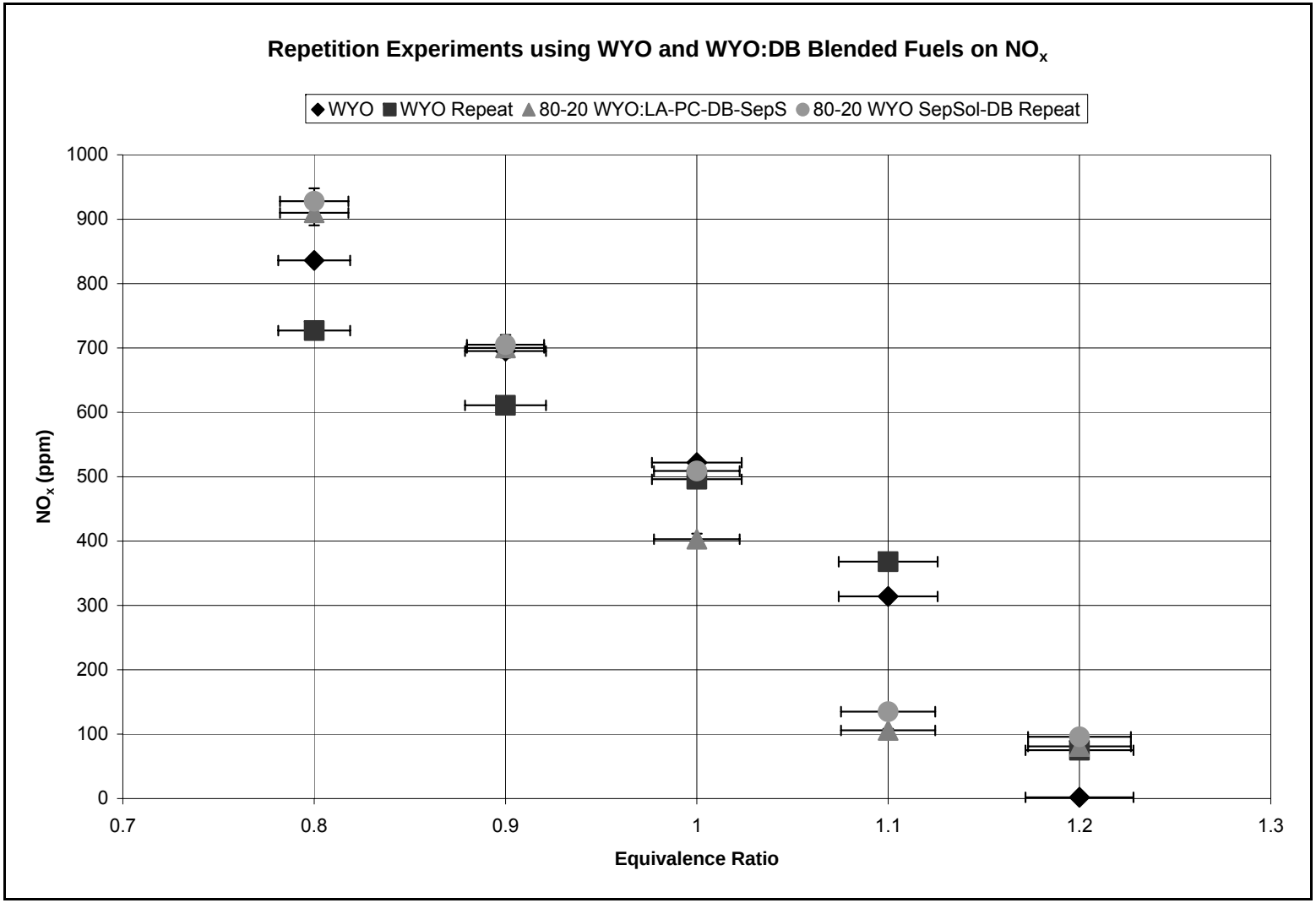

Figure D.11: Repetition of NO_x experiments for WYO and WYO:DB blended fuels. Note that the data points did not over lap as well as for the experiments using TXL:DB blended fuels.

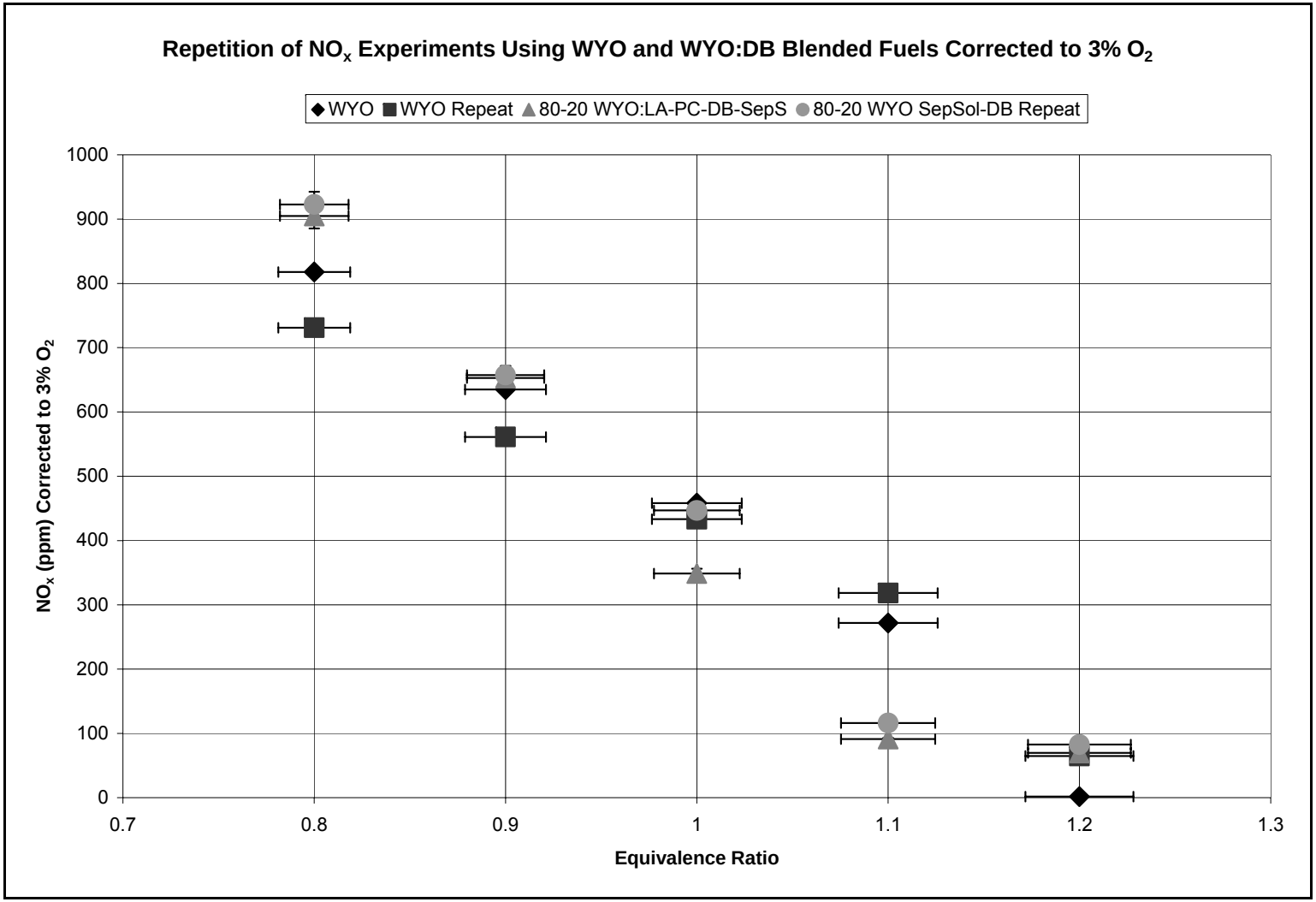

Figure D.12: Repetition of NO_x experiments for WYO and WYO:DB blended fuels corrected to 3% O_2. Correcting the NO_x emissions caused the fluctuations to slightly increase.

D.6 Fuel Nitrogen Conversion Efficiency

Figures D.13 and D.14 present the fuel nitrogen conversion efficiency for the repetition experiments using TXL:DB blended fuels and WYO and WYO:DB blended fuels, respectively. As figure D.13 shows, in the lean regime, the fluctuations between the original and repetition data were relatively small. As the equivalence ratio increased and crossed into the rich regime, the data points practically overlapped. The fuel nitrogen conversion efficiency is constant in the rich regime with very little fluctuation.

As Figure D.14 shows there were more fluctuations using WYO and WYO:DB blended fuels. In general, the fluctuations were still rather small, but they were larger than the fluctuations using TXL:DB blended fuels. In the rich regime, the fluctuations became larger than in the lean regime.

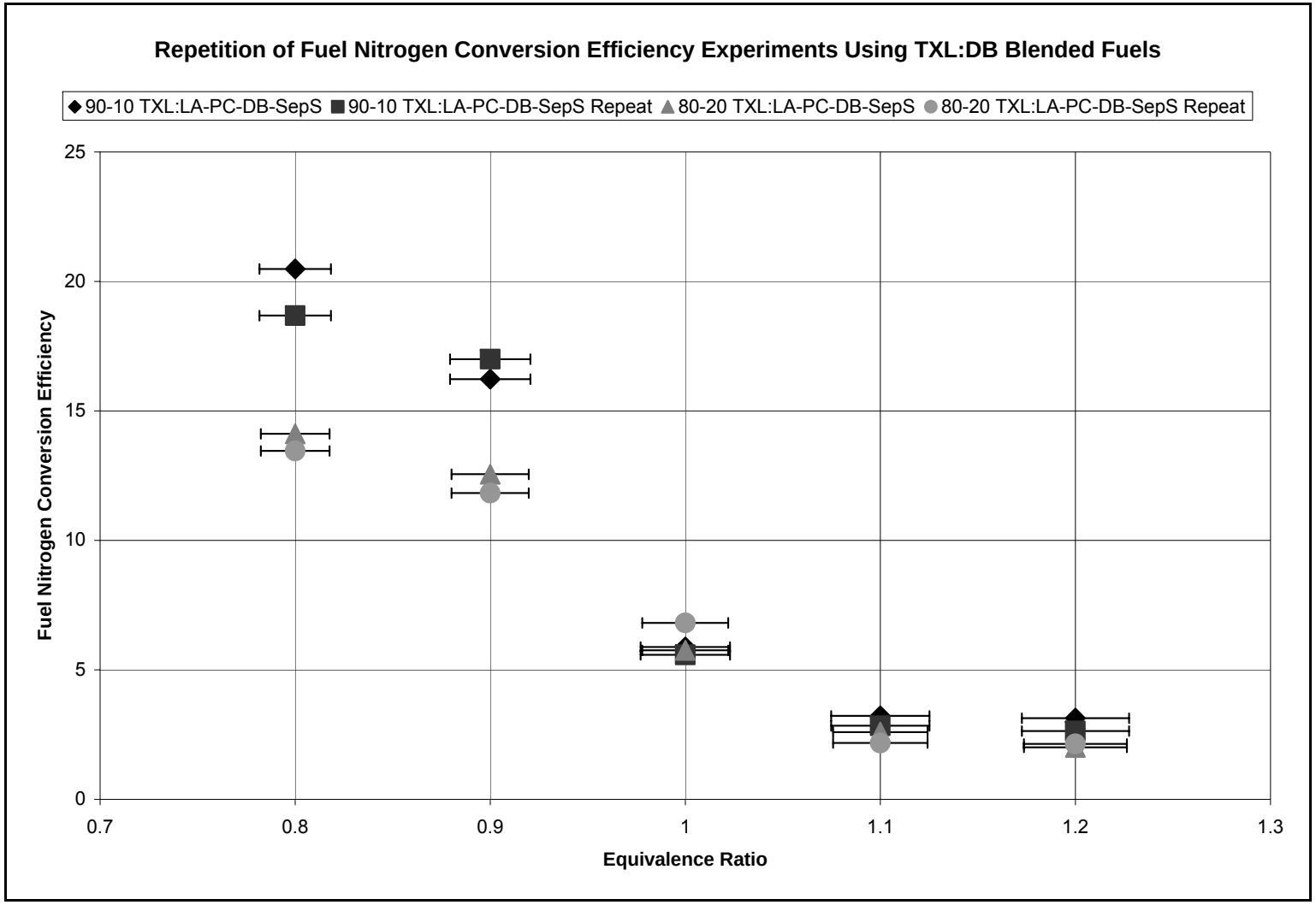

Figure D.13: Repetition of fuel nitrogen conversion efficiency experiments for TXL:DB blended fuels. In the stoichiometric and rich regimes, there were very little fluctuations between the original and repetition data.

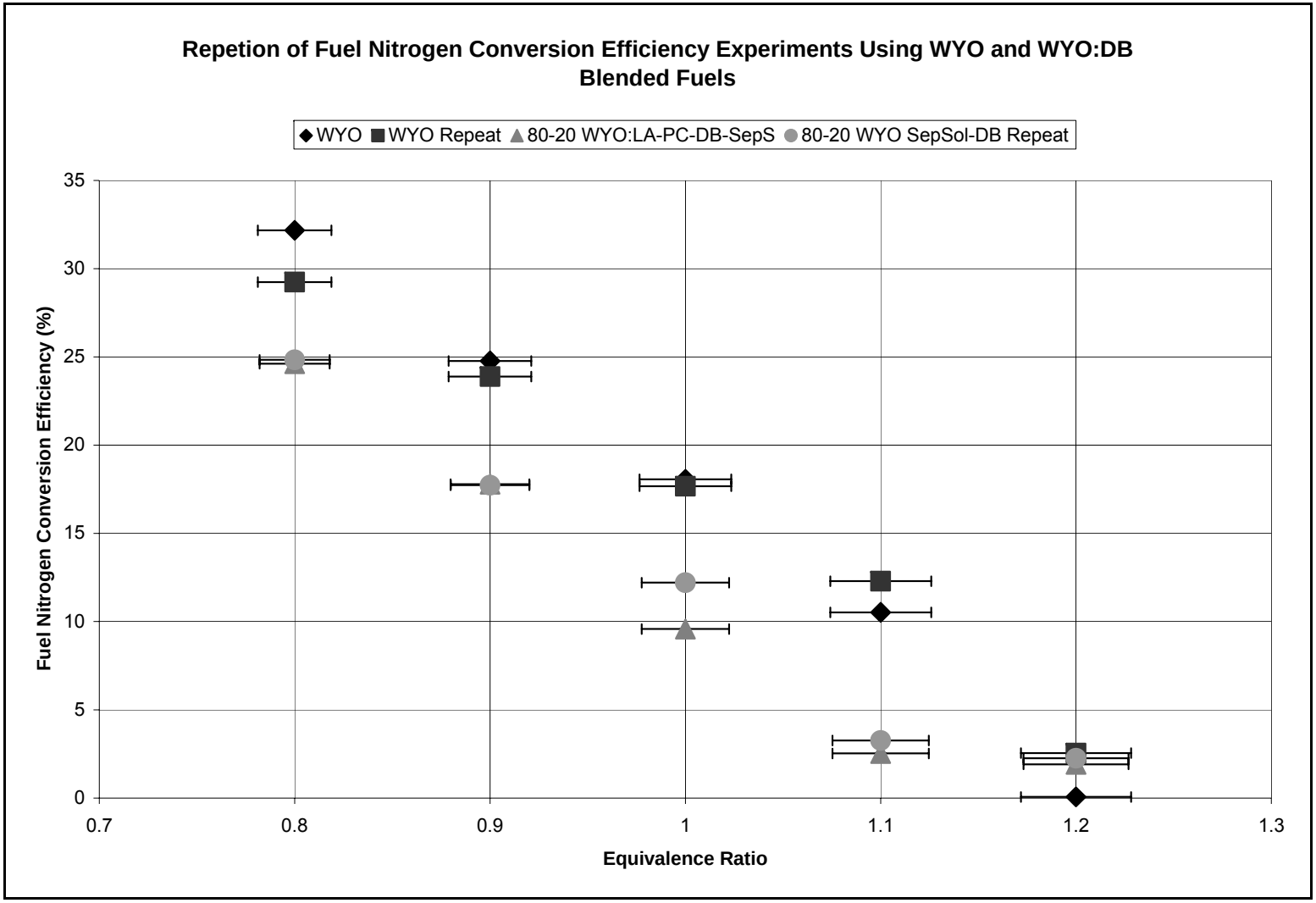

Figure D.14: Repetition of fuel nitrogen conversion efficiency experiments for WYO and WYO:DB blended fuels. Note that these data points had more fluctuations than the TXL:DB blended fuels.

VITA

Benjamin Daniel Lawrence received his Associate of Arts degree in liberal arts from Johnson County Community College in 2002 and received his Bachelor of Science in mechanical engineering from Kansas State University in 2005 where he was selected as an outstanding senior. He entered the mechanical engineering program at Texas A&M University in September 2005. He received a Master of Science in mechanical engineering from Texas A&M University in 2007. His research interests include thermodynamics, fluid mechanics, and heat transfer with a specific application to utility power generation and combustion science. He plans on pursuing a PhD in mechanical engineering in the same emphasis. After completing his education he plans on pursuing a tenured professorship at a major research university.

Mr. Lawrence may be reached at 1000 B Summer Cr., College Station, TX 77840. His email is ben.d.lawrence@gmail.com.